Electrochemical reduction of CO_2 to Oxalic Acid

Electrochemical conversion, down-stream processing and techno-economic analysis

V.S. Boor

TU Delft

Electrochemical reduction of CO_2 to Oxalic Acid

Electrochemical conversion, downstream processing and techno-economic analysis

by

V.S. Boor

to obtain the degree of Master of Science

at the Delft University of Technology,

to be defended publicly on Thursday April 9, 2020 at 14:30.

Student number:	4394062	
Project duration:	September 2, 2019 – April 9, 2020	
Thesis committee:	Prof. dr. ir. T.J.H. Vlugt,	TU Delft, supervisor
	Dr. M. A. Van Der Veen,	TU Delft
	Dr. T. E. Burdyny,	TU Delft

TU Delft

Abstract

Rising CO_2 levels in the atmosphere are becoming increasingly problematic, due to the effect of CO_2 on climate change. CO_2 capture and utilization has high potential as strategy to close the carbon cycle. An example of utilization of CO_2 is the electrochemical reduction of CO_2 to more valuable compounds. This thesis discusses the electrochemical reduction of CO_2 to oxalic acid. Until now, oxalic acid as target product of the electrochemical CO_2 reduction has not been studied in great depth, mainly because it only forms in non-aqueous solutions. The influence on several parameters, namely cathode material, applied potential, anolyte, catholyte, membrane, supporting electrolyte, and temperature, on the electrochemical conversion of CO_2 to oxalic acid has been studied. The first step in scaling-up has been taken, from a batch reactor (H-cell reactor) to a semi-continuous system (flow-cell reactor). In order to investigate the feasibility and its implementation in the industry, several options for the downstream processing of oxalic acid are discussed and a techno-economic analysis is performed on the proposed process design.

From the parametric study that was carried out, the parameters that had a considerable effect on the performance of the electrochemical reduction of CO_2 to oxalic acid were cathode and anode material, catholyte and anolyte, membrane, applied potential and temperature. With the batch reactor optimal results in terms of faradaic efficiency and current density have been found, using lead as cathode, platinum as anode, propylene carbonate+0.7M tetraethylammonium chloride as catholyte and 0.5M H_2SO_4 as anolyte in which the cathodic and anodic compartment are separated by a Nafion 117 membrane. At higher temperatures, higher current densities were induced by reduction of mass transfer limitations. Within the range of -2.2V to -2.7V vs Ag/AgCl, increasing current densities and decreasing faradaic efficiencies were found with increasing applied potential. Semi-continuous flow-cell was investigated as a strategy to increase the mass transfer in the system. Although higher reduction currents were measured during CO_2 reduction in a flow-cell compared to the batch reactor, the faradaic efficiency towards oxalic acid was lower. The oxalic acid produced during CO_2 reduction in the electrochemical reactor is dissolved in the liquid electrolyte. A further separation step of the oxalic acid from the liquid needs to be present to recover the product in a solid state. In order to assess the feasibility of the separation of oxalic acid, several technologies were addressed. Liquid-liquid extraction followed by crystallization is experimentally proved to be a suitable method for the separation and recovery of oxalic acid from the electrolyte. Based on this separation method, a process design is proposed and a techno-economic analysis has been performed. The techno-economic analysis showed a favorable economic potential for this technology if certain key performance indicators can be achieved. However, the maturity level of this process is still in early stages. Some of those key performance indicators still need to be experimentally improved, further research should focus on increasing the obtained current densities and obtaining stable faradaic efficiencies.

Acknowledgements

From a young age, I have always wanted to commit myself to the greatest challenge of our time - climate change. The past years in Delft have given me the knowledge and also, even more motivation, to work on solutions. Examples of current technological challenges are carbon capture and utilization and - even more than renewable energy generation - energy storage.

This thesis is about the electrochemical reduction of CO_2 to oxalic acid, which has not yet been widely researched. I hope that with this research I have been able to contribute to the development of this technique.

I would like to thank Thijs Vlugt, Mahinder Ramdin and Peter van den Broeke for all the ideas they generated, their encouragement and for keeping me focussed throughout the project. I got the opportunity of doing experiments at TNO, where I was surrounded by very smart and motivated people who were always willing to help. I would like to thank Elena Pérez Gallent in particular, for all the fruitful discussions we had, but also for listening to me expressing frustrations about the troubles experienced during the research. I would also like to thank Tom Burdyny and Monique van der Veen for being on my thesis committee.

Finally, I would like to thank my friends. My time in Delft would not have been the same without you. Also during this thesis you were always there to have coffee, lunch or drinks and to talk and laugh about all the things happening in our lives. Also, I would like to thank my family, for their unwavering support throughout my life.

V.S. Boor
Delft, March 2020

Contents

List of Figures

List of Tables

Nomenclature

Physics Constants

j	Current density	mA/cm^2
E	Potential	V
σ	conductivity	mS/cm
η	Overpotential	V
E_0	Standard potential	V
κ	Conductivity	S/m
n_e	Stoichometric number of electrons involved in an electrode reaction	(-)
l	Thickness,	m
A	Area,	m^2
F	Faraday's constant,	C/mol
Q	Energy requirement,	kJ
m	Mass flowrate,	ton/year
h	Enthalpy,	kJ/kg
N_{ts}	Number of theoretical stages,	(-)
σ	Surface tension,	N/m
μ	Viscosity,	$Pa \cdot s$
ρ	Density,	kg/m^3
D	Diameter,	m
n	Scaling factor,	(-)
T	Temperature,	°C
M	Molecular weight,	g/mol
K	Distribution coefficient,	(-)
E	Extraction factor,	(-)

Abbreviations

ACN acetonitrile. 7, 53

AEM anion-exchange membrane. 22

CAPEX Capital Expenditure. 50

CCS Carbon Capture and Sequestration. 1

CCU Carbon Capture and Utilization. 1

CE counter electrode. 13, 14

CEM cation-exchange membrane. 22

CEPCI Chemical Engineering Plant Cost Index. 47

CV cyclic voltammetry. 11, 24

DMF dimethylformamide. 7

DMSO dimethylsulfoxide. 7

FE faradaic efficiency. 6

GDEs Gas Diffusion Electrodes. 55

OPEX Operational Expenditure. 50

PC propylene carbonate. ix, 4, 7, 13, 16, 24

RE reference electrode. 13, 14

SHE Standard Hydrogen Electrode. 2

TBAP Tetrabutylammonium perchlorate. xi, 24–26, 53

TEAAce Tetraethylammonium acetate. xi, 24–26, 53

TEACl tetraethylammonium chloride. ix, xi, 13–16, 19, 21, 25, 26, 53

TEC Total Energy Consumption. 44

WE working electrode. 13, 14

1 Introduction

In the past centuries, the CO_2 levels in the atmosphere have risen from 280 ppm in the pre-industrial area to 418 ppm presently [4] due to deforestation and the use of fossil fuels. This rise is one of the main contributors to climate change by the greenhouse gas effect [5]. To limit the rise of the CO_2 level in the atmosphere, CO_2 emissions must be reduced and methods for removal of CO_2 from the atmosphere have been proposed. Examples of these methods are Carbon Capture and Storage (CCS), carbon sequestration but also Carbon Capture and Utilization (CCU). CCU closes the carbon cycle by capturing the emitted CO_2 and then recycle it by conversion to useful products. Methods for CO_2 conversion are photo-chemical reduction [6], gas-phase reaction [7], liquid-phase reaction [8] and electrochemical reduction [9].

CO_2 can be electrochemically converted to form added-value chemicals. The process shows great potential because CO_2 is a cheap carbon source for the production of renewable fuels and it would reduce the level of CO_2 in the atmosphere. Examples of organic feedstocks that can be produced are carbon monoxide, formic acid, formaldehyde, ethanol, and methane [10]. At the moment, none of these products are industrially produced by the electrochemical production process. Economic feasibility of the electrochemical reduction process is mainly dependent on how many electrons - which determines amount of energy - need to be transferred when forming one mole of product. Formic acid, carbon monoxide, and oxalic acid are all 2-electron transfer products and therefore show the most potential, in comparison to other products such as methane (8 electrons) and ethylene (12 electrons). Also, the atom efficiency of the reaction to oxalic acid is very high, especially compared to methane and ethylene.

Over the years, significant research effort is done towards the electrochemical reduction of CO_2 to formic acid (HCOOH), carbon monoxide (CO), methanol (CH_3), and syngas (mixture of CO + H_2) [11]. The product distribution of electrochemical reduction of CO_2 is dependent on conditions such as type of solvent, material and morphology of electrode and applied potential. Over the past years, the reduction to formate/formic acid has been investigated thoroughly worldwide. Within the TU Delft Process and Energy department, the process has been modelled [12] and bipolar membranes have been applied in the electrolysis [13]. Also, the opportunities for using Deep Eutectic Solvents with high CO_2 solubility have been investigated [14]. The formic acid process is not yet suitable for commercial production, because of the high capital investments needed for electrolyser units, the fast degradation of catalysts and the difficult downstream processing of the product [15, 16]. Therefore, alternative reaction products of electrochemical CO_2 reduction should be explored.

Oxalic acid has been overlooked as a potential promising product of the CO_2 reduction, mainly because it particularly forms in non-aqueous solutions. In aqueous solutions, there is too much competition with other electrochemical reduction reactions. Water has been preferred as a solvent for electrochemical reactions, as it is abundant and has many excellent solvent properties [17]. Although oxalic acid is formed in non-aqueous solutions, the CO_2 reduction to oxalic acid shows great potential, especially because oxalic acid can be converted to ethylene glycol [18, 19]. Oxalic acid has a market price of 1000 €/tonne [20] and an overall market value of 700M$ in 2020. It has applications in multiple industries such as pharmaceutical, textile and rare earth metal industry [21]. Two oxalic acid production processes are commercialized: the oxidation

of ethylene glycol with a mixture of nitric acid and sulfuric acid [22] and via the preparation of oxalic acid esters with the reaction of carbon monoxide with an ester of nitrous acid [23]. Ethylene glycol serves as reactant in the plastics industry and has a market price of 1500$ / tonne. Annually, 35M tonne of ethylene glycol is produced[24]. The formation of different oxalate based polymers has been reported with adjustable properties such as thermal stability, biodegradability, crystallinity and mechanical strength [25].

Reaction 1.1 shows the formation of the oxalate-anion in aqueous alkaline environment together with the standard reduction potential (E_0), which is given with reference to the standard hydrogen electrode (SHE). Reaction 1.2 shows the formation of oxalic acid in aqueous acidic environment.

$$2CO_2(g) + 2e^- \leftrightharpoons {C_2O_4}^{2-}, E^0 = -0.64V \text{ vs. SHE} \tag{1.1}$$

$$2CO_2(g) + 2H^+ + 2e^- \leftrightharpoons H_2C_2O_4, E^0 = -0.48V \text{ vs. SHE} \tag{1.2}$$

$$2H^+ + 2e^- \leftrightharpoons H_2(g), E^0 = 0V \text{ vs. SHE} \tag{1.3}$$

In aqueous solutions, the CO_2 reduction reactions compete with the hydrogen evolution reaction (reaction 1.3), which reduces the selectivity to the CO_2 reduction reaction products. Therefore, working with non-aqueous solvents is an interesting alternative. On the other side, foreseeable problems are the low conductivity of these solvents which leads to low current densities, the stability of membranes in organic solvents and the difficulty of keeping the solvent water-free.

This thesis presents research on optimization of the electrochemical conversion of CO_2 to oxalate in non-aqueous solvents and on the downstream processing of the produced oxalic acid. A production process for the electrochemical production of oxalic acid is proposed and the techno-economic feasibility of this process is evaluated. The research has been conducted based on the following research questions:

- What are the optimal experimental settings in batch-scale experiments for electrochemical conversion of CO_2 to oxalic acid?
- What is the influence of a semi-continuous experimental set-up for the electrochemical conversion of CO_2 to oxalic acid?
- What are the preliminary options for the separation and purification of oxalic acid?
- Which techno-economic conditions need to be satisfied before commercial application of the CO_2 reduction to oxalic acid is feasible?

2

Theory

In this section, a literature overview will be given of the electrochemical reduction of CO_2 to oxalic acid. First, general challenges for the electrochemical reduction of CO_2 are discussed. Then, the state-of-the-art of the electrochemical conversion from CO_2 to oxalic acid is reviewed.

2.1. General challenges for the electrochemical reduction of CO_2

Using CO_2 - one of the largest waste streams available [26] - as feedstock for fuels and chemicals is one of the few games where all players stand to win. So the question arises; why is it not applied on a large scale yet? Before the large-scale application of CO_2 reduction reaction is possible, several challenges must be overcome. The electrochemical reduction of CO_2 is the conversion of CO_2 into more valuable compounds using electrical energy. This process is called electrolysis and can be used to form lots of different products from CO_2, but the process has no industrial applications for CO_2 reduction yet. For the electrochemical reduction of CO_2 to formic acid, the high electricity consumption, the low electrode stability and the difficult downstream processing are the main reasons the process is not economically feasible yet [15]. CO_2 has a very stable, linear, symmetrical structure, which makes it non-polar. Due to the stability, lots of energy is needed for the first (rate-limiting) step in the reduction, which means that large overpotentials need to be applied. Using a catalyst could reduce the activation energy, however the non-polarity makes it difficult to selectively adsorb CO_2 on catalysts.

If the CO_2 reduction is performed in aqueous solution, there is competition at the working electrode with the hydrogen evolution reaction. The hydrogen evolution reaction in acidic and alkaline conditions is respectively described by reaction 2.1 and 2.2 [27].

$$2H^+ + +2e^- \leftrightharpoons H_2(g) \tag{2.1}$$

$$2H_2O + 2e^- \leftrightharpoons H_2(g) + 2OH^- \tag{2.2}$$

In aqueous media, water is abundant compared to CO_2, which favours the hydrogen evolution reaction. The kinetics of HER are also faster compared to CO_2 reduction and the both reactions occur in the same potential range. CO_2 is also a relatively large molecule, which leads to slow mass transfer and limits the rate of reaction. Besides the low mass transfer, CO_2 is poorly soluble in water (1.45 g/L STP [28]), which is also a factor why the reaction is mass-transfer limited.

2.2. Description of the mechanism

CO_2 has always been the source of carbon for life on earth. The conversion of CO_2 by photosynthetic organisms (such as plants, algae and cyanobacteria) closes the carbon cycle [29]. CO_2 is thermodynamically very

stable, which makes conversion quite difficult. Methods for CO_2 conversion are photo-chemical reduction [6], gas-phase reaction [7], liquid-phase reaction [8] and electrochemical reduction [9]. This work discusses the electrochemical reduction of CO_2. In this section, the mechanism and reaction of this electrochemical reduction will be discussed. It should be noted that the reaction products are different in aqueous and non-aqueous solvents. The reaction mechanisms differ based on the availability of a proton donor.

The mechanism of CO_2 reduction in aprotic solvent (DMF) on mercury is described by Gennaro et al. [30] on inert electrodes such as Pb and Hg. The first (and rate-limiting) step of CO_2 reduction in non-aqueous media is the formation of the bend CO_2-radical (reaction 2.3). The CO_2-anion is an unstable intermediate.

$$CO_2(g) + e^- \leftrightharpoons {CO_2}^-, E_0 = -1.90\text{V vs. SHE} \tag{2.3}$$

For the formation of oxalate, two CO_2-radicals need to react with each other, as described by reaction 2.4 [30].

$$2{CO_2}^- \rightarrow {C_2O_4}^{2-} \tag{2.4}$$

The other reaction products that form are carbon monoxide and carbonate, via the mechanism described by reaction 2.5 [30].

$$\begin{aligned} &{CO_2}^- + CO_2 \rightarrow {C_2O_4}^- \\ &{C_2O_4}^- + {CO_2}^- \rightarrow CO + {CO_3}^{2-} + CO_2 \end{aligned} \tag{2.5}$$

The reaction mechanism for the production of oxalate has also been described by Eneau-Innocent [1]. In Figure 2.1 an overview of the reaction steps for oxalate formation on lead in propylene carbonate (PC) is given. The mechanism starts with the formation of the CO_2-anion on lead, which reacts to form oxalate. Finally, the bond between oxalate and lead is broken and an oxalate-anion is formed.

The difference between the mechanisms of Gennaro [30] and Eneau-Innocent [1] lies mainly in the formation of byproducts. Gennaro described the formation of CO and ${CO_3}^{2-}$ as byproducts, while Eneau-Innocent analyzed the reaction with IR spectroscopy and did not find any formation of CO.

If there is water or protons available in the solvent, also other products can be formed. Reactions 2.6, 2.7, 2.8, 2.9 and 2.10 describe the electrochemical CO_2 reduction reaction and the standard reduction potentials to respectively formic acid, carbon monooxide, methane, ethylene and ethanol in aqueous solutions [31].

$$CO_2(g) + 2H^+ + 2e^- \leftrightharpoons HCOOH, E^0 = -0.25\text{V vs. SHE} \tag{2.6}$$

$$CO_2(g) + 2H^+ + 2e^- \leftrightharpoons CO + H_2O, E^0 = -0.106\text{V vs. SHE} \tag{2.7}$$

$$CO_2(g) + 6H_2O + 8e^- \leftrightharpoons CH_4 + 8OH^-, E^0 = -0.659\text{V vs. SHE} \tag{2.8}$$

$$2CO_2(g) + 8H^+ + 8e^- \leftrightharpoons CH_4 + 2H_2O, E^0 = -0.659\text{V vs. SHE} \tag{2.9}$$

$$2CO_2(g) + 12H^+ + 12e^- \leftrightharpoons C_2H_5OH + 3H_2O, E^0 = 0.084\text{V vs. SHE} \tag{2.10}$$

Ikeda et al. [2] described the several outcomes of CO_2 reduction reactions with the CO_2-anion as intermediate. In Figure 2.2 an overview of the the reaction products formed based on the type of solvent and type of electrode is given. In aqueous solvents on indium, lead and mercury formic acid is formed. CO is formed on zinc, silver and gold in aqueous solutions and on zinc, tin and gold in non-aqueous solvents. In non-aqueous solvents on lead, thallium and mercury oxalic acid is formed.

Oxalic acid can also be further reduced, to glycolic acid and glyoxylic acid [32]. In Figure 2.4 the reaction to glycolic acid is shown and in Figure 2.3 the reaction to glyoxylic acid is shown. Glyoxylic acid can be further reduced to tartaric acid and glycolic acid can be further reduced to maleic acid, but this does not occur on lead electrodes [32].

2.3. Characterization

Common electrochemical experiments used to evaluate the performance of electrochemical cells are cyclic voltammetry and chronoamperometry. In cyclic voltammetry, the potential is swept in time between two val-

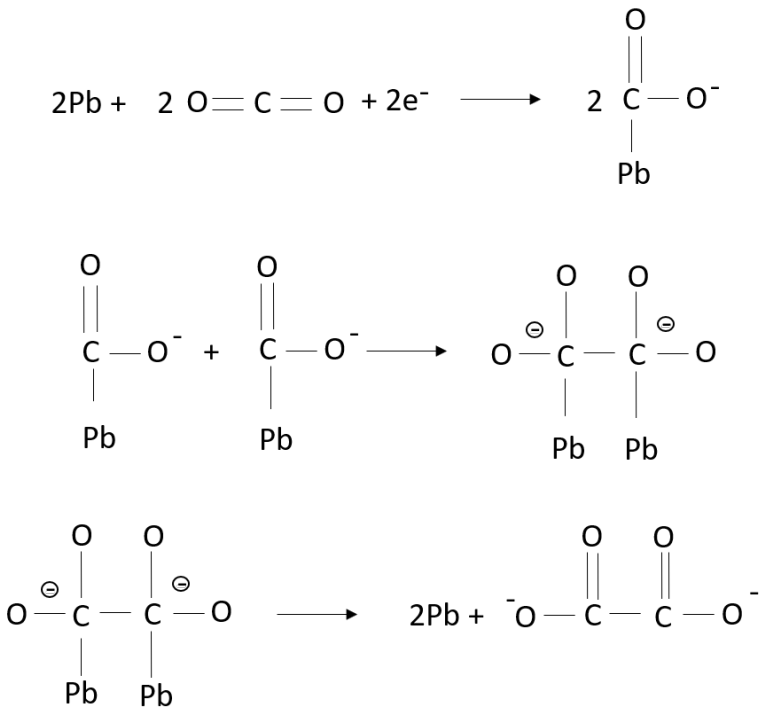

Figure 2.1: The mechanism for the formation of oxalate on lead as described by Eneau-Innocent [1]. It starts with the formation of the CO_2-anion stabilized by the catalyst (Pb). Two CO_2-anions together react to form oxalate. Finally, the bond between the lead and the oxalate breaks and an oxalate anion is formed.

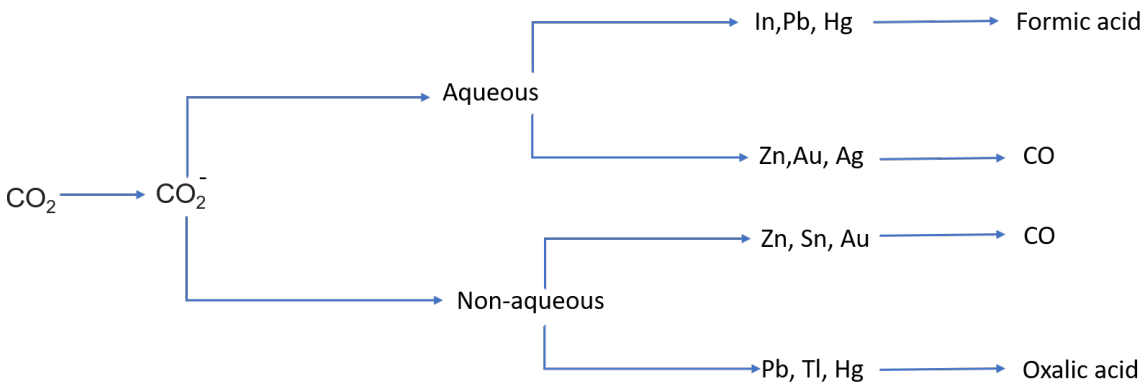

Figure 2.2: The CO_2 reduction reaction routes via the CO_2-anion as described by Ikeda et al. [2]. In aqueous solvents on indium, lead and mercury formic acid is formed. CO is formed on zinc, silver and gold in aqueous solutions and on zinc, tin and gold in non-aqueous solvents. In non-aqueous solvents on lead, thallium and mercury oxalic acid is formed.

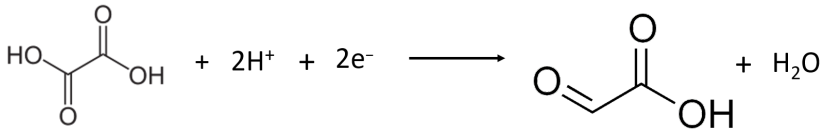

Figure 2.3: The reaction of oxalic acid to glyoxylic acid and water.

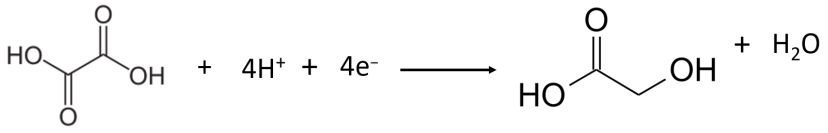

Figure 2.4: The reaction of oxalic acid to glycolic acid and water.

ues. The current is measured while the cell is scanned through different voltages. The voltammogram with the reactive species (CO_2) is compared to the voltammogram without reactive species. Reduction peaks in the voltammogram with reactive species, that are not available in the voltammogram without reactive species, show the reduction of the reactive species. A different electrochemical technique used is chronoamperometry. In this experiment, the potential is fixed and the current is measured for a certain time.

Figures of merits for electrochemical CO_2 reduction
Current density, faradaic efficiency, energetic efficiency and stability are the figures of merit characterizing the performance of an electrochemical system.

The current density (j) is the amount of current (I) per area of the electrode (A) (equation 2.11). The current of an electrochemical cell is the electron transport from the anode to the cathode as a consequence of the reactions taking place at the electrodes. Higher current indicates a higher reaction rate for both the cathodic and anodic reactions.

$$j = \frac{I}{A} \tag{2.11}$$

As the CO_2 reduction process has several products, the selectivity of the reaction to the desired product is of high importance. In electrochemistry, this is described by the faradaic efficiency (FE). The faradaic efficiency describes the efficiency with which charge is transferred in a system facilitating an electrochemical reaction to the desired product. The FE, calculated by equation 2.12, is the amount of electrons used for formation of the desired product divided by the total charge applied. The amount of electrons used for formation of the desired product is the product of the stoichometric amount of electrons needed in your reaction (n_e, the Faraday number (F) and the obtained concentration of the desired product obtained ([product]). The total charge applied is the product of the obtained current (I) and the amount of time (t) this current is applied.

$$\mathrm{FE} = \frac{n_e \cdot F \cdot [\mathrm{product}]}{I \cdot t} \tag{2.12}$$

Faradaic losses are experienced when electrons participate in unwanted side reactions. For the electrochemical reduction of CO_2 to oxalic acid, these unwanted side reactions appear in the form of the hydrogen evolution reaction, reduction of CO_2 to other carboxylic acids or CO and potential reduction of the solvent.

The energetic efficiency ($E_{\mathrm{energetic}}$) is given by equation 2.13. The energetic efficiency is the amount of energy in the products divided by the amount of electrical energy put into the system.

$$E_{\mathrm{energetic}} = \sum \frac{E_i^0 \cdot \mathrm{FE}}{E_i^0 + \eta} \tag{2.13}$$

The stability of the catalyst is an important indication for the characterization of an electrochemical cell because it largely influences the feasibility of the production process. Until now, no research has been done on the stability of the several electrocatalysts suitable for electrochemical conversion of CO_2 to oxalic acid.

Table 2.1: Different experimental settings of studies that have shown oxalic acid production including the solvent, electrolyte salt, working electrode and counter electrode used.

Solvent	Electrolyte	WE	CE	RE	Ref
PC,ACN,DMSO	0.1M TEAP	Pb, Hg, TI	Pt	Ag/AgCl	[2]
Aqueous	TMAOH	graphite	Pt	Ag/AgCl	[33]
ACN	0.1M TBAF	Pt	Pt	$Ag/AgNO_3$	[34]
ACN	TBAP	Stainless steel	Zn	-	[35]
PC	0.2M TEAP	Pb	Carbon	Ag/AgCl	[1]
AN	0.1M TBP	Stainless steel	Zn	Ag rod	[36]
DMF	0.1M Et_4Cl	Hg	-	Ag/AgI	[37]
CH_3OH	0.1M TMACl	Pb	Pt	Ag/AgCl	[32]

2.4. State of the art

In Table 2.1 an overview is given of the research into the electrochemical reduction of CO_2 to oxalate until now. The table discusses experimental settings that influence the selectivity to and the yield of oxalate. The research started late 70s - begin 80s with determining which conditions need to be fulfilled to produce oxalate. From then on, the research into the electrochemical reduction of CO_2 focused on other reaction products (mainly CO and formic acid). The past decade, renewed interest has focused on the development of electrocatalysts to reduce the overpotential of the reaction.

Ikeda et al. [2] tested different electrodes in non-aqueous electrolytes (PC) and found, without addition of water, 73.3% current efficiency for oxalic acid formation with a total applied charge of 100C. As soon as small amounts of water were added, the current efficiency to oxalic acid dropped, while the current efficiency to formic acid increased [2]. They also showed that at the start of the experiment the oxalic acid concentration increased linearly, but the growth slowed down, which happened simultaneously with the formation of glyoxylic acid and glycolic acid. They found lead, thallium and mercury as suitable metals for the electrochemical CO_2 reduction to oxalate and observed similar results in other non-aqueous electrolytes, such as acetonitrile (ACN) and dimethylsulfoxide (DMSO). Eggins described the electrochemical reduction of CO_2 in methanol and found at a voltage of -1.7V vs. Ag/AgCl current efficiency of up to up to 12.5% to oxalate, which decreased over time. At higher voltage, the reduction products were mainly glyoxalate and glycolate [32]. Oxalate was formed with 78 % current efficiency at a potential of -0.9V vs. Ag/AgCl for 3.25 hour at 1.2 mA in an aqueous solution of tetramethylammonium hydroxide [33]. IR analysis has been done on the electrochemical reduction of CO_2 in acetonitrile to understand the geometry of the formed oxalate-anion [34]. Using acetonitrile with tetrabutylammonium perchlorate as anode, current efficiencies of more than 90% towards oxalic acid have been achieved with stainless steel as cathode and zinc oxidation as anode reaction [35]. With similar settings, it has been shown that oxalate is formed between -2.5V and -3.5V vs. Ag, with maximum faradaic efficiency at -3.5V [36]. In situ infrared reflectance spectroscopy was used to determine adsorbed intermediates and reaction products in the CO_2 reduction process to oxalic acid. It was shown that the reaction is mass transfer limited and that there was no formation of CO during the process [1]. Also, the electrochemical reduction in dimethylformamide (DMF) has been examined with voltammetry experiments, where the formation of oxalic acid has been reported. In Table 2.1 an overview is given of the experimental settings used in the described experiments that reported the formation of oxalic acid.

Electrocatalysts for oxalic acid formation
In Table 2.2 an overview of the research into electrocatalysts for oxalate formation is given. The main goal of these catalysts is the reduction of the overpotential of the reaction. As the stability of these complexes is a problem, the development or use of them is not within the scope of this project.

2.5. Parameters

On of the goals of this research is the determination of the optimal combination of parameters that result in high and selective production of oxalic acid. Several factors influence the type and the amount of products formed during the electrochemical reduction of CO_2. These factors include the type and morphology of the metal electrode used as catalyst, the supporting electrolyte used, the catholyte used, the applied potential

Table 2.2: Different electrocatalysts described in literature studies that have been used as electrocatalyst for oxalate formation at reduced potentials.

Electrocatalyst	**Result**	**Ref**
Triangular rhodium cluster	Produced oxalate in the presence of Bu4NBF4 and LiBF4 at -1.5 V (vs. SCE) in ACN	[38]
Macrocyclic nickel complex	Most active metal complex electrocatalyst yielding selectively oxalate reported so far	[39]
Tetranuclear copper(II)complex	Low overpotential needed of only -0.03V vs. SHE, while being relatively stable.	[40]
Ag or Pd Porphyrins	Oxalic acid main product, no CO detected only H_2. At -1.50/1.65V current densities of 3 mA/cm2 achieved.	[41]
Pt coated with polyvinyl alcohol/[Ni(dppm)$_2$Cl$_2$]	oxalate formation at PVA/Ni(dppm)$_2$Cl$_2$ in acetonitrile	[42]
Cr-Ga Oxide on glassy carbon	In aqueous 0.1M KCl electrolyte FE of 59% were obtained -1.48V vs. Ag/AgCl	[43]

and the temperature and pressure.

Cathode
In electrochemical CO_2 reduction, the cathode mainly defines which products are selectively formed. Copper shows mainly potential for formation of hydrocarbons and alcohols, while Ag, Au and Zn are used for the target product carbon monoxide. Sn, In, Pb and Hg have been investigated as being selective for the production of formate [44]. Several factors influence the over-all performance of the cathode material. The faradaic efficiency, overpotential required for CO_2 reduction, the current density and the stability must be considered. Research has shown that in aprotic solvents the main products of CO_2 reduction are CO and $CO_3{}^{2-}$ when there is a strong metal-CO_2 interaction and the main product is $C_2O_4{}^{2-}$ when there is a weak metal-CO_2 interaction [45]. As previously described, working electrodes that have shown CO_2 reduction to oxalate are lead, mercury, thallium and stainless steel.

Catholyte/solvent
Several properties describe the suitability of a solvent for application of the electrochemical reduction of CO_2. The following list describes these properties:

- **CO_2 solubility** should be high to allow for high current densities.
- **Viscosity** should be low to increase mass transfer, increased mass transfer means increased conductivity.
- **Relative permittivity** shows the electrostatic interaction between two charges. A solvent always lowers this electrostatic interaction. A high relative permittivity allows for high electrostatic interaction between solutes and high dissolution and dissociation of electrolyte salts, which correlates to the conductivity of the solution [46].
- **Donor number** is a measure for the ability of a solvent to donate an electron. A higher donor number of the solvent correlates to higher selectively production of oxalic acid [45].
- **Oxalic acid solubility** should be as low as possible to enhance and facilitate downstream processing.

In Table 2.3 an overview is given of the relevant properties for the organic solvents that already have been used as solvents for the electrochemical reduction of CO_2 to oxalic acid.

The solvent dependence of the CO_2 reduction reaction was evaluated using a boron-doped-diamond working electrode, which showed the largest current at the lowest potential for acetonitrile [49], but similar onset potentials for the different solvents at -1.8V vs. Ag/Ag^+.

Supporting electrolyte
As described in section 2.2 the availability of protons in the solvent reduces the selectivity to oxalate formation. Therefore, the use of non-aqueous organic solvents is preferable. Organic solvents are generally low conductive, which leads to high resistance and large energy losses in the system. Therefore, supporting elec-

Table 2.3: Overview of relevant solvent properties, CO_2 solubility, viscosity, relative permittivity and the donor number, for the use of organic solvents as electrolyte in the electrochemical reduction of CO_2.

Solvent	**CO_2 solubility**	**Viscosity**	**Relative permittivity**	**Donor number**
	mmol/L	mPa·s	-	kJ/mol
PC	134 [47]	1.19 [48]	64.96 [48]	15.1 [48]
AcN	314 [47]	0.339 [48]	35.69 [48]	14.1 [48]
DMSO	131 [47]	0.802 [17]	36.7 [17]	124.8 [17]
DMF	194 [47]	1.99 [17]	46.5 [17]	111.4 [17]

trolyte salt is used. Tetraalkylammonium salts are suitable because of their solubility in most organic solvents. The properties of tetraalkylammonium salts differ based on the alkylgroup in the cation and on the type of anion. It has been proposed that the tetraalkylammonium-group work as catalyst for CO_2-reduction [50], but the opposite has been proven by Berto et al. by showing that the onset potential for CO_2 reduction is not dependent on the tetraalkylammonium-group [49]. The influence of addition of tetraalkylammonium salts to the solvent does not significantly influence the CO_2 solubility [47]. There is no data available for the influence of the type of tetraalkylammonium salt on electrochemical CO_2 reduction towards oxalic acid.

Anode (+ anode reaction)
The electrons for the electrochemical CO_2 reduction reaction at the cathode are delivered by an oxidation reaction at the anode. The anode reaction influences the cell voltage and thereby the electricity requirements of the production process. Also, a valuable reaction product increases the economic potential of the process. The kinetics of the anode reaction should not limit the reaction at the cathode.
The anode oxidation reactions chosen in previous research has been platinum, but without mentioning the anolyte used or the anode reaction [2, 32]. It is assumed that the same anolyte is used as the catholyte, which indicates that in this research the anode reaction was the oxidation of the tetraalkylammoniumsalt-anion. Another suitable reaction at the platinum anode could be the oxygen evolution reaction from water, with sulphuric acid added to enhance the conductivity [51]. Also, zinc has been used as anode in combination with oxalic acid production for zinc oxidation at a sacrificial zinc anode [35, 36].

Anolyte
The choice of anolyte is related to the choice of anode reaction, as the reactants for the anode reaction should be available in the anolyte. Another requirement for the anolyte is high conductivity, as this prevents losses due to large resistance. As mentioned in the previous paragraph, suitable anode reactions could be the oxidation of a tetralkylammoniumsalt-ion, oxygen evolution reaction or zinc oxidation. For the first two, suitable anolytes are an organic solvent with a tetraalkylammoniumsalt or a sulphuric acid solution. For the latter one, no anolyte is necessary as zinc is the reactant for the anode reaction.

Temperature of the catholyte
The temperature of the catholyte influences several reaction parameters: the CO_2 solubility, the conductivity of the solution, the viscosity of the catholyte and the diffusion rate of the reactants. In general, CO2 solubility decreases with increasing temperature, while the conductivity, viscosity and diffusion rate increases with increasing temperature. This indicates that, depending on which factors are limiting, the current density could change with changing temperature. Additionally, the selectivity of the reaction is influenced by the temperature. For the electrochemical reduction of CO_2 on copper, it has been shown that at low temperature (2 °C), optimal faradaic efficiencies for the conversion to ethylene and CH_4 were achieved [52]. Above room temperature, the hydrogen evolution reaction started to dominate, which shows that the selectivitiy of the reaction is dependent on temperature. For the electrochemical reduction of CO_2 to oxalic acid, no data is available on the influence of temperature on the faradaic efficiency or current densities achieved.

Pressure
Increasing the pressure under which the reaction takes place increases the CO_2 solubility, which increases the availability of the reactant (CO_2) at the electrode. If the reaction is mass-transfer limited, higher solubility of CO_2 will increase the current density and the reported concentration of the product. For the CO_2 reduction reaction to formate, increasing current density and concentration of the reactant have been reported until pressures of 50 bar. The faradaic efficiency increases until 40 bar, and after that decreases [13]. In aqueous solutions the CO_2 pressure effects the pH of the solution, which influences the favoured reactions and the products formed [53].

Batch vs. semi-continuous set-up

Up to now, the electrochemical conversion to oxalic acid has been performed in small-scale batch set-ups without, after the initial loading of CO_2, extra supply of reactants [2] or with continuous bubbling of CO_2 in the set-up [32]. As the CO_2 reduction to oxalic acid is mass transfer limited, a method to increase the production is by enhancing the mass transfer in the used set-up. Set-ups that have been developed to enhance mass transfer are the continuous flow-cell reactor and reactors with gas diffusion electrodes.

The continuous flow-cell continuously pumps the catholyte solution, freshly loaded with CO_2, to the electrode, which reduces the mass transfer limitations. The cell is designed to make the distance between the cathode and anode as small as possible, to minimize the energetic losses due to the electrical resistance of the cell. The continuous flow-cell reactor has shown increasing current densities for the electrochemical reduction of CO_2 to formic acid [54]. The gas-diffusion electrode is an electrode design in which the CO_2 directly diffuses onto the electrode area, which avoids the limitations of the low CO_2 solubility in many solvents. This electrode design also reduces the mass transfer limitations and also has shown increased current densities for the production of formate [55]. In chapter 3, the set-ups used will be further discussed.

3

Experimental procedure

Electrochemical conversion experiments have been performed in a single-cell set-up, batch-type set-up (H-cell) and a semi-continuous flow-cell set-up. All of this set-ups and the accompanying experimental procedures will be discussed in this section. As part of the exploration of the downstream processing options, several proof-of-concept experiments have been performed. Because the proof-of-concepts are small experiments that need some contextual explanation, a discussion of these experiments can be found together with results in Chapter 4.

3.1. Single-cell

The electrochemical window for CO_2 reduction in the solvent used has been determined by doing cyclic voltammetry experiments in a single-cell set-up. Cyclic voltammetry (CV is an electrochemical method in which the potential is swept between potential E_1 and potential E_2. The potential is applied and the resulting current is measured, which was done for the solvent in both the presence and absence of CO_2. If in the presence of CO_2 the reduction starts at a less negative potential than in the absence of CO_2, the catalyst and solvent used is suitable for CO_2 reduction. The suitable electrochemical window lies in between the starting potential for electrochemical CO_2 reduction and the starting potential for electrochemical solvent reduction. The set-up used is schematically shown in Figure 3.1.

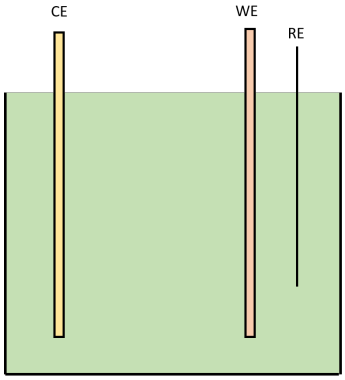

Figure 3.1: Schematic display of the single-cell experimental set-up, used for the performance of cyclic voltammetry experiments to determine the electrochemical window of the solvent used. The single-cell experimental set-up consists of the working electrode (WE), counter electrode (CE) and reference electrode (RE) in a beakerglass filled with the catholyte. The CE, RE and WE are connected to a potentiostat that applies potential and measures the current.

3.2. H-Cell

3.2.1. Preparation of set-up

In Figure 3.2 a schematic view of the H-cell is shown. In Figure 3.3, a picture is shown of the set-up of this experiments. The glassware was thoroughly cleaned by storing them overnight in $KMNO_4$ solution, which oxidizes all the organic impurities and reacts to MnO_2. The MnO_2 forms a brown precipitate, so the next step was washing the cell in a 0.1M H_2O_2 solution. A few drops of H_2SO_4 were added to catalyze this reaction. Then the cell was washed in deionized water to neutralize the cell. Hereafter, the H-Cell was built with a Nafion 117-membrane to separate the anode from the cathode compartment. The cell was tested for leakage by putting in acetone. Then, the catholyte side and anolyte side were filled with the catholyte and anolyte and the electrodes were placed. Before every experiment, the lead electrode was pretreated by applying -1.8V vs Ag/AgCl for 800 seconds in 0.5M H_2SO_4 solution. With this pretreatment, the lead oxide present on the surface of the electrode is reduced. The same procedure was applied for the pretreatment of platinum electrode which was used as a counter electrode. After this treatment, the electrodes were dried and rinsed with acetone to remove water, before being placed in the electrolyte solutions. The Ag/AgCl reference electrode was stored in 0.01M H_2SO_4.

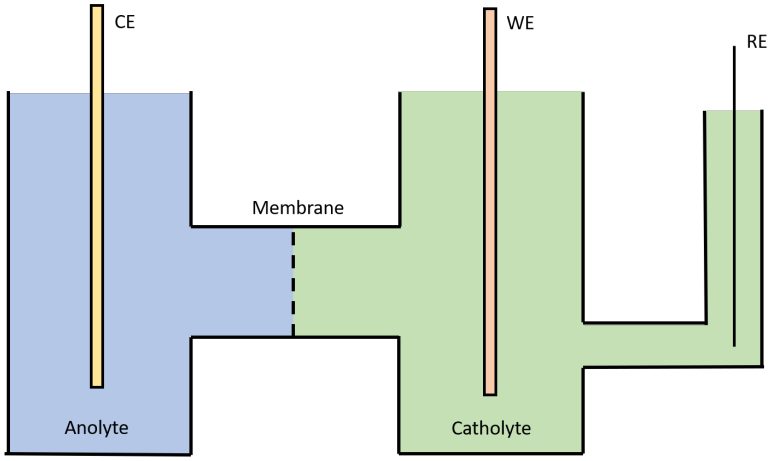

Figure 3.2: Schematic display of the H-Cell experimental set-up, which consists of a cathodic and anodic compartment separated by a membrane. The working electrode (WE) (in this case the cathode) was placed in the catholyte together with the reference electrode (RE). The counter electrode (CE) (in this case the anode) was placed in the anolyte.

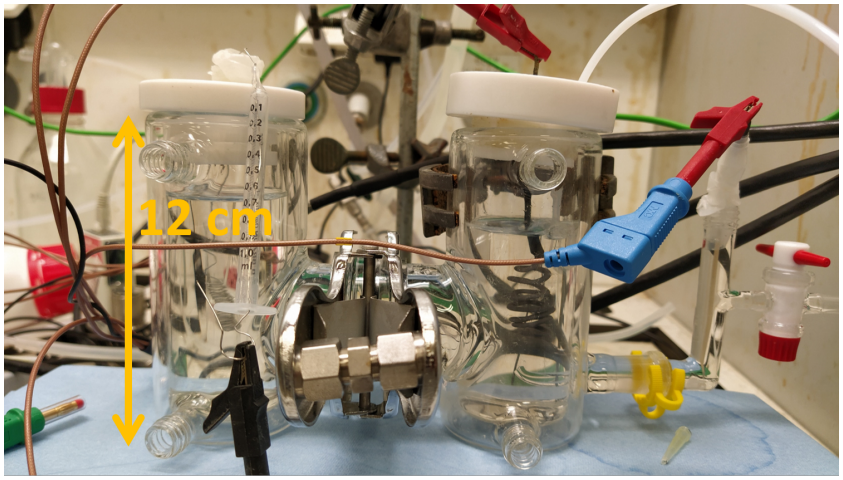

Figure 3.3: The actual set-up used for the H-Cell experiments, as schematically described in Figure 3.2. The compartment on the right was filled with 160 mL catholyte, while the left compartment was filled with 160 mL anolyte. In this case, the catholyte was 0.7M TEACl in propylene carbonate, the cathode was lead, the anolyte was 0.5M H_2SO_4 and the anode was platinum. The reference electrode was a leak-free Ag/AgCl electrode. The compartments are separated by a cation-exchange membrane.

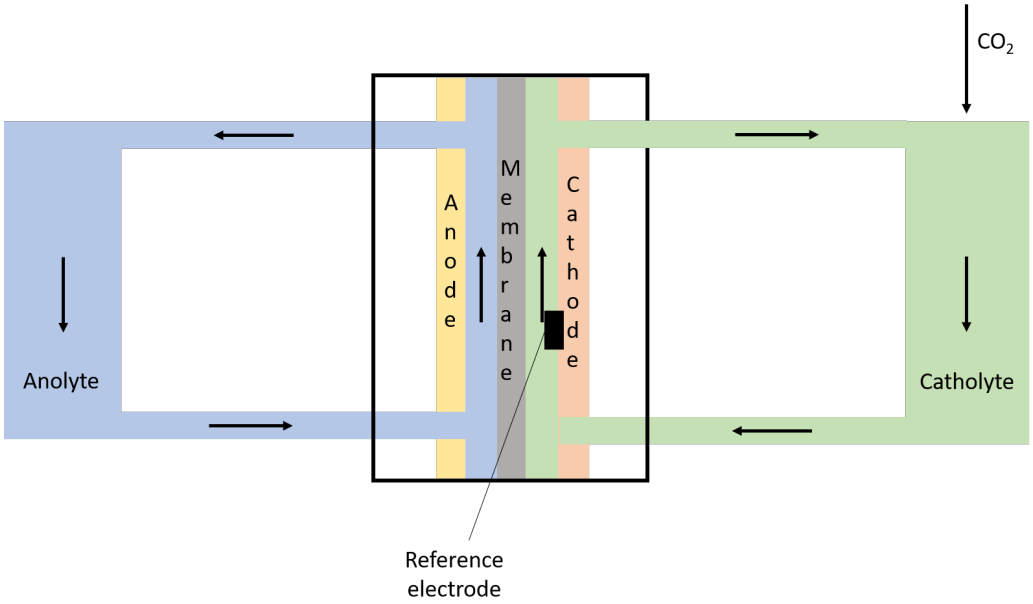

Figure 3.4: Schematic display of the flow-cell experimental set-up, which consisted of a cathodic and anodic compartment separated by a membrane. The anolyte and catholyte were pumped through the flow-cell. The flow-cell consisted of (from left to right) the anode, the anolyte compartment, a membrane, the catholytic compartment and the cathode.

3.2.2. Experiments

The working electrode (WE) consisted of a lead wire (Alfa Aesar, 99.9%) with a surface area of 10 cm^2. The counter electrode (CE) was a platinum wire with a surface area of 10 cm^2. Leak-free Ag/AgCl electrode (Innovative Instruments LF-1-100) was used as reference electrode (RE), situated in the cathodic compartment. All potentials in this work are reported against Ag/AgCl. The experiments were conducted in potentiostatic mode for 5 hours. The experiments were carried out in an H-Cell with two different compartments separated by a cationic exchange membrane (Nafion117). The catholyte consisted of a 0.7M tetraethylammoniumchloride (TEACl) in propylene carbonate (PC) solution where pure CO_2 was bubbled through with a flow rate of 18 l/h while the anolyte consisted of a 0.5M H_2SO_4 solution. The amount of anolyte and catholyte was 160 mL in each compartment. The liquid products produced on the cathode during the reduction of carbon dioxide were collected every 30 minutes and analyzed by an Agilent High performance liquid chromatographer (HPLC). The gaseous products were not analyzed. The water content in the catholyte was measured using Karl-Fischer titration. In different experiments, different variations have been made. The applied potential has been varied between -2.3V and -2.7 vs. Ag/AgCl. The catholyte, anolyte, membrane, temperature and working electrode have been varied, which will be further explained in Chapter 4.

3.3. Flow-cell

3.3.1. Preparation of set-up

In Figure 3.4 a schematic view of the flow-cell is shown and in Figure 3.5 a picture is shown of the flow-cell set-up. All of the components of the flow-cell, except the reference electrode, were stored overnight in a MilliQ solution. Prior to every experiment, the lead and platinum electrode were pretreated by applying -1.8V vs Ag/AgCl for 500 seconds in 0.2M H_2SO_4 solution. With this pretreatment, the lead oxide present on the surface of the electrode is reduced. After this treatment the electrodes were dried and rinsed with acetone to remove water, before being placed in the flow-cell. The Ag/AgCl reference electrode was stored in 0.01M H_2SO_4. The cell was tested for leakage by using water in the anolytic compartment and PC in the catholytic compartment.

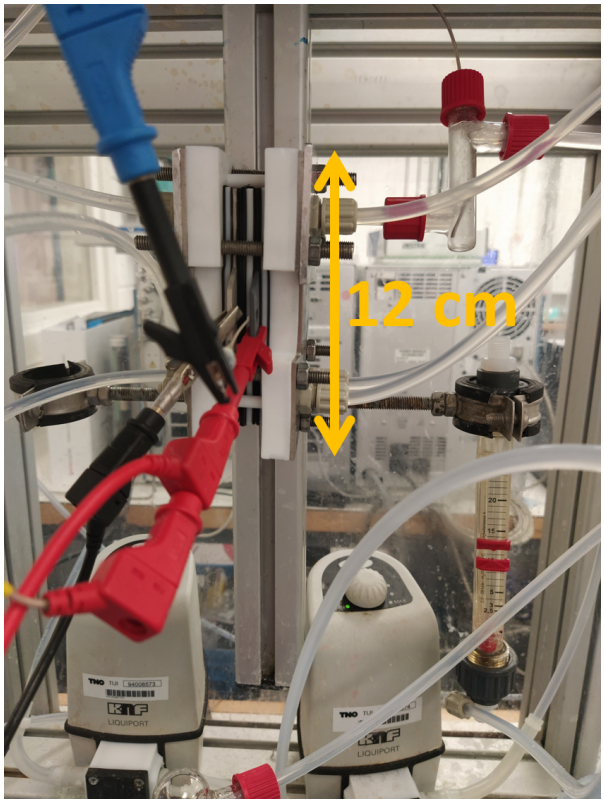

Figure 3.5: The actual set-up used for the flow-cell experiments, as schematically described in Figure 3.4. The flowcell is shown, with the connenctions to the potentiostat. The flow-cell consists of (from left to right) the anode (Pt), the anolytic compartment, the membrane, the catholytic compartment with the reference electrode and the cathode (Pb). On both sides of the flow-cell, the cell is connected to glass bottles - filled with the anolyte and catholyte - that were left out the picture. The connections the anolyte and catholyte flows trough and pumps are in the picture.

3.3.2. Experiments

The WE was a lead plate (Alfa Aesar, 99.9%) with a surface area of 10 cm^2. The CE was a platinum wire plate with a surface area of 10 cm^2. Leak-free Ag/AgCl electrode (Innovative Instruments LF-1-100) was used as (RE), situated in the cathodic compartment. All potentials in this work are reported against Ag/AgCl. The experiments were conducted in potentiostatic mode for 4.5 hours. The experiments were carried out in a flow-cell with two different compartments separated by a cationic exchange membrane (Nafion117). The catholyte consisted of a 0.7M TEACl in propylene carbonate solution where pure CO_2 was bubbled through with a flow rate of 18 L/h while the anolyte consisted of a 0.5 M H_2SO_4 solution. The amount of anolyte and catholyte was 150 mL. The anolyte and catholyte were pumped through with a flowrate of 3.6 L/h/cm^2. The liquid products produced on the cathode during the reduction of carbon dioxide were collected every 45 minutes and analyzed by an Agilent High performance liquid chromatographer (HPLC). The gaseous products were not analyzed. The water content in the catholyte was measured using Karl-Fischer titration. In different experiments, different variations have been made. For the flow-cell, the applied potential has been varied between -2.3V and -2.7 vs. Ag/AgCl. The catholyte used was in principal PC+0.7M TEACl, but this has been compared with using PC+0.3M TBAP.

4

Results and Discussion

4.1. Electrochemical conversion of CO_2 to oxalic acid

The electrochemical conversion of CO_2 to oxalic acid has been performed in an H-Cell set-up, flow-cell set-up and in the high-pressure flow-cell set-up. This section discusses the screening for optimal settings in the H-cell and the first steps to scale-up in the flow-cell.

4.1.1. Electroreduction of CO_2 in H-Cell type reactor

The H-cell reactor is used to screen the optimal settings for electrochemical CO_2 reduction to oxalic acid. The influence of the cathode material, applied voltage, catholyte, anolyte, membrane, supporting electrolyte and temperature have been researched and will be discussed in this section.

Influence of the cathode material during electrochemical reduction of CO_2

Different materials were tested as cathode for the electrochemical reduction of CO_2 to oxalic acid. Indium has been tested as cathode to selectively produce oxalic acid. After 5 hours in an H-Cell experiment with PC+0.7M TEACl as catholyte and 0.1M TEACl in ACN as anolyte at -2.5V vs. Ag/AgCl, there was no production of oxalic acid or any other carboxylic acid. Lead (Pb) has also been tested as cathode to selectively prodcuce oxalic acid. After 5 hours in an H-Cell experiment with PC+0.7M TEACl as catholyte and 0.5M H_2SO_4as anolyte at -2.5V against Ag/AgCl, production of oxalic acid and other carboxylic acids was observed. Figure 4.1 shows the current density, faradaic efficiencies for the liquid products and the concentration of oxalic acid obtained during this experiment.

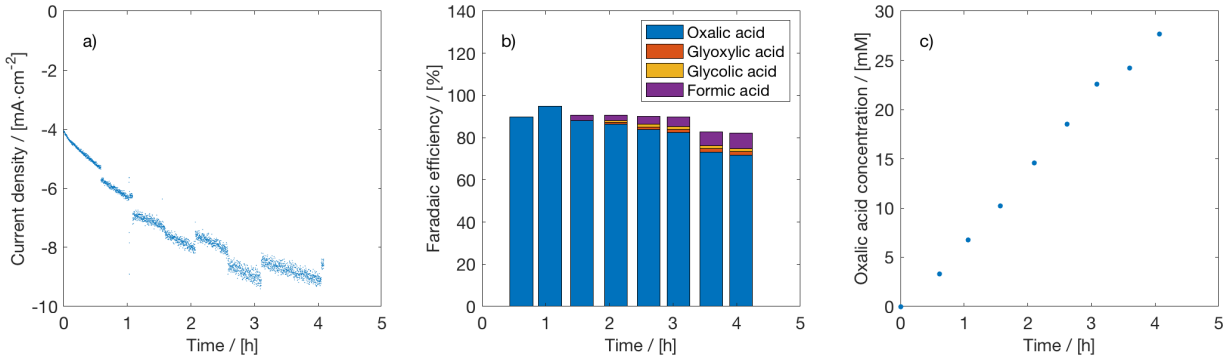

Figure 4.1: a) Current density, b) faradaic efficiency of liquid products formed and c) concentration of oxalic acid produced during electrochemical reduction of CO_2 using Pb as cathode in a 0.7M TEACl in propylene carbonate solution at -2.5V vs Ag/AgCl as a function of time. The anodic part of the reactor consisted of a platinum (Pt) anode in 0.5 M H_2SO_4. Both compartments were separated with a cation exchange membrane (Nafion 117).

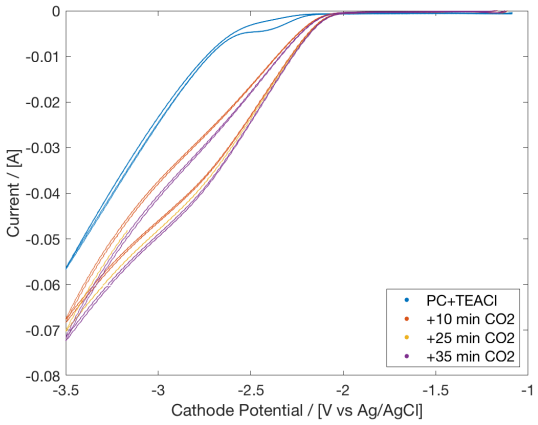

Figure 4.2: Cyclovoltammogram of cyclic voltammetry conducted in one-compartment cell with a Pb electrode in a 0.7M TEACl in PC solution in the absence of CO_2 (blue line) and in the presence of CO_2 (10 minutes of CO_2 bubbling (red line), 25 minutes of CO_2 bubbling (yellow line), 35 minutes of CO_2 bubbling (purple line).

Figure 4.1 shows the conversion of CO_2 to oxalic acid at faradaic efficiencies of up to 90 %. The current density increased from -4 mA/cm^2 to -10 mA/cm^2. After 4 hours, the oxalic acid concentration in the catholyte was 27 mM.

Voltage selection

Cyclic voltammetry measurements were performed on a Pb electrode in a 0.7M TEACl in propylene carbonate in the presence and absence of CO_2. Figure 4.2 shows that in the absence of CO_2 the catholyte starts reducing at a potential of -2.5V vs. Ag/AgCl, indicating that the operating potential window of this solvent is below this potential. With presence of CO_2, a reductive current is observed at lower onset potentials (-2.2V vs. Ag/AgCl). It follows that the optimal electrochemical window for CO_2 reduction in this catholyte is between -2.2V and -2.5V.

In order to test the influence of the potential applied during the reduction of CO_2 on Pb electrodes in terms of oxalic acid production and faradaic efficiency, several potentials in the range between -2.2 and 2.7V vs. Ag/AgCl were applied for 5 hours. Figure 4.2 shows that there is an optimal electrochemical voltage window where CO_2 reduction takes place, where there is almost no reduction of the catholyte. Several experiments are done in the range between -2.2V and -2.7V to see what the effect is on the faradaic efficiency and the production. The potentials studied were -2.2, -2.3, -2.4, -2.5 and -2.7 V vs Ag/AgCl and the obtained current densities (a), faradaic efficiencies to several carboxylic acid (b), and oxalic acid concentrations (c) are shown in Figures 4.3, 4.4, 4.5, 4.1 and 4.6 respectively.

In Figure 4.7, the current density, faradaic efficiency towards oxalic acid and the obtained oxalic acid concentrations are compared for H-Cell experiments at different applied potential. The faradaic efficiency towards oxalic acid increases when the voltage is reduced. At -2.2V vs. Ag/AgCl, the faradaic efficiency at the start of the experiment is 100% and it decreases to 86%. At -2.7V vs. Ag/AgCl, the faradaic efficiency at the start of the experiment is 80% and it decreases to 45%. However, the production of oxalic acid increases at higher voltage reaching a maximum of 36 mM after 5h at -2.7 V vs Ag/AgCl, while only a maximum of 6 mM is reached at -2.2V vs Ag/AgCl. As higher potentials lead, with same resistance, to higher current densities, there are more electrons available for electrochemical reactions when applying higher potentials, which explains the increasing production with increasing potential. Figure 4.2 shows that from -2.5V the catholyte starts to reduce. This extra side reaction leads to decreasing overall faradaic efficiencies to the carboxylic acids. When Figure 4.3b, 4.4b, 4.5b, 4.1b and 4.6b are compared it is also clearly seen that the reduction to carboxylic acid becomes more favorable with increasing voltage. The further reduction to glycolic acid and glyoxylic acid could be more favorable at higher potential, but another reason for the observed increasing faradaic efficiencies towards glycolic acid and glyoxylic acid is the increasing oxalic acid concentration. At higher oxalic acid concentration, the reaction from oxalic acid to glycolic acid and glyoxylic acid could become more favorable. Also increasing faradaic efficiencies towards formic acid are observed with increasing applied potential.

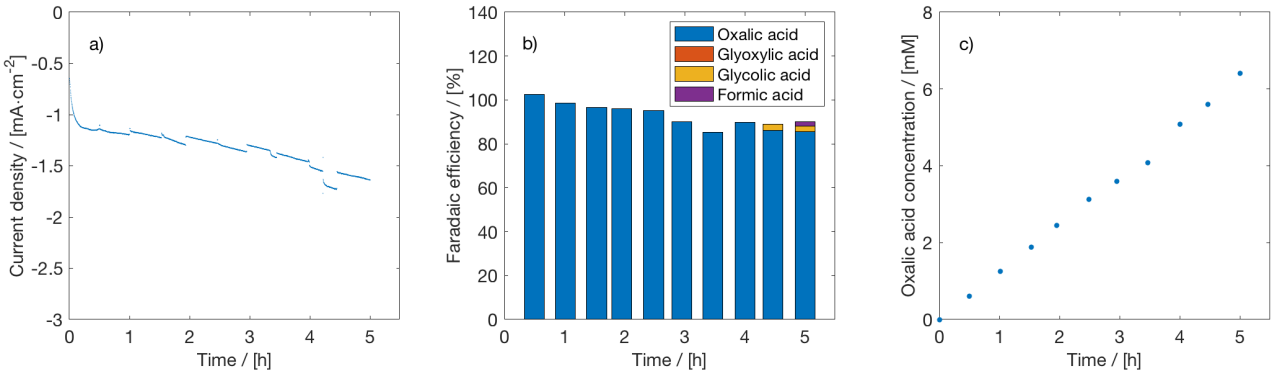

Figure 4.3: a) Current density, b) faradaic efficiency of liquid products formed and c) concentration of oxalic acid produced during electrochemical reduction of CO_2 using Pb as cathode in a 0.7M TEACl in propylene carbonate solution at -2.2V vs Ag/AgCl as a function of time. The anodic part of the reactor consisted of a Pt anode in 0.5M H_2SO_4. Both compartments were separated with a cation exchange membrane (Nafion 117).

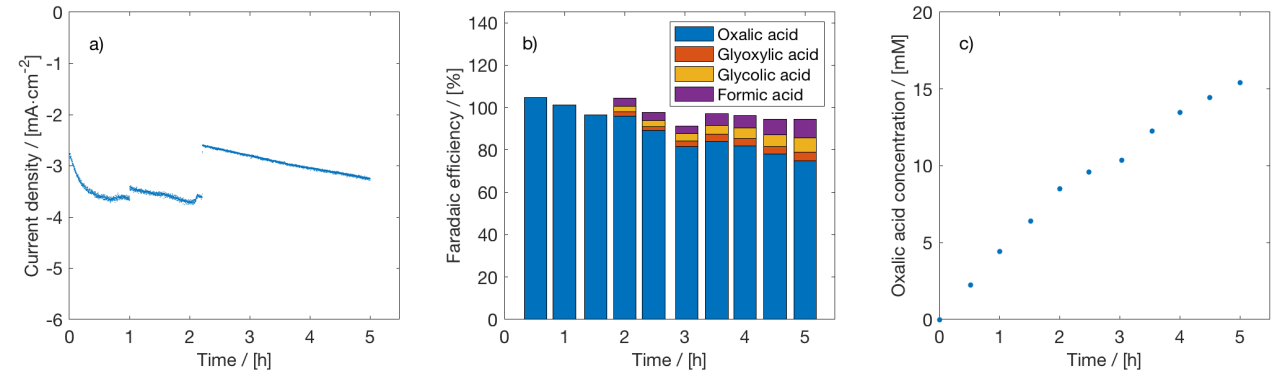

Figure 4.4: a) Current density, b) faradaic efficiency of liquid products formed and c) concentration of oxalic acid produced during electrochemical reduction of CO_2 using Pb as cathode in a 0.7M TEACl in propylene carbonate solution at -2.3V vs Ag/AgCl as a function of time. The anodic part of the reactor consisted of a Pt anode in 0.5M H_2SO_4. Both compartments were separated with a cation exchange membrane (Nafion 117).

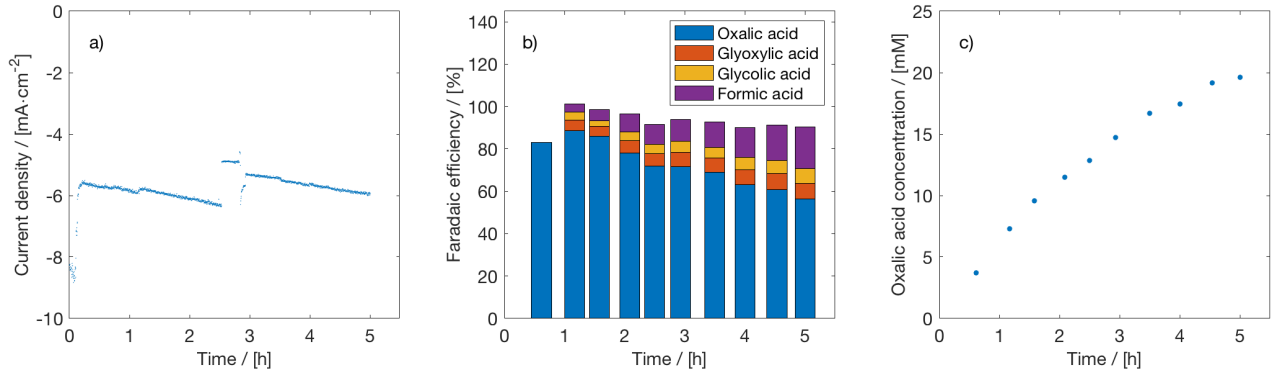

Figure 4.5: a) Current density, b) faradaic efficiency of liquid products formed and c) concentration of oxalic acid produced during electrochemical reduction of CO_2 using Pb as cathode in a 0.7M TEACl in propylene carbonate solution at -2.4V vs Ag/AgCl as a function of time. The anodic part of the reactor consisted of a Pt anode in 0.5M H_2SO_4. Both compartments were separated with a cation exchange membrane (Nafion 117).

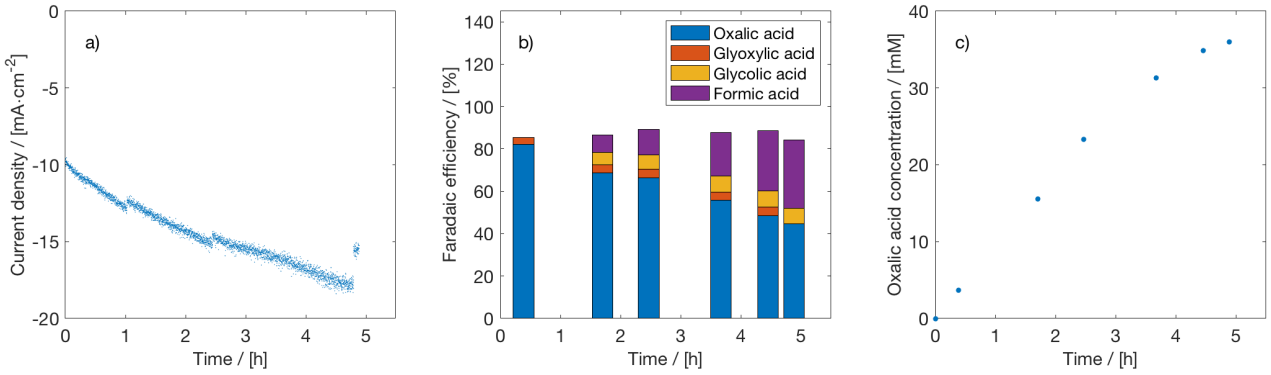

Figure 4.6: a) Current density, b) faradaic efficiency of liquid products formed and c) concentration of oxalic acid produced during electrochemical reduction of CO_2 using Pb as cathode in a 0.7M TEACl in propylene carbonate solution at -2.7V vs Ag/AgCl as a function of time. The anodic part of the reactor consisted of a Pt anode in 0.5M H_2SO_4. Both compartments were separated with a cation exchange membrane (Nafion 117).

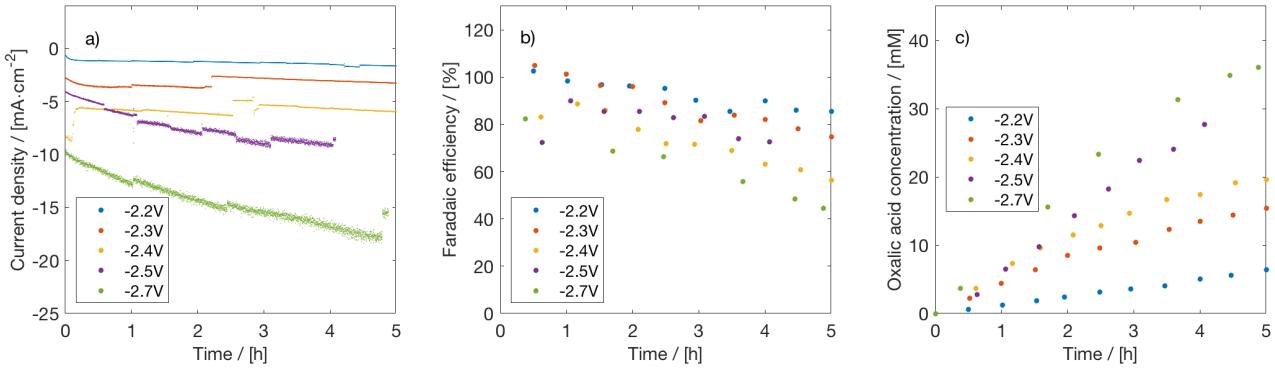

Figure 4.7: Comparison of a) current density, b) faradaic efficiency of oxalic acid formed and c) concentration of oxalic acid produced during electrochemical reduction of CO_2 using Pb as cathode in a 0.7M TEACl in propylene carbonate solution at different applied voltages (vs. Ag/AgCl) as a function of time. The anodic part of the reactor consisted on a Pt anode in 0.5 M H_2SO_4. Both compartments were separated with a cation exchange membrane (Nafion 117).

Influence of the catholyte

Different catholytes, acetonitrile and propylene carbonate, have been tested during the electrochemical reduction of CO_2 and the performance of the reaction has been assessed in terms of selectivity towards oxalic acid and oxalic acid production. Propylene carbonate and acetonitrile are organic solvents with relatively low conductivity. To propylene carbonate, tetraethylammoniumchloride has been added up to a concentration of 0.7M, which gives a solution with a conductivity of 8.8 mS/cm. Acetonitrile has been used with a concentration of 0.1M TEACl, which corresponds to a conductivity of 10.8 mS/cm. The current density, faradaic efficiency and obtained oxalic acid concentrations obtained with both the organic solvents used are given in figure 4.1 and 4.8. In Figure 4.1a) is shown that when propylene carbonate is used as catholyte, the current density at the start of the experiment is -4 mA/cm^2 and decreases to -9 mA/cm^2. In Figure **??**b) is shown that the faradaic efficiency to oxalic acid is 90 % at the start of the experiment and decreases to 70%. In Figure **??** is shown that the oxalic acid concentration after 4 hours is 28 mM. In Figure 4.8a) is shown that when acetonitrile is used as catholyte, the current density at the start of the experiment is -5 mA/cm$_2$ and decreases to -10 mA/cm^2. In Figure 4.8b) is shown that the faradaic efficiency at the start of the experiment is 50%, it decreases to 10% over the time period of the experiment. The faradaic efficiency to formic acid increases during the time of the experiment from 20 to 70%. Figure 4.8c shows that the oxalic acid concentration hardly increases after the second hour.

Figure 4.9 compares PC+0.7M TEACl with ACN+0.1M TEACl in terms of current density, faradaic efficiency and oxalic acid concentrations obtained during the experiments as discussed in figure 4.1 and 4.8. The figure shows large differences between the different catholytes in both faradaic efficiency and obtained oxalic acid concentration. The current densities obtained are similar, at the start of the experiment -4 mA/cm^2, decreasing to -10 mA/cm^2.

To see the influence of the water content in the catholyte, 1 vol.% water has been added to the catholyte. Figure 4.10a) shows that the current density obtained was 5 mA/cm^2 and relatively constant over the time frame of the experiment. Figure 4.10b) shows that the cumulative faradaic efficiency to oxalic acid decreased from 70 % at the start of the experiment to 45 % at the end of the experiment. Figure 4.10c) shows that the concentration of oxalic acid was at the end of the experiment 15 mM.

Figure 4.11 compares electrochemical reduction of CO_2 with and without addition of water to the catholyte. Figure 4.11a) shows that the current density is more constant with addition of water, that could be explained by an increasing stability of the membrane with increasing water content in the catholyte. Figure 4.11b) shows that the faradaic efficiency to oxalic acid is lower with addition of water, with a faradaic efficiency to oxalic acid of 80% without addition of water and 45% with addition of water. Figure 4.11c) shows that the concentration of oxalic acid obtained is lower with addition of water, namely 12mM compared to 27mM without addition of water.

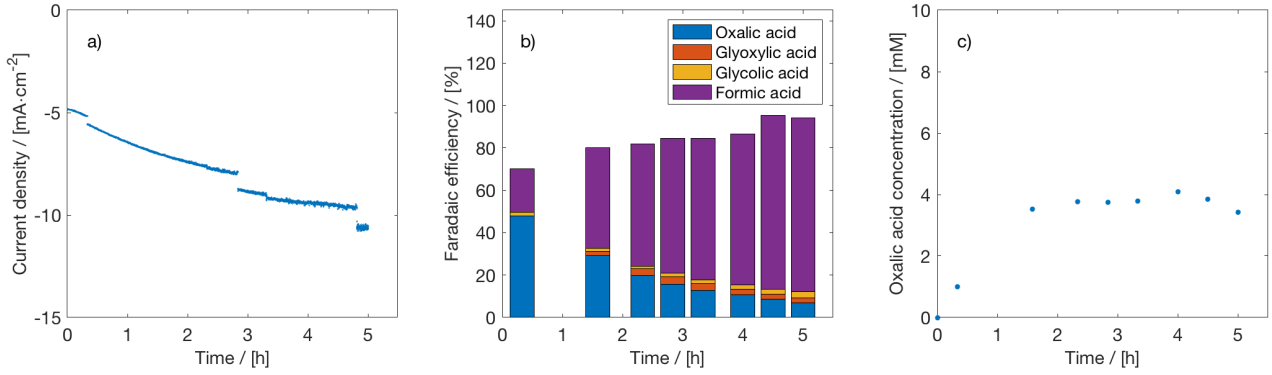

Figure 4.8: a) Current density, b) faradaic efficiency of liquid products formed and c) concentration of oxalic acid produced during electrochemical reduction of CO_2 using Pb as cathode in a 0.1M TEACl in acetonitrile solution at -2.5V vs Ag/AgCl as a function of time. The anodic part of the reactor consisted on a Pt anode in 0.5M H_2SO_4. Both compartments were separated with a cation exchange membrane (Nafion 117).

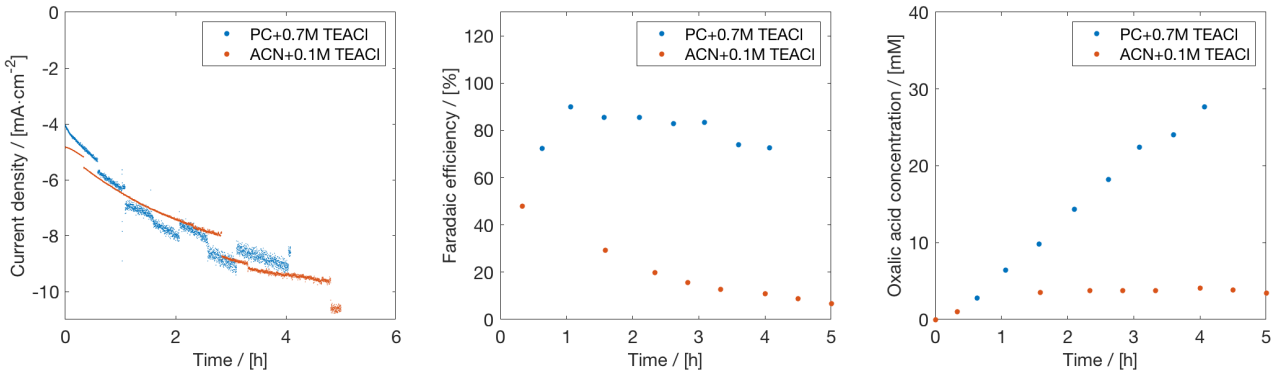

Figure 4.9: Comparison of a) Current density, b) faradaic efficiency of oxalic acid formed and c) concentration of oxalic acid produced during electrochemical reduction of CO_2 using Pb as cathode in a 0.7M+propylene carbonate (blue) or 0.1M TEACl+acetonitrile (red) solution at -2.5V vs. Ag/AgCl as a function of time. The anodic part of the reactor consisted on a Pt anode in 0.5M H_2SO_4. Both compartments were separated with a cation exchange membrane (Nafion 117).

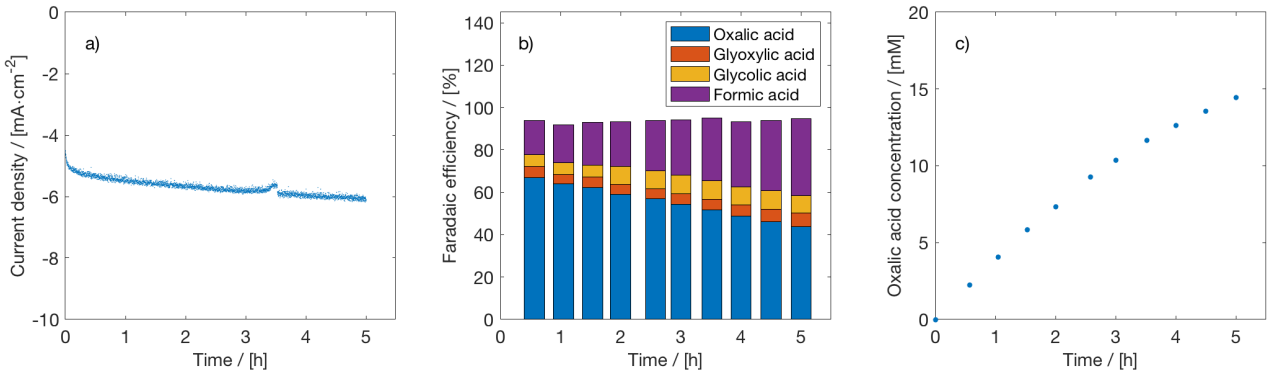

Figure 4.10: a) Current density, b) faradaic efficiency of liquid products formed and c) concentration of oxalic acid produced during electrochemical reduction of CO_2 using Pb as cathode in a 0.7M TEACl in propylene carbonate solution with 1 vol.% water at -2.5V vs Ag/AgCl as a function of time. The anodic part of the reactor consisted on a Pt anode in 0.5M H_2SO_4. Both compartments were separated with a cation exchange membrane (Nafion 117).

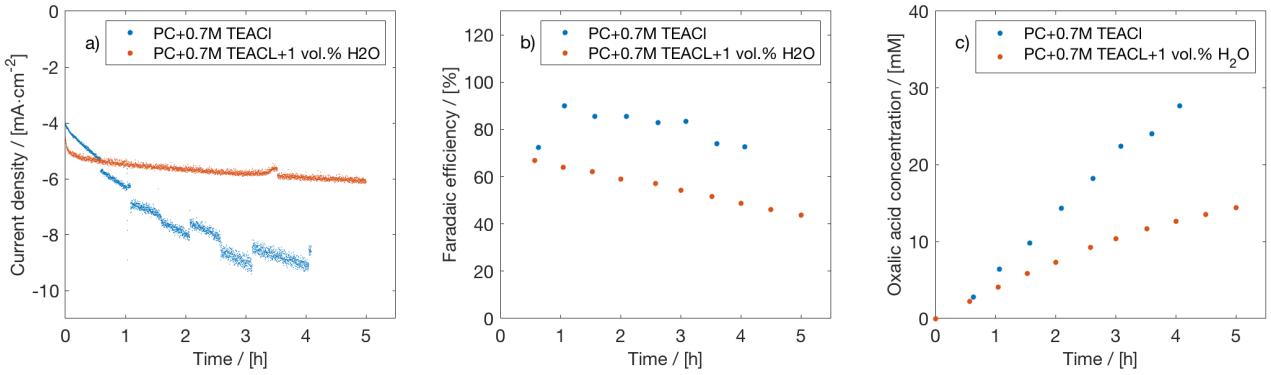

Figure 4.11: Comparison of a) current density, b) faradaic efficiency of oxalic acid formed and c) concentration of oxalic acid produced during electrochemical reduction of CO_2 using Pb as cathode in a PC (propylene carbonate) + 0.7M TEACl with (red) and without (blue) addition of water at -2.5V vs. Ag/AgCl as a function of time. The anodic part of the reactor consisted on a Pt anode in 0.5M H_2SO_4. Both compartments were separated with a cation exchange membrane (Nafion 117).

Influence of the anolyte

Different anolytes were tested during the electrochemical reduction of CO_2 and the performance of the reaction has been assessed in terms of selectivity towards oxalic acid and oxalic acid production. In Figure 4.12b) the faradaic efficiency of reducing CO2 to different liquid products with acetonitrile + 0.1M TEACl as anolyte is shown. In Figure 4.1b) the faradaic efficiency of reducing CO_2 to different liquid products with 0.5M H_2SO_4 as anolyte is shown. In Figure 4.13 the use of acetonitrile and 0.5M H_2SO_4 as anolyte is compared. As can be seen in figure 4.13a, the current density is higher when using 0.5M H_2SO_4 as anolyte. This can be explained by the higher conductivity of H_2SO_4 (211 mS/cm) in comparison to acetonitrile + 0.1M TEACl (10.8 mS/cm). Figure 4.13b shows that the faradaic efficiency for CO_2 reduction to oxalic acid is slightly lower when using acetonititrile as anolyte than when using 0.5M H_2SO_4 as anolyte, namely 83% compared to 80%. This could be explained because water can transfer through the membrane when 0.5M H_2SO_4 is used as anolyte, and an increasing water content causes higher faradaic efficiencies towards formic acid. As discussed in section 4.1.1, higher water content in the catholyte relates to lower oxalic acid faradaic efficiency. The higher selectivity to oxalic acid when using acetonitrile as anolyte and the higher current density when using 0.5M H_2SO_4 as catholyte combine together to similar concentrations of oxalic acid in the catholyte obtained during the experiment. The concentration of oxalic acid at the end of the experiment when 0.5M H_2SO_4 was 27mM and the concentration of oxalic acid at the end of the experiment when acetonititrile was used as anolyte was 23mM. When using acetonitrile with TEACl as anolyte, the anode reaction is the oxidation of chlorine ions in which chlorine gas is produced, which could be undesired. Also, the mechanical and chemical stability of the membrane used (Nafion 117) is higher when in contact with water.

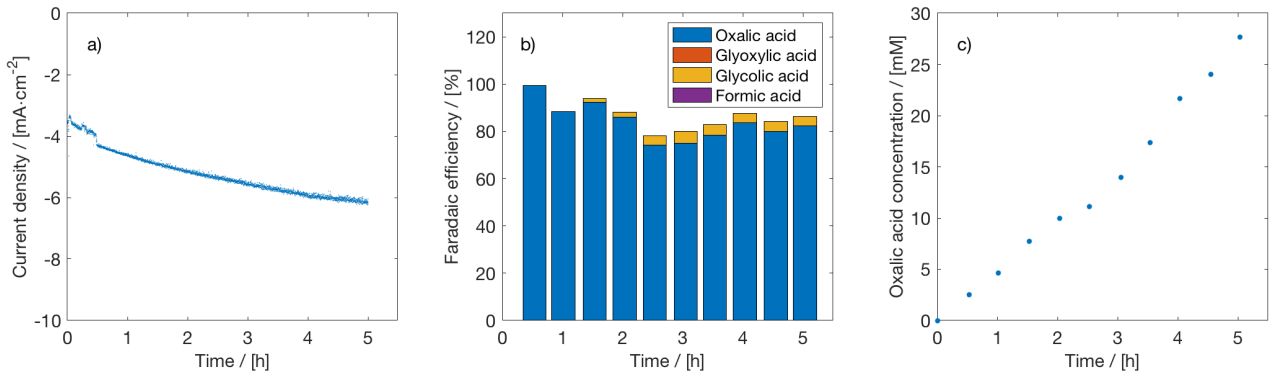

Figure 4.12: a) Current density, b) faradaic efficiency of liquid products formed and c) concentration of oxalic acid produced during electrochemical reduction of CO_2 using Pb as cathode in a 0.1M TEACl in acetonitrile solution at -2.5V vs Ag/AgCl as a function of time. The anodic part of the reactor consisted on a Pt anode in 0.5M H_2SO_4. Both compartments were separated with a cation exchange membrane (Nafion 117).

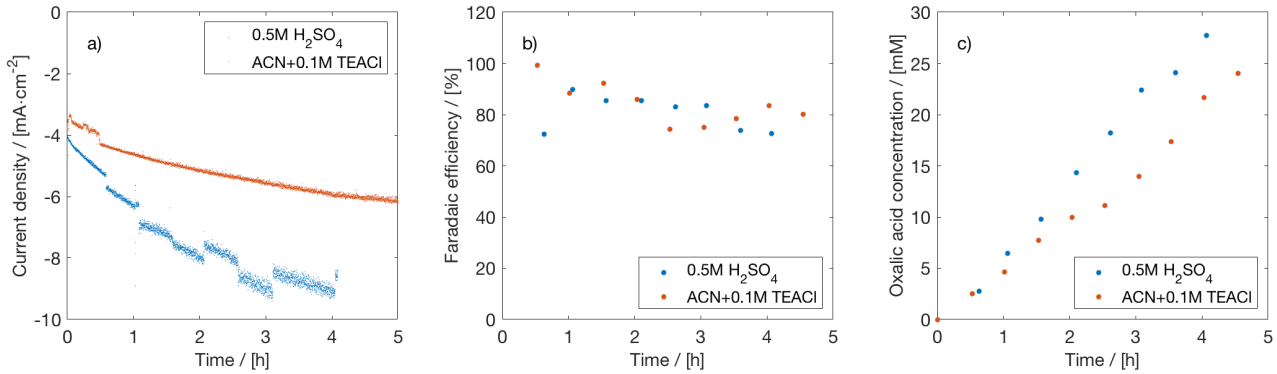

Figure 4.13: Comparison of a) Current density, b) faradaic efficiency of oxalic acid formed and c) concentration of oxalic acid produced during electrochemical reduction of CO_2 using Pb as cathode in a 0.7M TEACl in propylene carbonate solution at different applied voltages (vs. Ag/AgCl) as a function of time. The anodic part of the reactor consisted on a Pt anode in 0.5 M H_2SO_4 (red) or in 0.1M TEACl in ACN (blue).

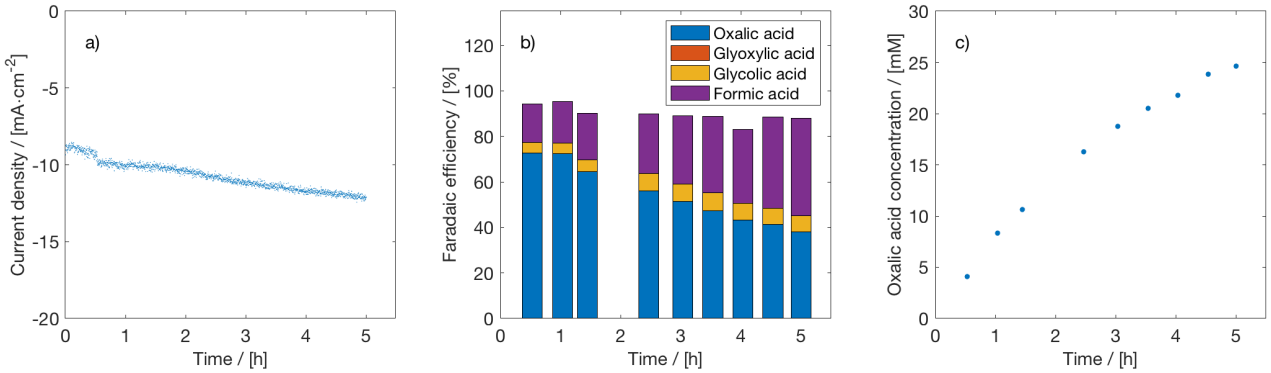

Figure 4.14: a) Current density, b) faradaic efficiency of liquid products formed and c) concentration of oxalic acid produced during electrochemical reduction of CO_2 using Pb as cathode in a 0.7M TEACl in propylene carbonate solution at -2.5V vs Ag/AgCl as a function of time. The anodic part of the reactor consisted of a Pt anode in 0.5M H_2SO_4. Both compartments were separated with an anion exchange membrane (Nafion 117).

Influence of the type of membrane used

During the electrochemical reduction of CO_2, electrons are transported from the anode to the cathode. To allow for electroneutrality, there is also transport of charged species, which occurs through the membrane. Cation-exchange membranes CEM transport positive ions and anion-exchange membrane (AEM) tansport negative ions. Membranes are never fully selective, which means that also other molecules of the catholyte and the anolyte will cross-over. In this section, the use of an anion-exchange membrane (Fumasep) and a cation-exchange membrane (Nafion117) is compared. Figure 4.14 shows, for the electrochemical reduction of CO_2 using an AEM, the current density obtained, the faradaic efficiency and the concentration of oxalic acid in the catholyte over the time period of the experiment. In figure 4.16 a picture is shown of the AEM at the end of the experiment. A white sticky layer is formed on the membrane which show probable degradation of the membrane. Figure 4.1 shows, for the electrochemical reduction of CO_2 using a CEM, the current density, the faradaic efficiency and the concentration of oxalic aid in the catholyte over the time period of the experiment. In Figure 4.15 the CEM at the end of the experiment is shown. The membrane looks 'dehydrated', which means that it is swollen and wrinkled. It is assumed that the selectivity of the membrane decreases when it becomes swollen and wrinkled. Figure 4.17 compares the electrochemical reduction of CO_2 using the AEM and CEM. Figure 4.17a) shows, that the AEM allows for higher current densities namely -12mA/cm^2 compared to -9 mA/cm^2. In Figure 4.17c) is shown that with both the membranes, similar amounts of oxalic acid are formed with final concentrations of 25 mM (AEM) and 27 mM (CEM). Figure 4.17b) shows that higher faradaic efficiencies are obtained with the CEM, namely 80% at the end of the experiment compared to 39% for the AEM. Both of the membranes have reduced chemical stability in non-aqueous solvents, but for the anion-exchange membrane the degradation was visually seen, as shown in figure 4.14.

Influence of the supporting electrolyte

For the production of oxalic acid, it is required to work with organic non-aqueous solvents such as propylene carbonate or acetonitrile. Electrolytes, that increase the conductivity of the solvent, are typically poorly soluble in organic solvents. Low conductivity of the solvent indicates high resistance, which causes high ohmic losses. As a result, lower currents will be achieved with the same applied voltage. Different supporting electrolytes have been tested and the results will be further discussed in this section. Tetraethylammonium-chloride (TEACl) has been dissolved in the propylene carbonate with a concentration of 0.7M, which leads to a conductivity of 8.8 mS/cm. Figure 4.1 shows the current density, faradaic efficiency of the liquid products formed and the concentration of the oxalic acid produced during electrochemical reduction of CO_2 with propylene carbonate with 0.7M TEACl as catholyte.

Another electrolyte salt tested was the ionic liquid Bmim-Otf at concentrations of 0.3M. At the start of the experiment, the catholyte was transparent, but during the experiment the color changed to dark brown/red which can be seen in figure 4.18. This implies decomposition of the catholyte. The experiment consisted

Figure 4.15: Cation exchange membrane at the end of the electrochemical reduction of CO_2 using Pb as cathode in a 0.7M TEACL in propylene carbonate solution at -2.5V vs Ag/AgCl. The anodic part of the reactor consisted of a Pt anode in 0.5M H_2SO_4. Both compartments were separated by an anionic exchange membrane. The membrane is swollen, which reduces the selectivity of the membrane.

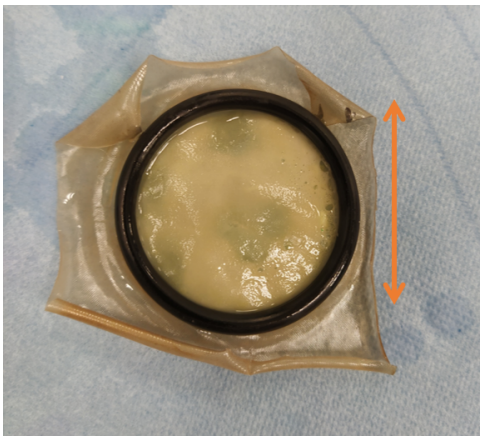

Figure 4.16: Anion exchange membrane at the end of the electrochemical reduction of CO_2 using Pb as cathode in a 0.7M TEACL in propylene carbonate solution at -2.5V vs Ag/AgCl. The anodic part of the reactor consisted of a Pt anode in 0.5M H_2SO_4. Both compartments were separated by an anionic exchange membrane. A white sticky layer is formed on the membrane, which shows degradation of the membrane.

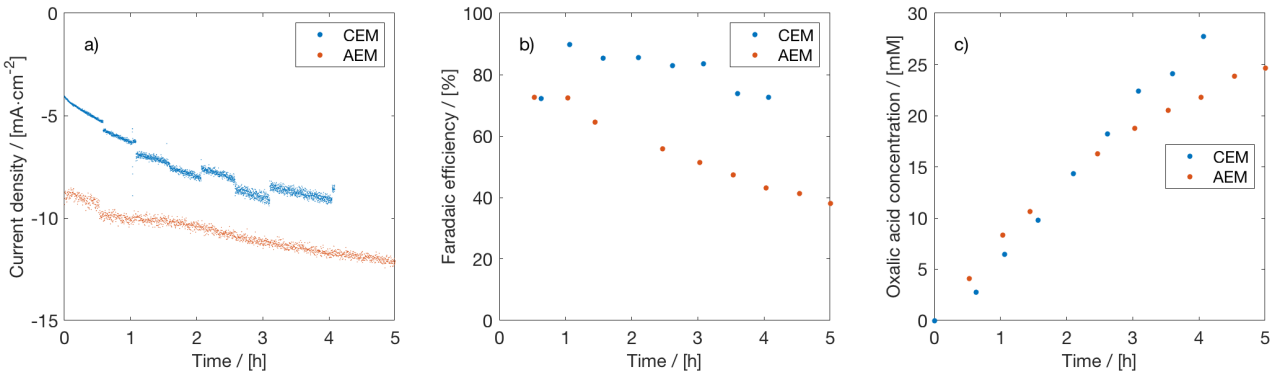

Figure 4.17: Comparison of a) Current density, b) faradaic efficiency of oxalic acid formed and c) concentration of oxalic acid produced during electrochemical reduction of CO_2 using Pb as cathode in a 0.7M TEACl in propylene carbonate solution at different applied voltages (vs. Ag/AgCl) as a function of time. The anodic part of the reactor consisted of a Pt anode in 0.5M H_2SO_4. Both compartments were separated with a Nafion 117 cation exchange membrane (blue) or with Fumasep anion exchange mebrane (red).

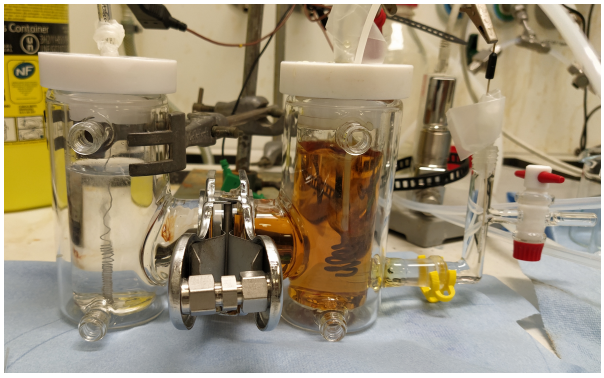

Figure 4.18: Appearence of the experimental set-up after application of -2.5V vs. Ag/AgCl for 5 hours with lead as cathode, platinum as anode, 0.5M H_2SO_4 as anolyte and PC + 0.3M Bmim-Otf as catholyte. The catholyte has turned from transparent to orange/brown, which implies decomposition of the catholyte.

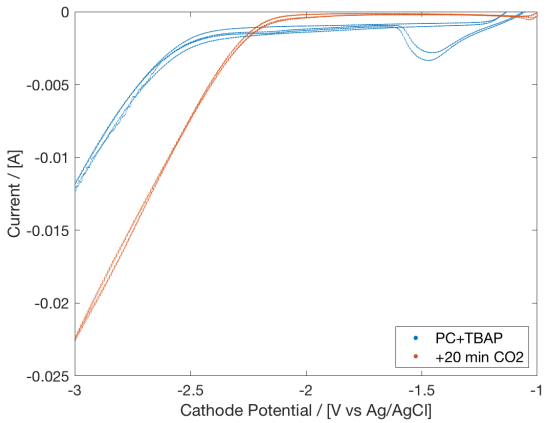

Figure 4.19: Cyclic voltammogram obtained after cyclic voltammetry experiment in one-compartment cell with a Pb electrode in a 0.3M TBAP in PC solution in the absence of CO_2 (blue line) and in the presence of CO_2 after 20 minutes of bubbling (red line).

of application of -2.5V vs. Ag/AgCl for 5 hours with lead as cathode, platinum as anode, 0.5M H_2SO_4 as anolyte and PC + 0.3M Bmim-Otf as catholyte. There was no production of oxalic acid during the experiment.Therefore, no further studies were carried out using Bmim-Otf as supporting electrolyte.

Tetrabutylammonium perchlorate (TBAP) is another salt that has been tested at concentrations of 0.3M in PC with a conductivity of 4.3 mS/cm. Figure 4.19 shows cyclic voltammetry (CV) experiments with this catholyte. When CV experiments with TBAP as supporting electrolyte are compared with CV experiments with TEACl (Figure 4.2), it is remarkable that the obtained current densities are lower, what is caused by the relative low conductivity. Electrochemical reduction of CO_2 has been performed with TBAP as supporting electrolyte. Figure 4.20a shows that the current density decreases from -2 mA/cm^2 to -3mA/cm^2 over the time period of the experiment. As shown in Figure 4.20b, there is no formation of glycolic acid and glyoxylic acid. The faradaic efficiency to oxalic acid decreases over the time of the experiment from 74% to 45%. The concentration of oxalic acid at the end of the experiment is 7mM.

Also, tetraethylammonium acetate (TEAAce) has been tested as electrolyte salt at concentrations of 0.5M TEAAce. The solution of 0.5M TEAAce in propylene carbonate has a conductivity of 3.6 mS/cm. Figure 4.21 gives the current density, faradaic efficiency of the liquid products formed and the concentration of the oxalic acid produced during electrochemical reduction of CO_2 with propylene carbonate with 0.5M TEAAce as catholyte. Figure 4.21a shows that the current density is between -1 and -2 mA/cm^2 during the whole experiment. Figure 4.21b shows that the faradaic efficiency at the start of the experiment is 64% and reduces to 42%. There is no formation of glyoxylic acid, and very small formation of glycolic acid. It should be noted that the current density and therefore the oxalic acid concentration is low, which could be the reason that there is no further reduction of oxalic acid to glycolic and glyoxylic acid. It could also be that the supporting electrolyte

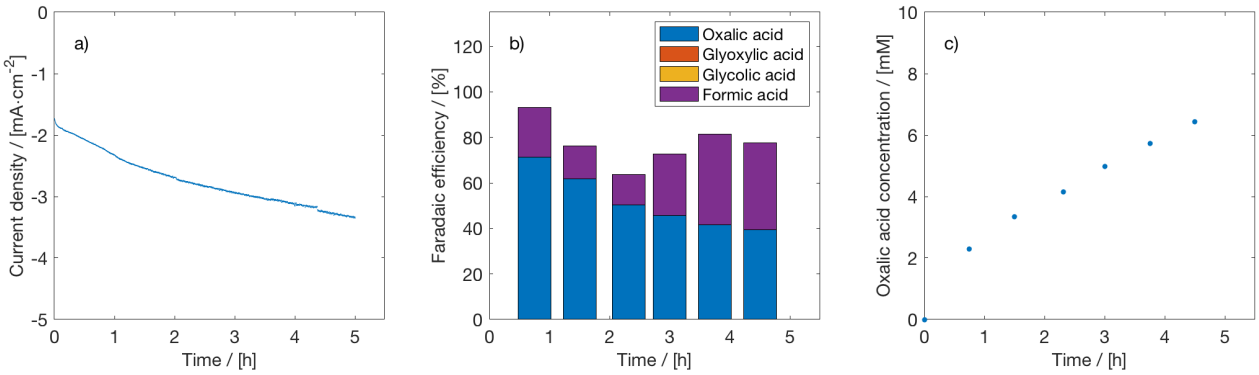

Figure 4.20: a) Current density, b) faradaic efficiency of liquid products formed and c) concentration of oxalic acid produced during electrochemical reduction of CO_2 using Pb as cathode in a 0.3M TBAP in PC solution at -2.6V vs Ag/AgCl as a function of time. The anodic part of the reactor consisted of a Pt anode in 0.5M H_2SO_4. Both compartments were separated with a cation exchange membrane (Nafion 117).

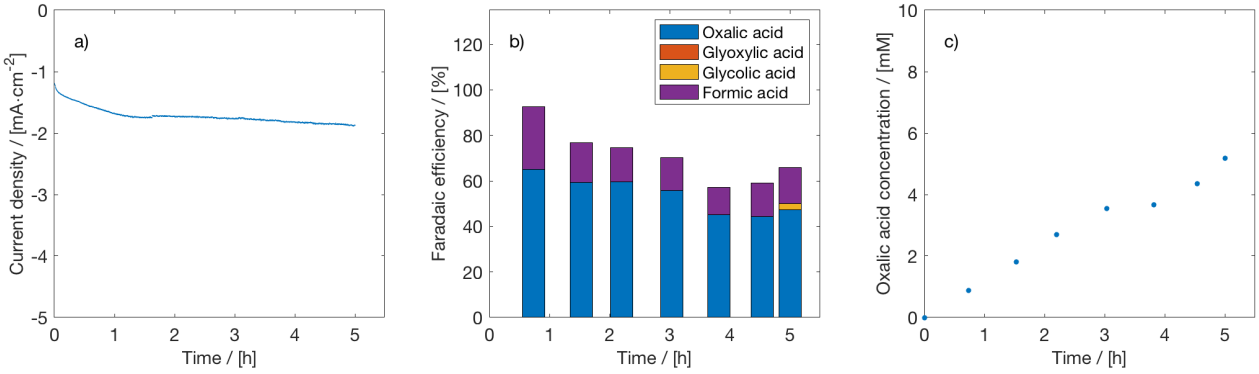

Figure 4.21: a) Current density, b) faradaic efficiency of liquid products formed and c) concentration of oxalic acid produced during electrochemical reduction of CO_2 using Pb as cathode in a 0.5M TEAAce in propylene carbonate at -2.4V vs Ag/AgCl as a function of time. The anodic part of the reactor consisted of a Pt anode in 0.5M H_2SO_4. Both compartments were separated with a cation exchange membrane (Nafion 117).

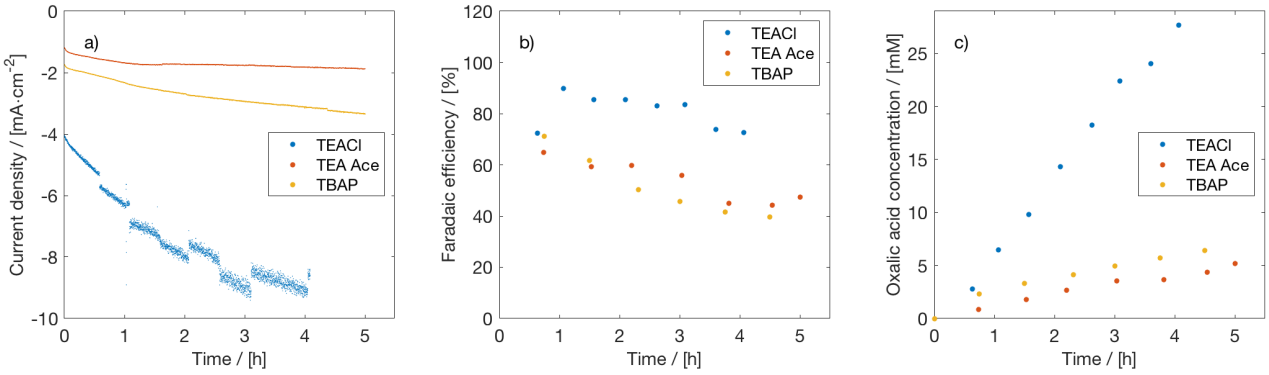

Figure 4.22: Comparison of a) Current density, b) faradaic efficiency of oxalic acid formed and c) concentration of oxalic acid produced during electrochemical reduction of CO_2 using Pb as cathode at -2.5V vs Ag/AgCl as a function of time. The catholyte used was 0.7M TEACl, 0.3M TBAP or 0.5M TEAAce in propylene carbonate. The anodic part of the reactor consisted of a Pt anode in 0.5M H_2SO_4. Both compartments were separated with a Nafion 117 cation exchange membrane.

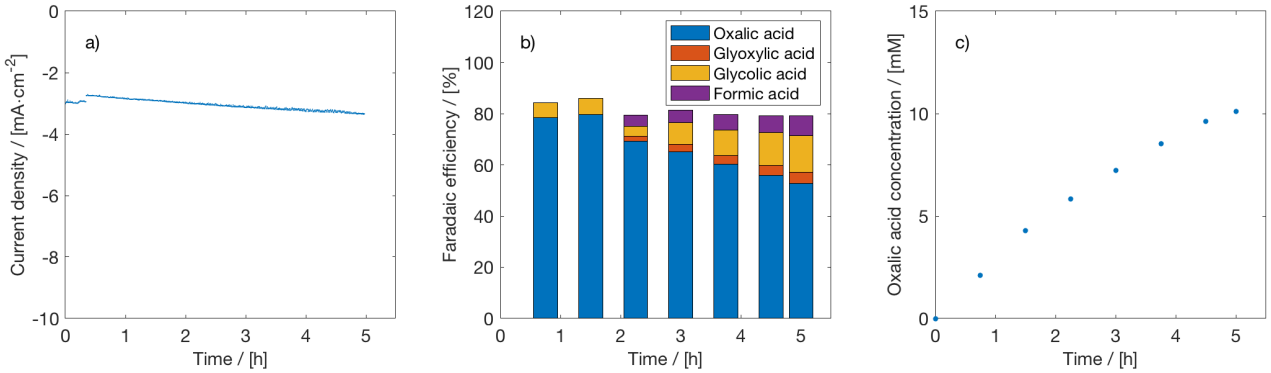

Figure 4.23: a) Current density, b) faradaic efficiency of liquid products formed and c) concentration of oxalic acid produced during electrochemical reduction of CO_2 using Pb as cathode in a 0.7M TEACl in propylene carbonate at -2.5V vs Ag/AgCl at 15 °C as a function of time. The anodic part of the reactor consisted of a Pt anode in 0.5M H_2SO_4. Both compartments were separated with a cation exchange membrane (Nafion 117).

salt influences the selectivity of the electrochemical CO_2 reduction. As shown in Figure 4.21c, the oxalic acid concentration at the end of the experiment is 5 mM. Figure 4.22 compares electrochemical reduction of CO_2 using TEACl, TBAP and TEAAce in terms of current density (a), faradaic efficiency (b) and obtained oxalic acid concentration (c). It is shown that both the current densities obtained as the faradaic efficiencies with both TBAP and TEAAce are remarkably lower than the current density obtained with TEACl. Also, the obtained oxalic acid concentration is lower using both TEAAce and TBAP, compared to TEACl. It should be noted that the solvent conductivity of 0.3M TBAP and 0.5 TEAAce in PC was lower than 0.7M TEACl, which stands in the way of a fair comparison. With larger concentrations of TBAP and TEAAce, similar conductivity could be obtained. This low current densities imply less electron transport and thus less electrochemical CO_2 reduction to oxalic acid. Therefore, lower concentrations of oxalic acid in the catholyte have been achieved during the experiments conducted with TBAP and TEAAce than during the experiment conducted with TEACl. The disadvantage of using TEACl is the formation of hydrochloric acid when the salt comes in contact with water. Hyrochloric acid is very corrosive and cannot be used in stainless steel reactors, which is a problem with an eye on potential scale-up.

Influence of temperature

The influence of temperature on the electrochemical reduction of CO_2 to oxalic acid has been examined. The temperature of the catholyte can both influence the current densities obtained as well as the faradaic efficiency. Figure 4.23, 4.24 and 4.25 show the current density, faradaic efficiency and oxalic acid concentrations obtained of experiments performed at 15 °C, 55 °C and 75°C respectively. In figure 4.23a) is shown that the maximum current density obtained at a temperature of 15°C is -3 mA/cm^2. In figure 4.23b) is shown that at the end of the experiment the faradaic efficiency towards oxalic acid is 60%. The obtained oxalic acid concentration was 10 mM, as shown in 4.23c. In figure 4.24a) is shown that the maximum current density obtained at a temperature of 55°C is -11 mA/cm^2. In figure 4.24b is shown that at the end of the experiment the faradaic efficiency towards oxalic acid is 60%. The obtained oxalic acid concentration was 34 mM, as shown in 4.24c. In figure 4.25a) is shown that the maximum current density obtained at a temperature of 75°C is -10 mA/cm^2. In figure 4.25b) is shown that at the end of the experiment the faradaic efficiency towards oxalic acid is 60%. The obtained oxalic acid concentration was 33 mM, as shown in 4.25c. In Figure 4.26 compares the experiments performed at 15 °C, 55 °C and 75 °C. Figure 4.26a shows that remarkable higher currents are obtained at both 55 and 75 °C. The currents obtained at 55 and 75 °C are similar. Figure 4.26b shows that similar faradaic efficiencies are obtained at different temperatures, from 80% faradaic efficiency at the start of the experiment towards 60% faradaic efficiency at the end of the experiment. It follows that at 55 °C and at 75 °C larger oxalic acid concentrations are obtained, which is shown in figure 4.26c.

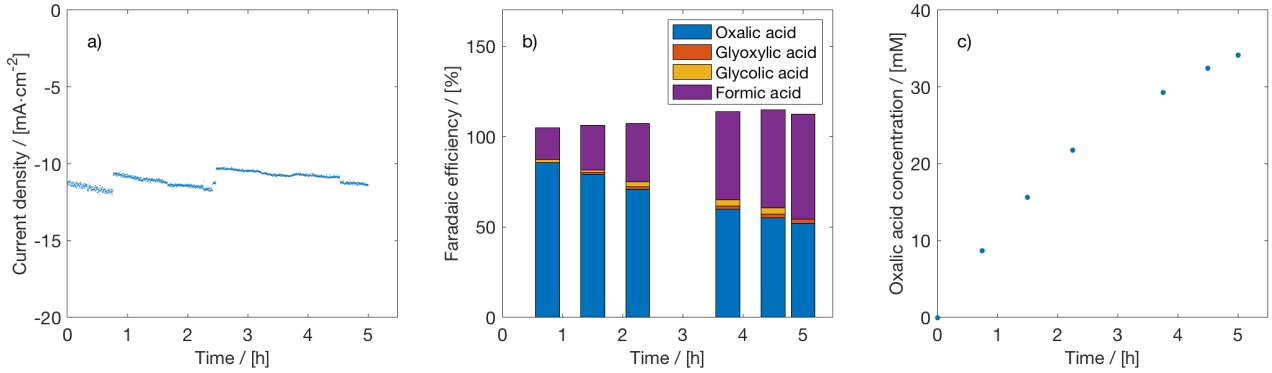

Figure 4.24: a) Current density, b) faradaic efficiency of liquid products formed and c) concentration of oxalic acid produced during electrochemical reduction of CO_2 using Pb as cathode in a 0.7M TEACl in propylene carbonate at -2.5V vs Ag/AgCl at 55 °C as a function of time. The anodic part of the reactor consisted of a Pt anode in 0.5M H_2SO_4. Both compartments were separated with a cation exchange membrane (Nafion 117).

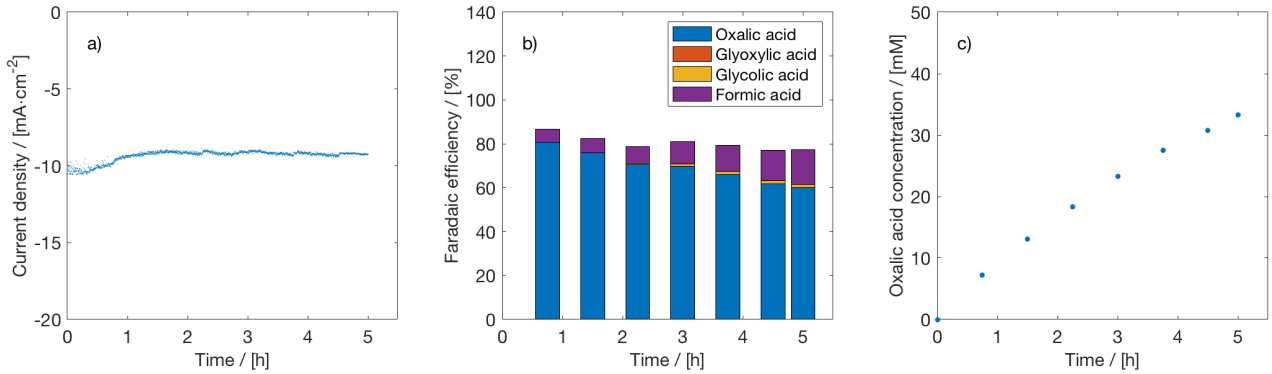

Figure 4.25: a) Current density, b) faradaic efficiency of liquid products formed and c) concentration of oxalic acid produced during electrochemical reduction of CO_2 using Pb as cathode in a 0.7M TEACl in propylene carbonate at -2.5V vs Ag/AgCl at 75 °C as a function of time. The anodic part of the reactor consisted of a Pt anode in 0.5M H_2SO_4. Both compartments were separated with a cation exchange membrane (Nafion 117).

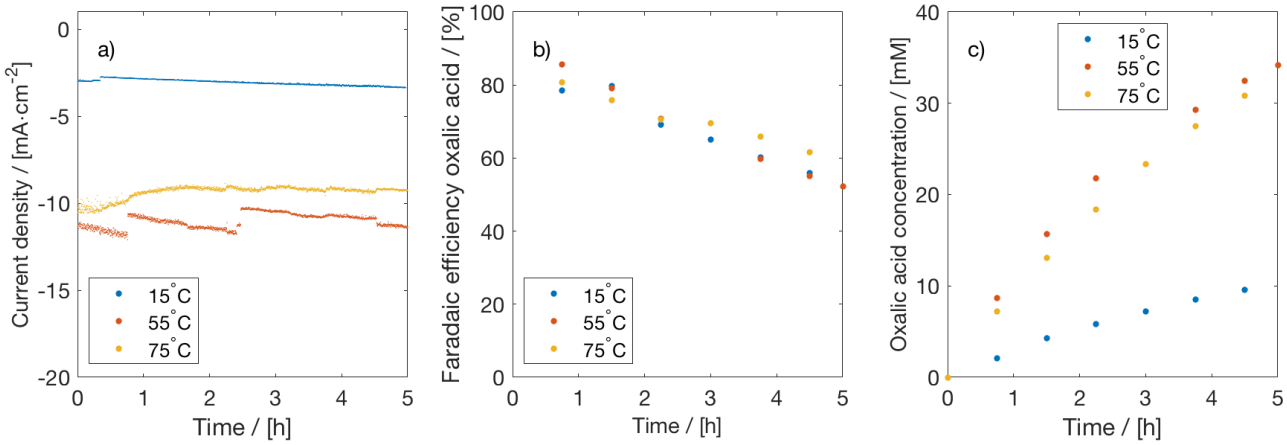

Figure 4.26: Comparison of a) Current density, b) faradaic efficiency of oxalic acid formed and c) concentration of oxalic acid produced during electrochemical reduction of CO_2 using Pb as cathode in a 0.7M TEACl in propylene carbonate solution at -2.5V vs. Ag/AgCl as a function of time. The anodic part of the reactor consisted of a Pt anode in 0.5M H_2SO_4. Both compartments were separated with a cation exchange membrane (Nafion 117). The temperature of the cathode compartment is 15 °C (blue), 55 °C (red) or 75 °C (yellow).

4.1.2. Electroreduction of CO_2 in Flow-Cell type reactor

Based on the results of the H-Cell experiments, the preferred conditions have been tested in the flow-cell set-up. A flow-cell is a (semi-)continuous set-up, in which the reactants are continuously fed to the electrode. This leads to higher reactant availability at the electrode, which reduces the mass transfer limitations. Because the reaction is less mass-transfer limited, the current density and the production should increase. The flow-cell has been tested with the following set-up with Pb as cathode, PC+0.7M TEACl as catholyte, Pt as anode and 0.5M H_2SO_4 as anolyte. The catholyte and anolyte are pumped through at a flowrate of 3.6 L/h/cm^2. In Figure 4.27b is shown that for the experiments performed with an applied potential of -2.3V vs. Ag/AgCl, the faradaic efficiency to oxalic acid at the start of the experiment is on average 75%, which drops over time to 45%. For the three different experiments performed, different current densities are found (Figure 4.27a), while the oxalic acid concentrations obtained are similar (Figure 4.27c). Figure 4.28b shows that the faradaic efficiency to oxalic acid at the start of the experiment is on average 60%, which drops over time to 30%. For the different experiments, the current density is at the start of the experiment -5 mA/cm^2 and increases over time, as shown in Figure 4.28a). In Figure 4.28c is shown that the oxalic acid concentrations obtained in the two different experiments are similar.

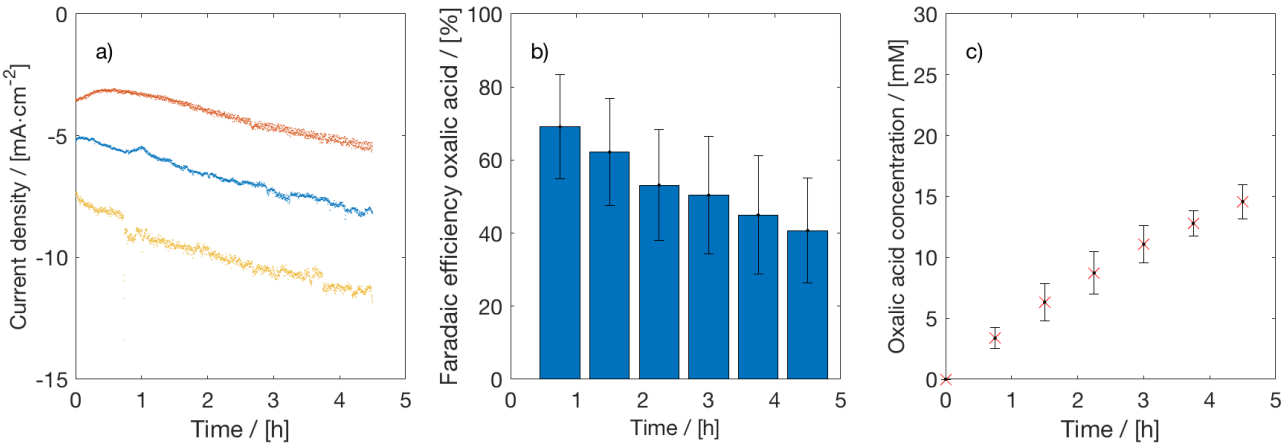

Figure 4.27: a) Current density of three duplicated experiments, b) average oxalic acid faradaic efficiency and c) average concentration of oxalic acid produced during electrochemical reduction of CO_2 using Pb as cathode in a 0.7M TEACl in propylene carbonate at -2.3V vs Ag/AgCl as a function of time. The anodic part of the reactor consisted on a Pt anode in 0.5M H_2SO_4. Both compartments were separated with a cation exchange membrane (Nafion 117). The catholyte and anolyte are pumped through at 3.6 L/h/cm^2.

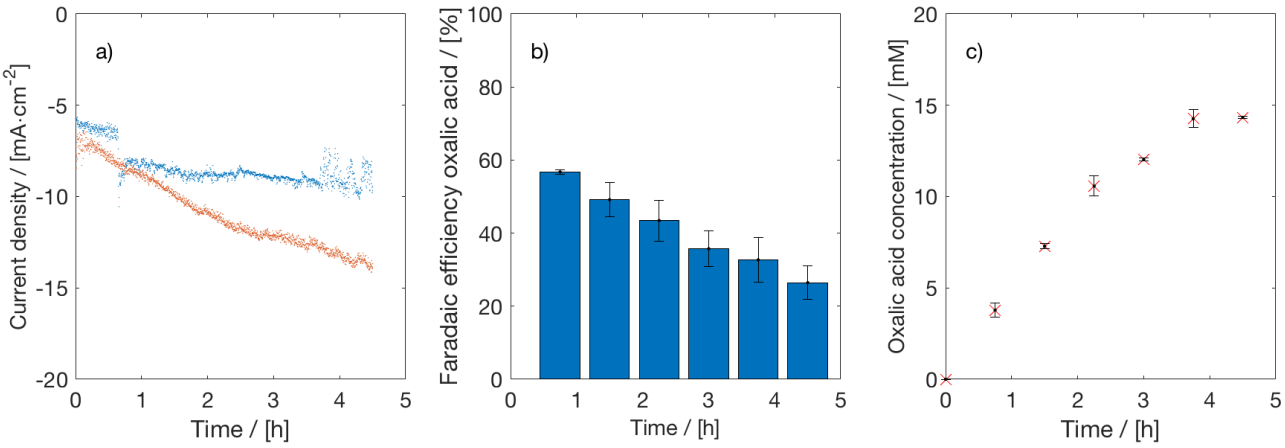

Figure 4.28: a) Current density of two duplicated experiments, b) average oxalic acid faradaic efficiency and c) average concentration of oxalic acid produced during electrochemical reduction of CO_2 using Pb as cathode in a 0.7M TEACl in propylene carbonate at -2.5V vs Ag/AgCl as a function of time. The anodic part of the reactor consisted on a Pt anode in 0.5M H_2SO_4. Both compartments were separated with a cation exchange membrane (Nafion 117). The catholyte and anolyte are pumped through at 3.6 L/h/cm^2.

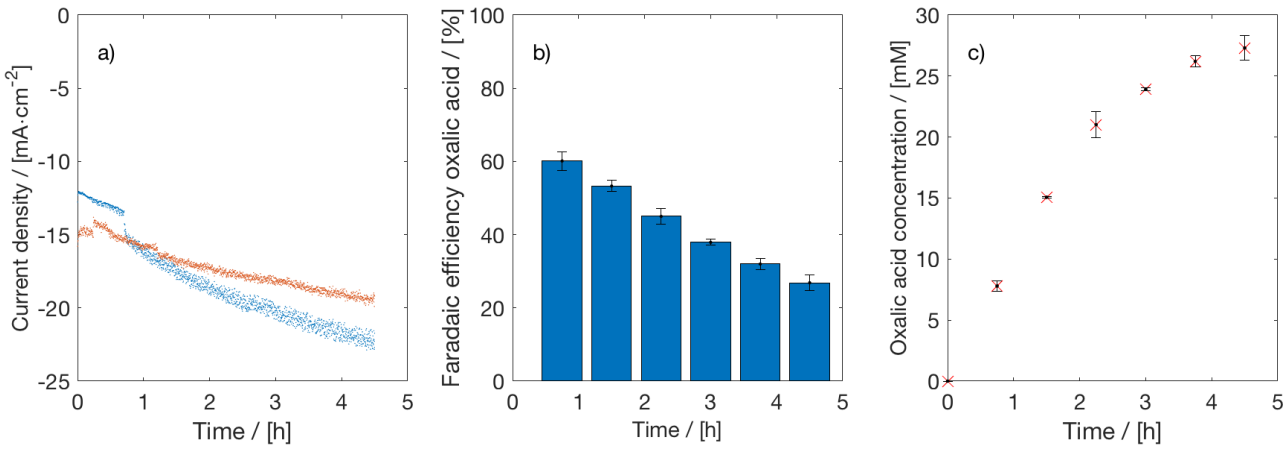

Figure 4.29: a) Current density of two duplicated experiments, b) average oxalic acid faradaic efficiency and c) average concentration of oxalic acid produced during electrochemical reduction of CO_2 using Pb as cathode in a 0.7M TEACl in propylene carbonate at -2.7V vs Ag/AgCl as a function of time. The anodic part of the reactor consisted of a Pt anode in 0.5M H_2SO_4. Both compartments were separated with a cation exchange membrane (Nafion 117). The catholyte and anolyte are pumped through at 3.6 L/h/cm^2.

In Figure 4.29b is shown that the faradaic efficiency to oxalic acid at the start of the experiment is on average 60%, which drops over time to 30%. For the different experiments, the current density is at the start of the experiment -12 mA/cm^2 and increases over time to -20 mA/cm^2, as shown in Figure 4.29c. In figure 4.29 the average oxalic acid concentration of the two experiments is shown, with small standard deviation values, so the concentrations obtained in the two different experiments are similar. It is remarkable that the standard deviations found for the faradaic efficiencies and current densities obtained with the experiments performed at -2.7V vs. Ag/AgCl are much smaller than the experiments performed at -2.3V and -2.5V vs. Ag/AgCl. The main reason for this seems to be that similar values for current densities are found in both experiments. It is proposed that the most probable reason for the large variations found in current densities of the same experiment is the large variations found in the water content of the catholyte. Figure 4.30 shows the mean water content per experiment with the standard deviation. The large standard deviation in water content of the experiments at -2.3V and -2.5V vs. Ag/AgCl corresponds with the high standard deviation for faradaic efficiencies seen in figure 4.27 and 4.28. The small standard deviation values of the water content at -2.7V vs. Ag/AgCl corresponds also with the small deviations for the faradaic efficiencies at -2.7V vs. Ag/AgCl. As soon as there are water molecules present, the production of formic acid is in favor as well as the hydrogen evolution reaction. Therefore, the larger amount of water reduces the selectivity and faradaic efficiency to oxalic acid. It is remarkable to see that the oxalic acid production, shown in the obtained oxalic acid concentrations, stays relatively constant and is not necessarily influenced by the water content.

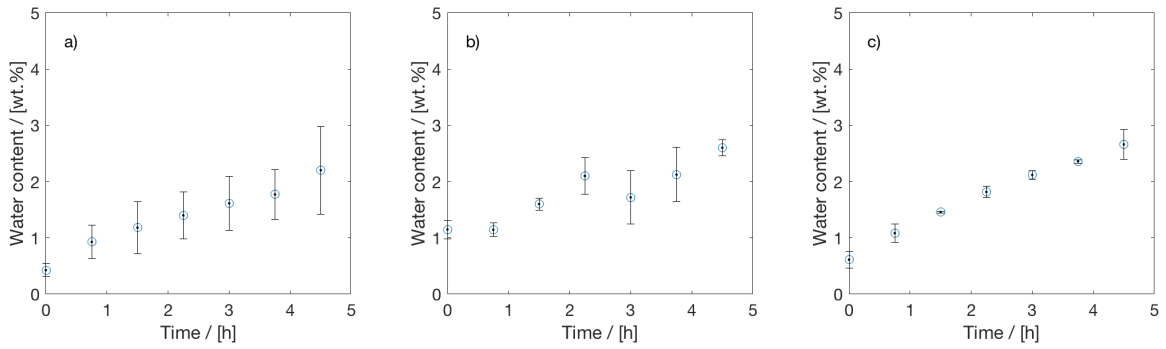

Figure 4.30: The avarage water content with the standard deviations for the flow-cell experiments performed at a) -2.3V, b) -2.5V and c) -2.7V vs. Ag/AgCl. This figure relates the large variations between the experiments with the large variations in water content. For the experiments performed at -2.7V vs. Ag/AgCl, small deviations in terms of current density, faradaic efficiency and obtained oxalic acid concentrations are perceived, as seen in figure 4.29 as well as small deviations in the water content as seen in figure c. The large deviations in terms of current density, faradaic efficiency and obtained oxalic acid concentrations for the experiments performed at -2.3V and -2.5V vs. Ag/AgCl relate to the large deviations in water content as seen in figure a and b.

The flow-cell set-up has also been tested with tetrabutylammonium perchlorate as supporting electrolyte. Figure 4.31 gives the current density (a), faradaic efficiency (b) and oxalic acid concentration (c) obtained of three experiments performed with the same experimental settings. Again, large variations in the current densities, but also in the faradaic efficiency and concentrations obtained were found. In figure 4.31d, the water content in the catholyte has been shown for the different experiments. The experiment with the lowest observed water content has (red) is also the experiment where the highest faradaic efficiency is observed and the lowest current density. The experiment with the highest observed water content (yellow) is also the experiment with the lowest observed faradaic efficiency.

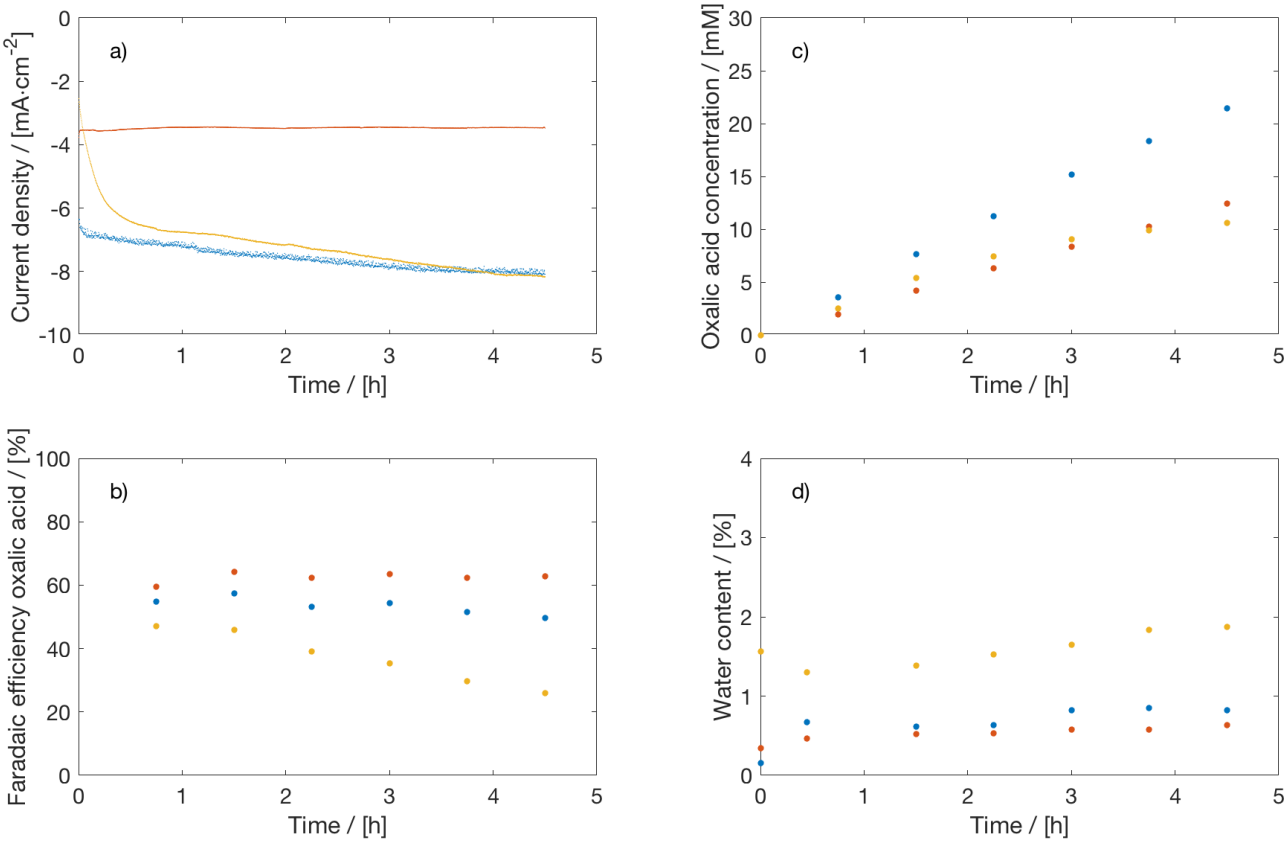

Figure 4.31: a) Current density, b) oxalic acid faradaic efficiency, c) concentration of oxalic acid produced d) and water content of the catholyte of of three duplicated experiments where the electrochemical reduction of CO_2 using Pb as cathode in a 0.3M TBAP in propylene carbonate at -2.7V vs Ag/AgCl as a function of time for three duplicated experiments. The anodic part of the reactor consisted of a Pt anode in 0.5M H_2SO_4. Both compartments were separated with a cation exchange membrane (Nafion 117). The catholyte and anolyte are pumped through at 3.6 L/h/cm^2.

4.1.3. Electroreduction of CO_2 in High-pressure set-up

The electrochemical reduction of CO_2 has been performed in a flow-cell under high-pressure. A 0.7M TBAP in propylene carbonate solution with a conductivity of 6.0 mS/cm has been used as catholyte. 0.5M H_2SO_4 has been used as anolyte. Pb and Pt plates have been used as respectively the cathode and anode. A Nafion 117 membrane is used to separate the compartments. A potential of 4.5V has been applied between the anode and the cathode. Figure 4.32a) shows the current density obtained during the performed experiment, which is higher than the obtained current densities in the normal flow-cell experiments, namely 23 mA/cm^{c}ompared to maximum 8 mA/cm^2 as shown in figure 4.31. Figure 4.32b) shows the faradaic efficiencies to oxalic acid, formic acid, hydrogen and carbon monoxide during the performed experiment. It is clear that mainly formic acid is formed. As shown in figure 4.32 was the water content at the start of the experiment 4% and increased over time to 6%.

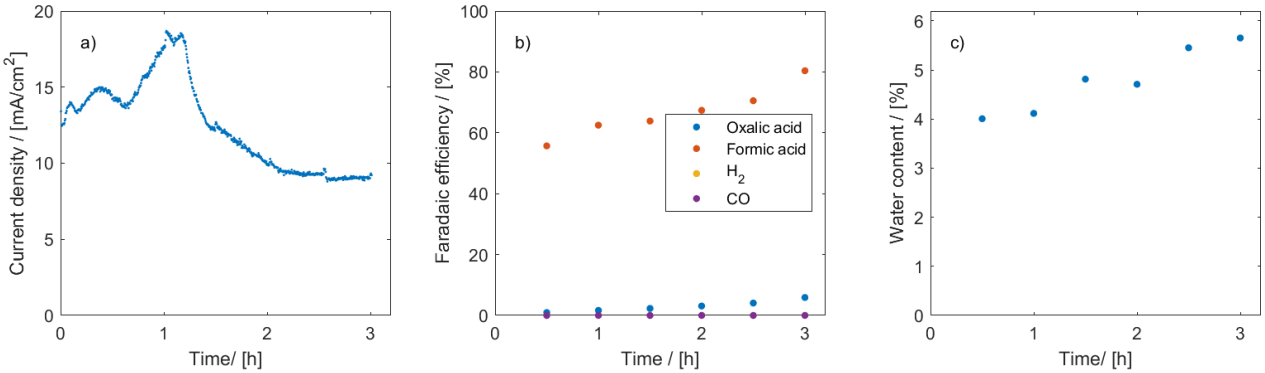

Figure 4.32: a) Current density, b) faradaic efficiency to both liquid and gaseous products and c) the water content in the catholyte during the electrochemical reduction of CO_2 under high-pressure. Pb was used as cathode in a 0.7M TBAP in propylene carbonate. The anodic part of the reactor consisted of a Pt anode in 0.5M H_2SO_4. Both compartments were separated with a cation exchange membrane (Nafion 117). The anolytic and catholytic flowrate was 0.11 L/h/cm^2.

4.1.4. Summary and General remarks

In this chapter, the electrochemical conversion from CO_2 to oxalic acid has been performed under many different circumstances in the H-cell set-up, flow-cell set-up and in a high-pressure flow-cell set-up.The H-cell experiments have been used to screen for optimal conditions. Based on the results of the H-cell experiments, the configuration of Pb as cathode, PC+0.7M TEACl as catholyte, Pt as anode and 0.5M H_2SO_4 in which the anodic and cathodic compartment are separated by a cation-exchange membrane has been selected. With this configuration, flow-cell experiments and high-pressure experiments have been performed. There are some general remarks that should be taken into account with regard to the electrochemical conversion experiments, which will be further discussed.

Gaseous and other liquid products

It has been shown that during none of the experiments, 100% faradaic efficiency has been achieved. This can be explained by the formation of gaseous products, not observed liquid products and the decomposition of the catholyte. During the H-Cell and Flow-Cell experiments, the gaseous products have not been measured. The only experiment where an analysis of the gaseous products is done was by the high-pressure experiment. The high-pressure experiment showed that there was some formation of H_2 and CO, but very small amounts, making the contribution to the faradaic efficiency negligible. Ofcourse, this can not be concluded for all the performed experiments, but it is not expected that in the other experiments there was large production of H_2 and CO. Figure 4.33 shows an HPLC chromatogram of a sample taken at the end of an electrochemical reduction of CO_2 experiment. The peaks identified by a blue arrow are the peaks that were also found in the

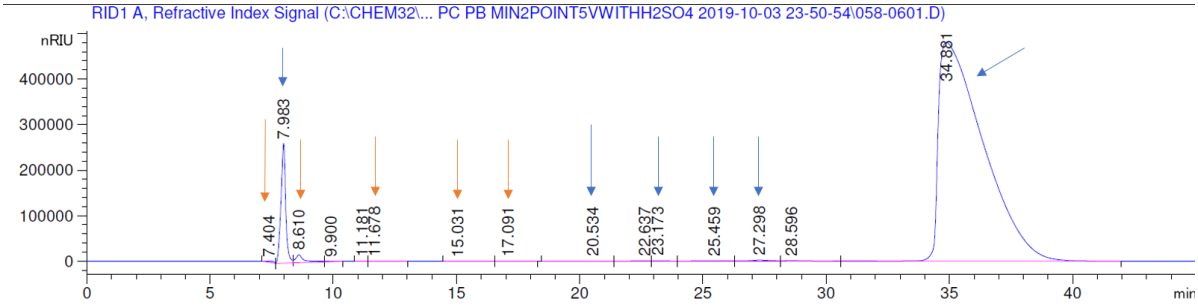

Figure 4.33: The HPLC chromatogram of a sample taken at the end of an electrochemical reduction of CO_2 experiment performed in the H-Cell with Pb as cathode, PC+0.7M TEACl as catholyte, Pt as anode and 0.5M H_2SO_4 as anolyte. The chromatogram has been compared with the chromatogram of a sample taken at the start of the start of the experiment. The matching peaks are indicated by blue arrows. For several carboxylic acids a calibration has been done, which finds retention time of oxalic acid (8.5 min), glyoxylic acid (11.8 min), glycolic acid (15 min) and formic acid (17 min). The peaks of the carboxylic acids are indicated by the orange arrows. The peaks at 9.9, 11.1, 22.6 and 28.6 remain unidentified, but could be products of the electrochemical reduction of CO_2 or the catholyte, as well as the chemical decomposition of the catholyte.

blank, a sample taken at the start of the experiment. The peaks identified by an orange arrow are carboxylic acids that are products of the electrochemical reduction of CO_2. It should be noted that there are unidentified peaks left and therefore potential unidentified liquid products of the electrochemical CO_2 reduction.

Faradaic efficiency over time

It is clear from the experiments performed both in the H-Cell and the flow-cell that the faradaic efficiency decreases over time. This could be explained by contamination of the electrode during the experiment. Before the start of the experiment, the lead electrode is electrochemically polished in 0.5M H_2SO_4. During the experiment, the lead could be oxidized or contaminated in a different way. To test the influence of contamination of the lead electrode, an H-Cell experiment has been performed in which the electrode is removed and cleaned after 3 hours. The periodic faradaic efficiency for each sample period is given in figure 4.34. It is shown that the periodic faradaic efficiency to oxalic acid decreases over time and there is no positive influence of cleaning the electrode observed. It is also shown that the periodic faradaic efficiency to formic acid increases over time. Another reason for the decrease in faradaic efficiency over time is the increasing water content over time, which has been seen in different experiments (Figure 4.32c, 4.31d,4.30). Larger water content is related to lower oxalic acid faradaic efficiency and higher formic acid faradaic efficiency. Finally, a reason for decreasing faradaic efficiency could be the further reduction of oxalic acid to glycolic acid and glyoxylic acid, which increases with increasing oxalic acid concentration.

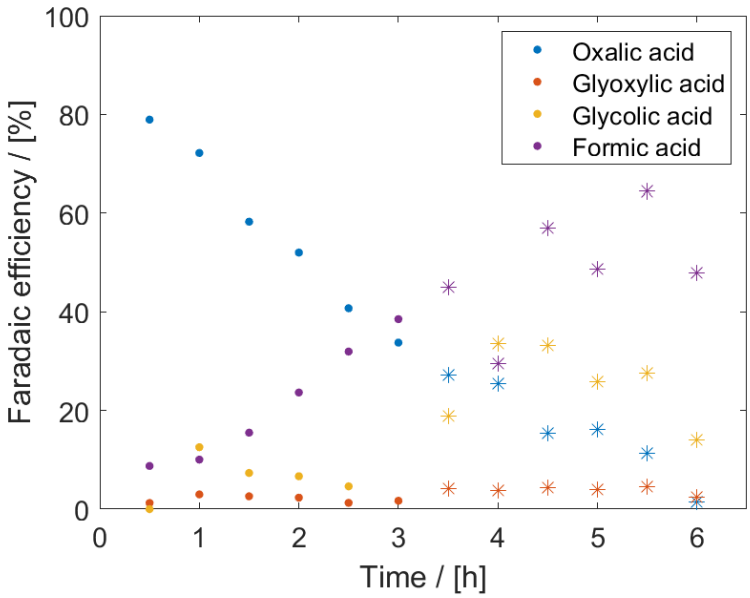

Figure 4.34: Faradaic efficiency to oxalic acid (blue), glyoxylic acid (red), glycolic acid (yellow) and formic acid (purple) before (●) and after (∗) cleaning of the electrode. It is shown that over the time period of the experiment, the faradaic efficiency to oxalic acid decreases. The faradaic efficiency to formic acid, glyoxylic acid and glycolic acid generally increases over the time of the experiment. No influence of cleaning the electrode is perceived.

Formation of oxalic acid/oxalate salts

The entire chapter discussed the formation of oxalic acid, but it should be pointed out that there is no certainty about whether oxalic acid or other oxalate salts are formed. During the electrochemical reduction of CO_2, electrons flow from the anolytic compartment to the cathodic compartment. By the concept of electroneutrality, also positive ions must flow from the anolytic compartment to the cathodic compartment (or negative ions should flow from cathodic to anodic compartment). In most of the experiments a cation-exchange membrane is used, which only allows for transport of positive ions. In most of the experiments, the anolyte consists of 0.5M H_2SO_4, so the only positive ions available in the anode compartment are protons. Therefore, it is expected that with the formation of oxalate, protons are transported through the membrane to the catholyte. In the catholyte, initially only TEA^+ and Cl^- ions are present. The oxalate-ions therefore can combine with protons or TEA^+-ions.

To test if there is transfer of protons to the catholyte, liquid-liquid extraction has been performed with the same volume catholyte as water and the pH is measured. Afterwards, the concentration of oxalate-ions has

been determined. The measured pH was 1.39 and 1.69 in the duplo. The oxalate concentration in water was 20.7 mM, which corresponds to a pH of 1.8 via the Henderson-Hasselbalch equation (equation 4.1). This corresponds quite well with the expected pH for oxalic acid. It should be noted that there were also glycolate-, glyoxalate-, formate- and chlorine-ions in the solution which also influences the pH.

$$pH = pK_a + \log\left(\frac{[A^-]}{[HA]}\right) \tag{4.1}$$

Reproducibility of the experiments

An important note to the results of the H-Cell experiments is that they have not been performed in duplo. Therefore, it is difficult to review the reproducibility and reliability of the results. The decision to not perform them in duplo was because the experiments were mainly conducted as screening, where the qualitative data is more important than the quantitative data. The idea was to find the optimal settings with the H-cell experiments and then achieve reproducible results with the flow-cell set-up, also because the flow-cell set-up is more suitable to reproduce experiments. It has turned out to be difficult to find reproducible results in the flow-cell setup, which has been related to the water content in the catholyte. Other probable differences between the experiment are the contamination and available reaction surface area at the cathode. Further research should focus on finding out where the different results come from and try to narrow the differences between the experiment down.

4.2. Downstream processing experiments

When evaluating a new production method, the separation step that is always needed in chemical processes is important. This section explores several methods for the downstream processing of oxalic acid after production by electrochemical conversion of CO_2. The H-cell and flow-cell experiments give some process parameters to work with. The oxalic acid is formed in a solution of 0.7M TEACl in PC, which means that the oxalic acid needs to be separated from both the PC and the TEACl. Additional requirement is that the PC and TEACl need to be recycled if possible, to keep the production costs as low as possible. Table 4.1 gives an overview of properties related to separation of PC, TEACl and oxalic acid.

The objective of the separation step is to form pure oxalic acid, while the TEACl and PC both are recycled. In this section several potential options for the separation of oxalic acid from the solution are discussed. Until now, maximum concentrations of 40 mM have been achieved. It is expected that by improving the cell design, oxalic acid concentrations in the catholyte of 1M could be achieved. This concentration will be used as value for the separation process design. Industrial separation processes exploit property differences. Properties separations could be based on are density, particle size, volatility, solubility, adsorbability, chemical reaction or melting point. The separation methods explored in this section are vacuum distillation (volatility), crystallization (solubility or melting point), filtration (particle size), precipitation (solubility) and extraction (solubility).

4.2.1. Vacuum distillation

Vacuum distillation is distillation performed under reduced pressure, which reduces the energy requirements for obtaining the boiling point of the desired product. Distillation is a method based on differences in boiling point of the different products. The boiling point of oxalic acid is lower than the boiling point of propylene carbonate and the boiling point of TEACl. Separation based on difference in volatility therefore could be a potential option for the recovery of oxalic acid. A proposed process scheme is found in Figure 4.35. Decomposition of oxalic acid starts at 80 °C [56], while the temperature of sublimation is at 160 °C [57]. Even at reduced pressure, the sublimation only takes place at temperatures higher than 100 °C [58]. Sublimation is only possible at temperatures decomposition will occur, so vacuum distillation is unfavorable for the separation of oxalic acid.

Table 4.1: The chemical formula, molecular weight, boiling point, density and solubility in water of the compounds involved in the to be designed separation process

Properties	**Oxalic acid**	**TEACl**	**PC**
Chemical formula	$H_2C_2O_4$	$C_8H_{20}ClN$	$C_4H_6O_3$
Molecular weight / g/mol	90	165.7	102
Boiling point / °C	160 (subl.)	n.a.	242
Density	1.9	1.08	1.2
Solubility in water at STP / g/L	90-100	very soluble	240

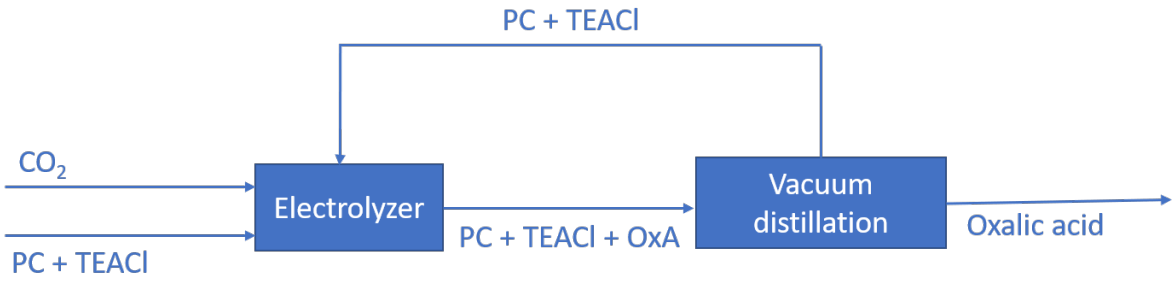

Figure 4.35: Proposed process using vacuum distillation as separation method, with OxA (oxalic acid) as the lowest boiling compound. After leaving the electrolyzer, the catholyte is directly fed into the distillation column. Oxalic acid is the distillate, while PC (propylene carbonate)+TEACl (tetraethylammoniumchloride) are the bottom products and recycled as catholyte.

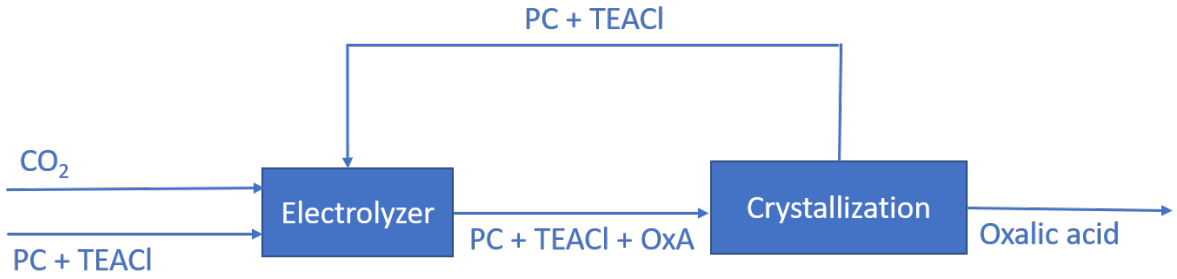

Figure 4.36: Proposed process using crystallization as separation method. After leaving the electrolyzer, the catholyte is directly fed into the crystallizer. OxA (oxalic acid) crystallizes, while PC+TEACl (propylene carbonate + tetraethylammoniumchloride) stay in solution and are recycled as catholyte.

Table 4.2: Experimentally determined solubility limits of oxalic acid in propylene carbonate and in a mixture of propylene carbonate + 0.7M TEACl at 25 °C.

Solvent	**Solubility (g/L)**	**Solubility (M)**
PC	120	1.3
PC + 0.7M TEACl	208	1.9

4.2.2. Crystallization

Crystallization is a seperation method in which the desired product is converted from dissolved state into solid state. It is based on the solubility of the desired product in the solvent. The method proposed is the direct crystallization of oxalic acid, dissolved in propylene carbonate. Crystallization of oxalic acid in organic solvents has been reported in binary solvents of acetone and water and glycerol and water [59]. An extra factor to take into account is the presence of TEACl, which could lead to simultaneous crystallization of TEACl and oxalic acid, after which an extra separation step is needed. The proposed process using crystallization as separation method is shown in Figure 4.36. The solubility limit of oxalic acid in propylene carbonate and in oxalic acid + 0.7M TEACl has experimentally been determined at room temperature, as shown in Table 4.2. The solubility limit is higher than the expected concentration of oxalic acid at the end of the experiment (1M), so the solution needs to be cooled.

It is shown that in presence of TEACl, the solubility limit of oxalic acid is higher. To evaluate the crystallization behaviour of oxalic acid in propylene carbonate, a Crystal16 experiment has been performed. Crystal16 measures the transmission coefficient of samples, while the temperature is varied at different cooling rates. Figure 4.37 shows crystallization behaviour in the samples at several cooling rates. Samples have been prepared with PC and oxalic acid, PC and TEACl and with both TEACl and oxalic acid. It is shown that there is no crystallization behaviour shown between 60 °C and -10 °C. The Crystal16 experimt shows that direct crystallization does not seem to be a potential separation method for the recovery of oxalic acid.

4.2.3. Liquid-liquid extraction

Liquid-liquid extraction is a separation method based on the relative solubility of the desired product in two immiscible solvents. If oxalic acid is more soluble in another solvent than in propylene carbonate, it can be extracted. Water and propylene carbonate form a two-phase system, although they are also partially soluble in eachother. The solubility at room temperature of water in propylene carbonate is 5wt.%, while the solubility of propylene carbonate at room temperature in water is 20 wt.% [60]. The density of water is 1000 kg/m^3, while the density of propylene carbonate is 1200 kg/m^3. The feasibility of liquid-liquid extraction using water as extractant has been tested by measuring the distribution ratio of oxalic acid between water and propylene carbonate.The distribution ratio of TEACl between water and propylene carbonate also has been measured. The experimental procedure was as follows: a liquid-liquid extraction separation funnel with a total size of 1 liter was filled with 500 mL propylene carbonate in which 10 mM oxalic acid and 0.7M TEACl has been dissolved to which the desired amount of water is added. The solution is mixed and settled for 48 hours. Then, the water phase and propylene carbonate phase were separated and the concentration of both TEACl and oxalic acid is measured using HPLC.

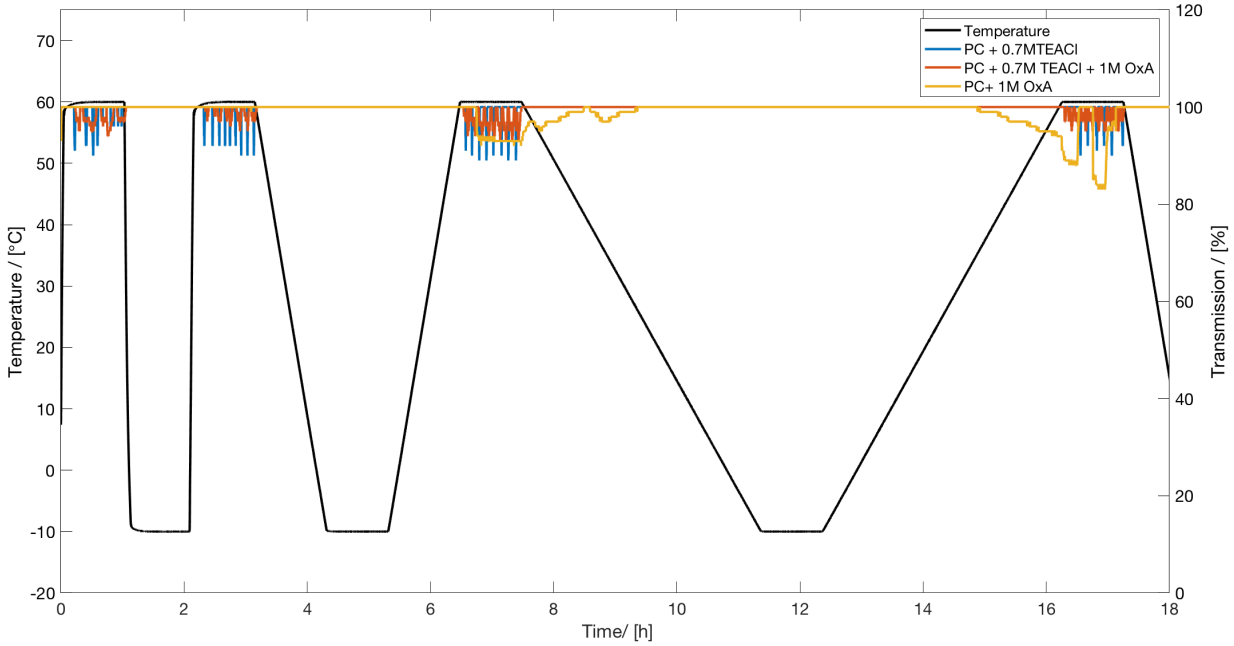

Figure 4.37: Transmission trough samples of PC (propylene carbonate) +1M OxA (oxalic acid), PC+0.7M TEACl (tetraethylammonium-chloride) and PC+1M oxalic and TEACl at different temperatures. Low transmission indicates crystallization. During the whole experiment, except when the temperature was held constant at 75°C, there was no lower transmission than 100% observed so no crystallization behaviour observed. An explanation for the noisy transmission at 75°could be some condensation, which is observed more often in similar experiments. The cooling rates tested are 20°C/min, 1°C/min and 0.3°C/min between 75 °C and -10 °C.

Table 4.3: Determination of the distribution ratio by measuring the oxalic acid (OxA) peak area with UV-HPLC in both the propylene carbonate-phase and water-phase after liquid-liquid extraction at 25 °C.

Ratio water/PC	**OxA in water** UV-HPLC	**OxA in PC** UV-HPLC	$K_{\mathbf{OxA}}$ water/PC
2/5	23930	2489	9.6
5/5	12467	1272	9.8
7/5	8081	864	9.4
Average			9.6

Table 4.4: Determination of the distribution ratio by measuring the TEACl peak area with RID-HPLC in both the propylene carbonate-phase and water-phase after liquid-liquid extraction at 25 °C.

Ratio water/PC	**TEACl in water** RID-HPLC	**TEACl in PC** RID-HPLC	$K_{\mathbf{TEACl}}$ water/PC
2/5	4.37E+06	510309	8.6
5/5	2.18E+06	251286	8.7
7/5	1.45E+06	266908	8.7
Average			8.6

Table 4.3 shows the experimentally determined distribution ratio of oxalic acid. It shows that the concentration of oxalic acid in water is 9.5 times higher than the concentration of oxalic acid in propylene carbonate. Table 4.4 shows the experimentally determined distribution ratio of TEACl. The concentration of TEACl is more than 8.6 times higher in the water phase than in the propylene carbonate phase. This distribution values show that liquid-liquid extraction with water is a suitable method for separation of oxalic acid from propylene carbonate. It is not a suitable method to separate oxalic acid from TEACl. Additional separation steps are necessary to handle the oxalic acid-TEACl-water stream. Two methods are further researched to separate oxalic acid and TEACl: precipitation and crystallization. These methods will be further discussed in

the following sections. The preferred option would be to extract oxalic acid with a solvent in which TEACl is not soluble. The search for a selective solvent should be subject of further research.

Liquid-liquid extraction followed by precipitation

After the liquid-liquid extraction step, there will be a water stream with TEACl and oxalic acid. Calcium oxalate is poorly soluble in water. By addition of a soluble calcium salt, such as $CaCl_2$, the oxalate-ions will precipitate in the form of calcium oxalate. Figure 4.38 gives a compact overview of the proposed process.

A proof-of-concept has been performed to show the possibilities of this process. The experiment is done with a concentration of 0.7M TEACl and 50 mM oxalic acid in propylene carbonate. Liquid-liquid extraction has been performed to extract the oxalic acid from the propylene carbonate. Then, 50mM of calcium chloride has been added, the solution has been mixed and filtrated. As is shown in table 4.5 the concentration of oxalic acid in the solution dropped to 0.5 mM, while the concentration of TEACl remained the same. It is shown that precipitation is a suitable method to separate oxalate-ions from TEACl. This method is not favorable, as calcium oxalate is not valuable. Also, the evaporation step to recover TEACl is expensive.

Liquid-liquid extraction followed by crystallization

Another option for the separation of the waterstream with TEACl and oxalic acid is crystallization. Figure 4.39 gives a compact overview of the proposed process. In literature, crystallization behaviour of oxalic acid in water between 60 to 10 °C with different cooling modes has been described [61]. The proof-of-concept focusses on the occurrence of crystallization in presence of TEACl.

For the proof of concept of crystallization of oxalic acid in presence of TEACl, first the crystallization behaviour of oxalic acid in water and the crystallization behaviour of TEACl in water has been tested with the same temperature program. The starting position of the downstream processing process is a solution of 1M

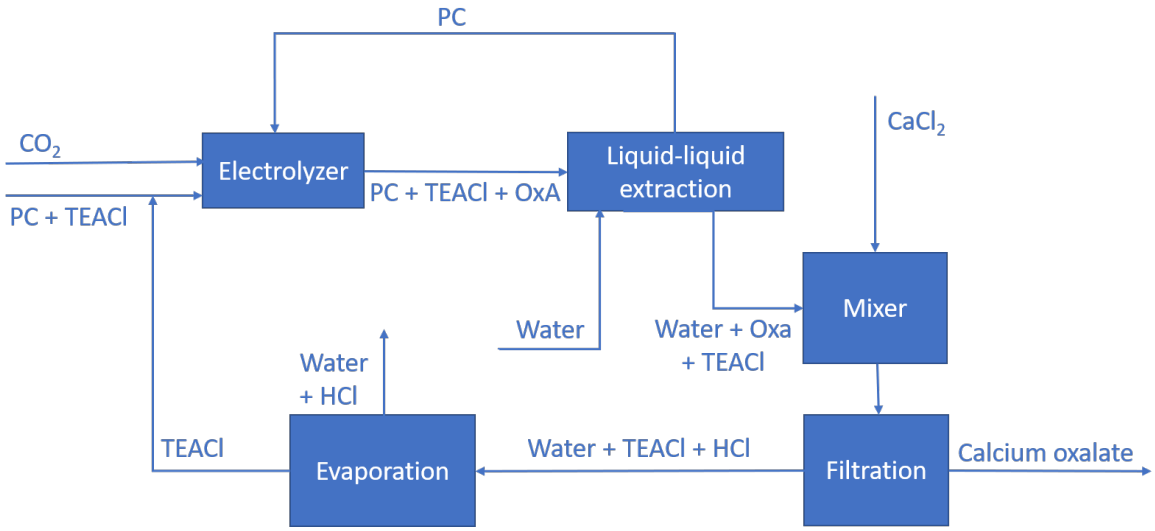

Figure 4.38: Proposed process using liquid-liquid extraction followed by precipitation as separation method. After leaving the electrolyzer, the catholyte is fed into an extraction column in which TEACl and oxalic acid are extracted by water. $CaCl_2$ is added to the extract and calcium oxalate precipitates.

Table 4.5: The concentrations of TEACl and oxalic acid in propylene carbonate, water and water after addition of $CaCl_2$. The concentration of oxalate drops from 34 mM in the water phase to 0.5 mM after addition of $CaCl_2$ due to precipitation of calcium oxalate.

Sample	**[TEACl] / M**	**[Oxalic acid] / mM**
PC + TEACl + OxA	0.7	50
Water phase after liquid-liquid extraction	0.49	34
Water phase after addition $CaCl_2$ and filtration	0.48	0.5

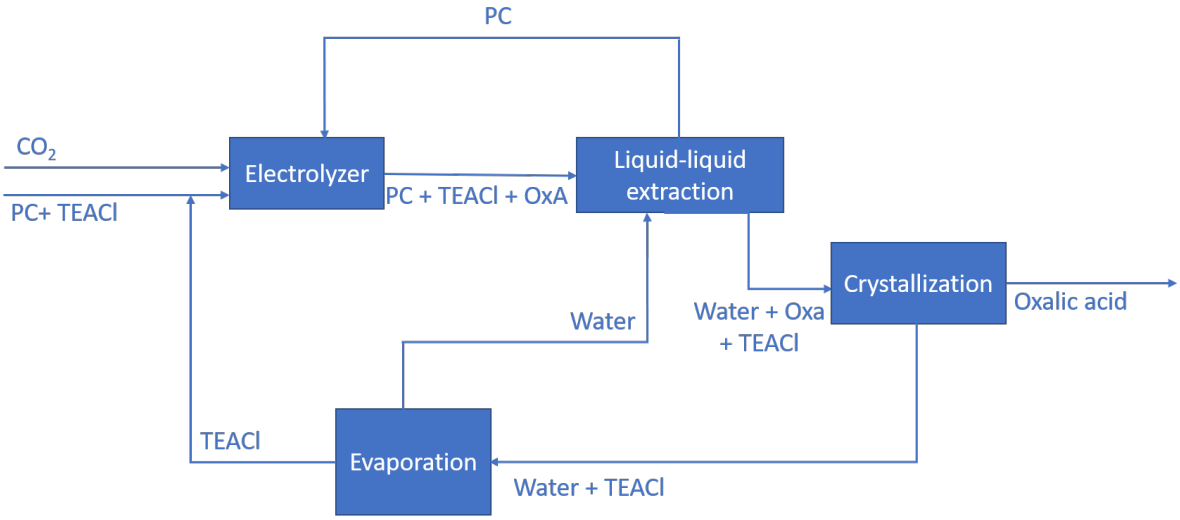

Figure 4.39: Proposed process using liquid-liquid extraction followed by crystallization as separation method. After leaving the electrolyzer, the catholyte is fed into an extraction column in which TEACl and oxalic acid are extracted by water. The oxalic acid is separated from this stream by crystallization, after which TEACl will be separated to be recycled from the water by evaporative crystallization.

Table 4.6: Concentrations of TEACl and oxalic acid in water at the start of crystallization and at the end of the crystallization.

	Solution A	**Solution B**	**Solution C**
Before crystallization	440 g/L OxA	508 g/L TEACl	440 g/L OxA + 508 g/L TEACl
Crystallization behaviour?	Yes	No	Yes
Concentration after crystallization	OxA: 100 g/L	TEACl: 508 g/L	OxA:165 g/L,TEACl:505 g/L

(90 g/L) oxalic acid and 0.7M (116 g/L) TEACl in PC, for this experiment the assumption has been made that both the solutes are fully extracted by the same volume of water, which corresponds to a solution of 0.7M TEACl (116 g/L) and 1M (90 g/L) oxalic acid in water. Crystal16 analysis has been performed to evaluate the crystallization behaviour of oxalic acid and TEACl in water. As is shown in Figure 4.40, there is no reduced transmission when the solution is cooled down up to 2 °C, so there is no crystallization behaviour of neither oxalic acid nor TEACl reported. Further crystallization test will be performed with higher oxalic acid concentrations.

The next step to enhance crystallization behaviour is to perform an experiment with higher concentrations of oxalic acid. For this proof-of-concept experiment, it is chosen to prepare a saturated oxalic acid solution (440 g/L) in water at 60 °C and then slowly cool the solution. In the process design this high concentrations could be achieved by evaporation of the residual water. To achieve the solubility limit of oxalic acid (440g/L) at 60 °C from a solution of 90 g/L, 77.3% of the water should be evaporated. In this case, the concentration of TEACl at the starting point of the crystallization is 508 g/L. For the proof-of-concept, a solution with 440 g/L oxalic acid, a solution with 508 g/L TEACL and a solution with both 440 g/L oxalic acid as 508 g/L TEACl has been prepared. Then, the solution is heated to 60 °C and after this, the solution is slowly cooled until room temperature.

As is shown in table 4.6, the concentration of oxalic acid in the solution decreases due to crystallization, while the concentration of TEACl remained constant. The possibility to crystallize oxalic acid from a solution of water and TEACl has been proven. Further research should focus on the optimization of the crystallization behaviour, based on cooling rate and temperature program. The further separation of water and TEACl can be done by evaporation of water, based on the difference in boiling points of TEACl and water.

4.2.4. Anti-solvent precipitation

A method to separate organic solvents from their solutes is by using supercritical CO_2 as anti-solvent [62]. This could be a potential method for separation of oxalic acid and the organic solvent propylene carbonate. No proof-of-concept has been performed yet. The drawback of this process is that the supporting electrolyte

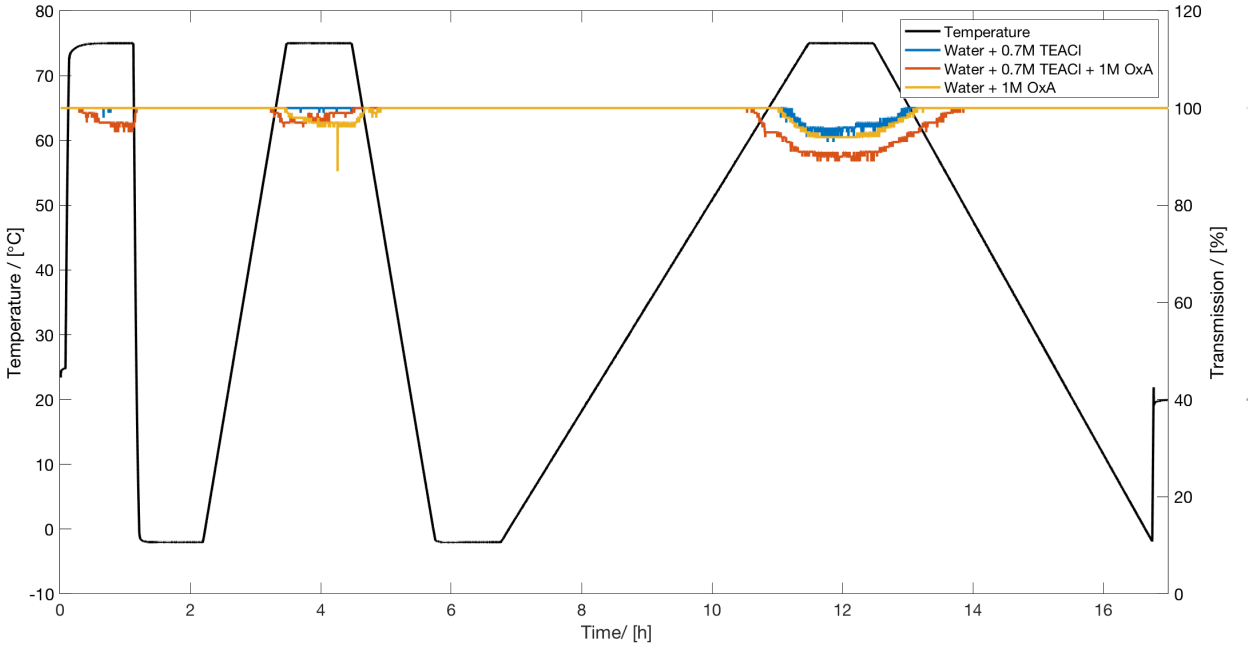

Figure 4.40: Transmission trough samples of water+1M OxA (oxalic acid), water+0.7M TEACl (tetraethylammoniumchloride) and water+1M oxalic and TEACl at different temperatures. Low transmission indicates crystallization. During the whole experiment, except when the temperature was held constant at 75°C, there was no lower transmission than 100% observed so no crystallization behaviour observed. An explanation for the noisy transmission at 75°could be some condensation, which is observed more often in similar experiments. The cooling rates tested are 20°C/min, 1°C/min and 0.3°C/min between 60 °C and -2 °C. No crystallization behaviour at low temperatures is found.

salt (TEACl) also precipitates, so an additional separation step, such as crystallization, is still necessary to separate the oxalic acid and the electrolyte salt. In Figure 4.41 the proposed process, with the anti-solvent precipitation as separation method, is shown.

4.2.5. Direct further reaction in methanol to ethylene glycol

Oxalic acid can be converted to ethylene glycol, which has a larger volume market and a higher market price than oxalic acid. [20, 21, 24]. Ethylene glycol has applications as antifreeze, heat transfer agent and as precursor to polymers. The conversion of oxalic acid to ethylene glycol proceeds via methylation of oxalic acid to dimethyl oxalate in methanol and then further hydrogenation to ethylene glycol, as described in Figure

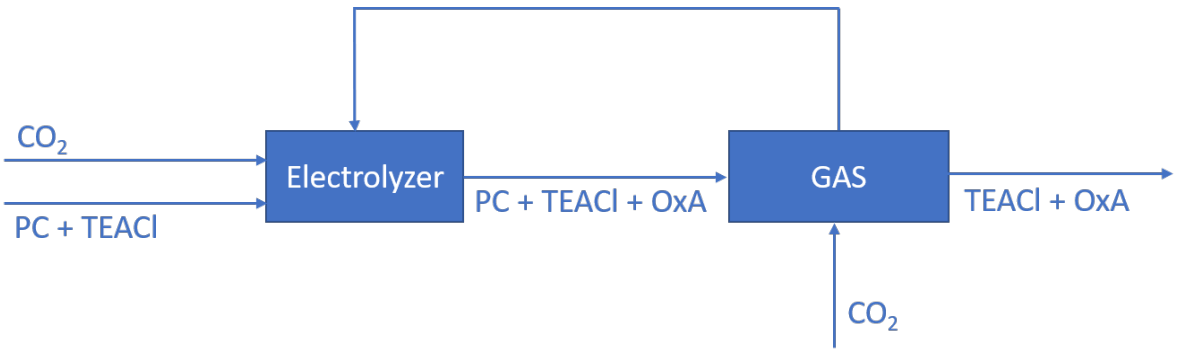

Figure 4.41: Proposed process using Gas AntiSolvent precipitation as separation method. After leaving the electrolyzer, the catholyte pressurized with supercritical CO_2 which causes precipitation of the solvents present in the catholyte. After this an additional separation step is necessary to separate the oxalic acid and TEACl.

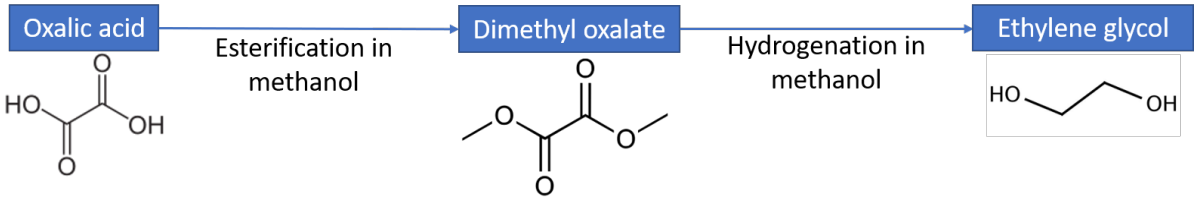

Figure 4.42: Proposed process for direct further conversion to ethylene glycol. For this process, the electrochemical conversion step should be done in methanol.

4.42. If the electrochemical reduction of CO_2 to oxalic acid occurs in methanol, there are no separation steps necessary between the further reactions and the oxalic acid production which would increase the potential of this production process. Therefore, the electrochemical CO_2 reduction in methanol has been performed. The experiment has been performed with a lead cathode, platinum anode, 0.5M H_2SO_4 as anolyte, 0.7M TEACl in methanol as catholyte at -2.5V vs. Ag/AgCl for 3 hours. During the experiment, no formation of oxalic acid has been observed. The direct further reaction in methanol to ethylene glycol is therefore not a possible process design. The further reaction to ethylene glycol is still of high potential, but the oxalic should be separated from the solvent before further reaction is possible.

4.2.6. Summary and general remarks

In this section, several methods for downstream processing of oxalic acid have been explored and proof-of-concepts have been performed for liquid-liquid extraction followed by crystallization and precipitation. Liquid-liquid extraction followed by crystallization is preferred, because the more valuable compound oxalic acid is recovered. It must be emphasized that both of this methods probably are not the most efficient separation methods possible. Nevertheless, it was decided to perform a techno-economic analysis on the process design, to get a view of the potential of electrochemical oxalic acid production.

4.3. Techno-economic analysis

To estimate the economic feasibility of the formation of oxalic acid using the electrochemical reduction of CO_2, a techno-economic analysis has been performed. The process design is based on the results of the electrochemical conversion experiments as well as the proof-of-concepts of the downstream processing. For the downstream processing, liquid-liquid extraction followed by crystallization has been selected as process to be further analyzed in the techno-economic analysis.

The process design will first be discussed separately for every different step: the electrolyzer, the liquid-liquid extraction and the crystallization. For each process step, the CAPEX and OPEX are discussed. After this, the full process design and the economics for oxalic acid production are discussed. A sensitivity analysis is performed to see the influence of different parameters on the production cost of oxalic acid.

The operational costs for oxalic acid production will depend on the price of CO_2 and the price of utilities.The price of CO_2 including the cost of capture using mono-ethanolamine is 70 $/tonne and is expected to fall during the coming years down to 44 $/tonne [63]. An EU-dollar conversion-rate of 0.9 has been used [64]. The same production rate has been chosen as has been used in earlier research, that performed the techno-economic analysis for formic acid production [65]. The CO_2 conversion is based on the assumption that no gaseous byproducts are formed during the reaction, so unlimited recycling of CO_2 is possible. The price of the utilities (steam, cooling water and electricity) are consistent with the currently available industry prices. For some of this parameters, sensitivity analysis will be performed. The economic assumptions are summarized in table 4.7.

4.3.1. Electrolyzer

The electrolyzer unit is the unit where the electrochemical reaction occurs. In Table 4.8 the mass balance of the electrolyzer unit is shown. In Figure 4.43 the process flow diagram of the electrolyzer is given. The anode compartment is included, which serves as both the electron and proton donor of the reduction reaction. The reaction at the anode is the oxygen evolution reaction. The reaction at the cathode is the CO_2 reduction. The anode compartment is further excluded from economical calculations as both the reactant (H_2O) cost as the product (O_2) price is very low. To simplify the process, it is assumed that the only byproduct formed is formic acid. The oxalic acid production rate is 4000 tonne/year, which corresponds to a production rate of 500 kg/h for 8000 hours.

Table 4.7: Economic assumptions for the overall cost of the production process

Parameter	**Base case**
CO_2 capture (€/tonne)	63
Oxalic acid production rate (tonne/year)	4000
CO_2 conversion (-)	1
Electricity price (€/kWh)	0.05
Steam price (€/tonne)	25
Cooling water price (€/m^3)	0.05

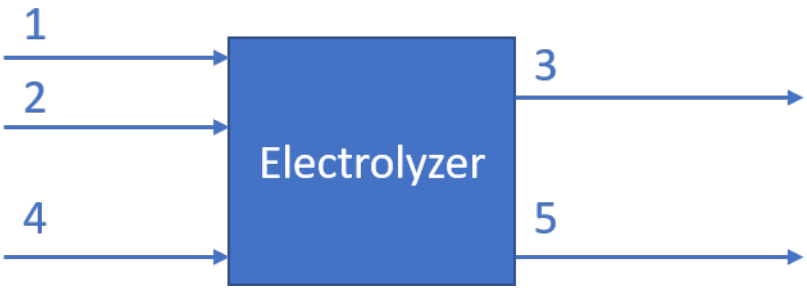

Figure 4.43: Process flow diagram of the electrolyzer unit. The numbers correspond to stream numbers, of which the composition is described by the mass balance of the electrolyzer unit (table 4.8).

Table 4.8: Mass balance of the electrolyzer unit. This includes the cathode compartment where CO_2 is reduced to both oxalic acid and formic acid and the anode compartment where the oxygen evolution reaction takes place. TEACl and propylene carbonate is continuously recycled and because the separation process is not ideal, also oxalic acid is recycled back into the system. The stream numbers correspond to the streams shown in the process flow diagram of Figure 4.43.

	1	**2**	**3**	**4**	**5**
	In (tonne/year)	*In* (tonne/year)	*Out* (tonne/year)	*In*(tonne/year)	*Out* (tonne/year)
CO_2	4889				
Oxalic acid		1000	5000		
Formic acid			1022		
PC		64000	64000		
TEACl		6098	6098		
H_2O				1200	
O_2					1067

Table 4.9: The total electrolyzer cost (€/m^2/year), based on the cost of the separate compartments, assuming a lifetime of 7 years of the separate compartments.

Pb-coated electrode (€/m^2/year)	33 [66]
Pt-coated electrode (€/m^2/year)	100 [67]
Nafion CEM (€/m^2/year)	231 [68]
Cell mechanical elements	40% total electrolyzer cost [69]
Total electrolyzer cost (€/m^2/year)	607

First, the cost of the electrolyzer per year per m^2 is calculated. This is done based on a lifetime of 7 years for the electrodes, membrane and the rest of the cell mechanical elements. The total lifetime of the plant should be 15 years, therefore the cost of the electrolyzer units is given as cost per year. In table 4.9 the total electrolyzer cost, made up of the price of the anode and cathode material, the membrane and the cell mechanical elements, of 607 €/m^2/year is shown. It is assumed that the CAPEX scales linearly with the electrode area, as the reactor design will consist of stacked electrochemical reactors.

The life time of the plant is assumed to be 15 years. The balance of plant is a factor to estimate all the cost for building your electrolyzer, based on the separate cost of the major technical components (electrodes and membranes).This is assumed to be 2.5 [70]. In Table 4.10, the total electrolyzer cost of 23 k€/m^2 is given, based on electrolyzer cost per year, the life time of the plant and the balance of plant cost.

The area of the electrolyzer needed to achieve the desired production capacity is depending on the current density and the faradaic efficiency obtained. The faradaic efficiency has been experimentally determined. An optimal current density can be determined, as increasing current density reduces the area of the electrolyzer needed (lower CAPEX), but increases the energy consumption (higher OPEX). Higher current density requires higher cell voltage, as the ohmic drop increases with increasing potential, shown in equation (4.3. The cell voltage, and therefore the electricity consumption, is based on the ohmic overpotential (η_{ohm}), as described by equation 4.2.

$$E_{\text{cell}} = |E^{exp}_{\text{anode}}{}^{ox} - E^{exp}_{\text{cathode}}{}^{red}| + \eta_{\text{ohm}} \tag{4.2}$$

η_{ohm} is the ohmic drop, which can be calculated with equation 4.3. It is the product of the current density and the sum of the resistance in each compartment. The resistance is dependent on the distance between

Table 4.10: The electrolyzer cost (€/m^2), based on the cost of the total electrolyzer cost (€/m^2/year), the total lifetime of the plant and the balance of plant factor.

Total electrolyzer cost (€/m^2/year)	607
Lifetime (year)	15
Balance of plant (-)	2.5 [70]
Electrolyzer cost (k€/m^2)	23

Table 4.11: Values used to calculate the optimum current density. $l_{anodecomp}$, $l_{membrane}$ and $l_{cathodecomp}$ are depending on the cell design. $\kappa_{anodecomp}$,$\kappa_{membrane}$ and $\kappa_{cathodecomp}$ are respectively the conductivity of 0.5M H_2SO_4 the membrane and 0.7MTEACl in PC. The ohmic drop can be calculated with equation 4.3, based on the value in this table.

$l_{anodecomp}$ (mm)	2
κ $_{anodecomp}$ (S/m)	21.1
$l_{membrane}$ (mm)	0.086
κ $_{membrane}$ (S/m)	1.03
$l_{cathodecomp}$ (mm)	2
κ $_{cathodecomp}$ (S/m)	0.85

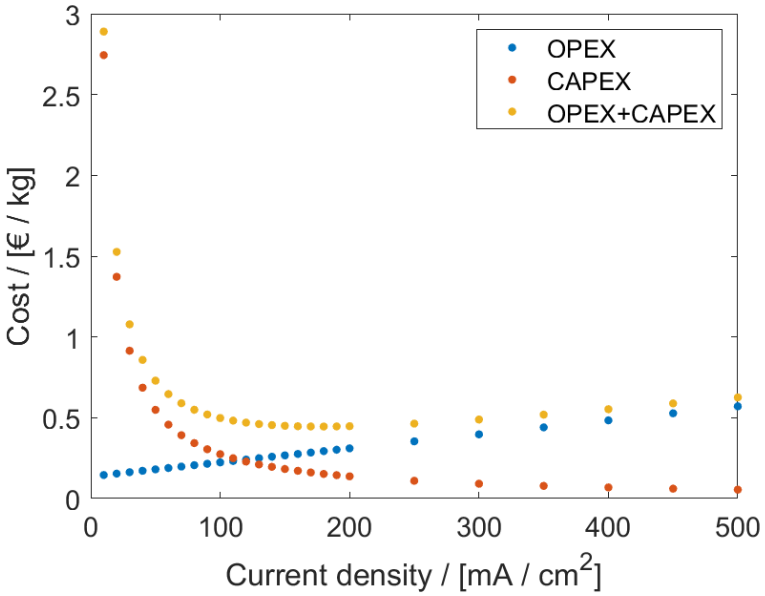

Figure 4.44: OPEX (electricity and CO_2 capture cost), CAPEX (electrolyzer investment) and total oxalic acid production cost (€/kg) as a function of the current density of the process. This calculations only include the electrolyzer OPEX and CAPEX without any costs for downstream processing. The CAPEX decreases with increasing current density, as less electrode area is necessary resulting in the same production. The OPEX increases with increasing current density because the total energy consumption increases.

the cathode and the anode and the conductivity.

$$\eta_{ohm} = j \cdot \left(\frac{l_{anodecomp}}{\kappa_{anodecomp}} + \frac{l_{membrane}}{\kappa_{membrane}} + \frac{l_{cathodecomp}}{\kappa_{cathodecomp}} \right) \tag{4.3}$$

Based on the influence of the current density on ohmic drop and therefore the cell voltage and the price of electrolyzer per m^2 and the electricity price, the optimal current density can be calculated. For the determination of the optimum current density, the values as described in Table 4.11 are used.

In Figure 4.44 is shown that lowest production cost are found with current density values between 100-180 mA/cm^2. Therefore, it has been chosen to assume a current density value of 120 mA/cm^2 for the further techno-economic calculations.
The cathode and anode reduction potential, ohmic overpotential and the faradaic efficiency achieved are based on experimental results. The corresponding current density achieved will not be used in the techno-economic analysis because of the low technological readiness of the performed experiments. It is expected that with improved cell design the current densities will increase. During the experiments, maximum current densities of only 23 mA/cm^2 are obtained. The current density value used in the techno-economic evaluation is 120 mA/cm^2, based on the production cost optimization (Figure 4.44). In the sensitivity analysis, the production costs for lower current density values will be calculated. In Table 4.12, the experimentally obtained values used to calculate the area of the electrolyzer needed are summarized.

From the parameters mentioned in Table 4.12, the productivity (kg product/m^2 is calculated (equation 4.4).

Table 4.12: Process parameters based on experimental results used in this techno-economic analysis. The current density is not based on performed experiments, but on the optimization of the total production cost.

Cathode reduction potential (V vs. Ag/AgCl)	-2.5
Anode oxidation potential (V vs. Ag/AgCl)	1.5
Ohmic overpotential (V)	0.5
Faradaic efficiency (%)	80
Current density (mA/cm^2)	120

Table 4.13: The overall capital investment necessary for the electrolyzer unit. The area is calculated from the capacity and productivity via equation 4.5. The CAPEX of the electrolyzer is the electrolyzer cost/m^2 multiplied by the area. The productivity is calcukated with equation 4.4

Productivity (tonne product/(m^2 annum)	12.6
Capacity (tonne/year)	4000
A_{elec} (m^2)	317
Electrolyzer cost (k€/m^2)	23
CAPEX electrolyzer (M€)	7.2

The productivity in mol/s is based on the current density (j), faradaic efficiency (FE), electron transfer during the cathode reaction (n_e) and the faraday number (F). If those are multiplied by the molecular weight and the amount of seconds in a year ($t_{\text{operational}}$ = 28800000s), the production per m^2 per year is found.

$$\text{Productivity} = \frac{j \cdot \text{FE}}{n_e \cdot F} * M * t_{\text{operational}} \tag{4.4}$$

If the overall production capacity (kg/year) is divided by the productivity, the total area (A_{elec}) of the electrolyzer can be found. This is described by equation 4.5.

$$A_{\text{elec}} = \frac{\text{capacity}}{\text{productivity}} \tag{4.5}$$

The total capital investment for the electrolyzer unit follows from the area needed and the electrolyzer cost (k€/m^2) and is given in Table 4.13.

The total electricity consumption (TEC) of the electrolyzer unit is calculated by equation 4.6. It is the product of the current density (j), area (A) and voltage applied (E_{cell}) multiplied by the amount of operational hours ($t_{\text{operational}}$).

$$\text{TEC} = j * A_{\text{elec}} * E_{\text{cell}} * t_{\text{operational}} \tag{4.6}$$

In Table 4.15, an overview is given of the operational cost per year of the electrolyzer unit. The only operational cost included are the reactant cost and electricity cost. No other costs, such as labour, maintenance and depreciation are considered.

Table 4.14: The total electricity consumption (TEC) of the electrolyzer unit, calculated by equation 4.6 based on the values of $t_{\text{operational}}$, area, current density and cell voltage as given in the table.

$t_{\text{operational}}$ (h/year)	8000
A_{elec} (m^2)	317
Current density (mA/cm^2)	120
E_{cell} (Cell voltage + ohmic overpotential (V)	7.0
TEC (MWh)	21433

Table 4.15: The operational cost of the electrolyzer per year, consisting of raw material (CO_2) cost and electricity cost. The cost is based on the consumption multiplied by the cost of the utility. No other costs, such as labour, maintenance and depreciation are considered.

General CO_2 capture (€/tonne)	63
CO_2 consumption (tonne/year)	4889
CO_2 cost (M€/year)	0.31
Electricity consumption electrolyzer (MWh)	21433
Electricity price (€/MWh)	50
Electricity cost (M€/year)	1.07

4.3.2. Liquid-liquid extraction

For the liquid-liquid extraction unit, large simplifications have been made which will be further explained. The distribution coefficient of oxalic acid and TEACl between propylene carbonate and water have been experimentally determined in section 4.2. The distribution coefficient (K_{OxA}) of oxalic acid between water and propylene carbonate is 9.6 and the distribution coefficient of TEACl (K_{TEACl}) is 8.7, so both oxalic acid and TEACl are more soluble in water than in propylene carbonate. The assumption is made that all of the oxalic acid and TEACl are in the water-phase at the end of the liquid-liquid reaction. In reality, TEACl and oxalic acid will be left in the propylene carbonate and will recycle back into the electrolyzer, but it is not expected this will cause problems in the electrolyzer. Another assumption that was made is that the solvents are substantially immiscible. With this assumptions, the mass balance of the extraction unit is as given in Table 4.16. The process flow diagram for the liquid-liquid extraction is given in Figure 4.45.

With the additional assumption that the distribution constant is constant, the required number of theoretical stages of the extraction column, N_{ts}, can be calculated with the Kremser equation (equation 4.7). The kremser equation calculates N_{ts} using the extraction factor (E), the distribution coefficient (K) and the mole fraction

Table 4.16: Mass balance of the extraction unit. To simplify the process, the assumption has been made that propylene carbonate and water are immiscible and that all of the OxA and TEACl end up in the water phase.

	1	**2**	**3**	**4**
	In (tonne/year)	*In* (tonne/year)	*Out*(tonne/year)	*Out* (tonne/year)
Oxalic acid	5000		5000	
Formic acid	1022		1022	
PC	64000			64000
TEACl	6098		6098	
Water		52800	52800	

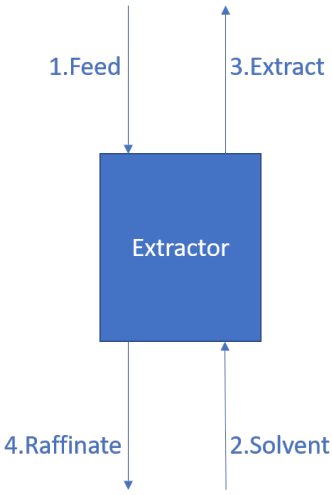

Figure 4.45: Process flow diagram of the extraction unit. The numbers correspond to stream numbers, of which the composition is described by the mass balance of the extraction unit (Table 4.16).

of the desired product in the feed(x_{in}), raffinate (x_{out}) and extracting solvent (y_{in}).

$$N_{ts} = \frac{\ln\left[\frac{x_{\text{in}} - \frac{y_{\text{in}}}{k}}{x_{\text{out}} - \frac{y_{\text{in}}}{k}}\left(1 - \frac{1}{E}\right) + \frac{1}{E}\right]}{\ln E} \tag{4.7}$$

The sizing of the liquid-liquid extraction unit is done based on the method described by Seader, Henley and Roper, in their book Separation process principles [71]. The selection of propylene carbonate as the dispersed phase is based on the following rules of thumb: the phase with the higher volumetric flowrate and viscosity should be selected as the dispersed phase. The assumption has been made that the specific gravity of the feed is the same as the density of propylene carbonate. For the extract, the specific gravity is assumed to be the same as the density of water. The ratio of the velocities of the dispersed and continuous phase (U_D/U_C) is given by equation 4.8.

$$\frac{U_D}{U_C} = \frac{m_{\text{Feed}}}{SG_{\text{Feed}}}\frac{SG_{\text{Extract}}}{m_{\text{Extract}}} = \frac{9515}{1.2}\frac{1}{8115} = 0.98 \tag{4.8}$$

For systems, in which one of the phases is water, the characteristic rise velocity u_0 of a single droplet is given by equation 4.9.

$$u_0 = \frac{0.01\sigma\Delta\rho}{\mu_c\rho_c} = \frac{0.01 \cdot 0.029\text{N/m} \cdot 200\text{kg/m}^3}{0.001\text{Pa}\cdot\text{s} * 1000\text{kg/m}^3} = 0.058\text{m/s} \tag{4.9}$$

The phase ratio is related to the total capacity of the column, which is described by Seider [71]. For U_c/U_D = 0.98, $\frac{(U_D+U_C)_f}{u_0}$ is 0.31. The actual superficial velocity is taken as 50% of the superficial velocity at flooding [72].

$$(U_D + U_C)_{50\%\text{offlooding}} = 0.5\frac{(U_D + U_C)_f}{u_0} * u_0 = 0.5 \cdot 0.31 \cdot 0.058 * 3600\text{s/h} = 32\text{m/h} \tag{4.10}$$

The total volumetric flowrate (ϕ) of the two phases is the mass flowrate divided by the specific gravity (eq. 4.11).

$$\phi = \frac{9515\text{kg/h}}{1.2\text{kg/m}^3} + \frac{8115\text{kg/h}}{1\text{kg/m}^3} = 16\text{m}^3\text{/h} \tag{4.11}$$

The required column area (A_{column}) is found by dividing the volumetric flowrate (ϕ) divided by the actual superficial velocity ($(U_C + U_D)_{50\%}$) , as seen in equation 4.12.

$$A_{\text{column}} = \frac{\phi}{(U_C + U_D)_{50\%}} = \frac{16\text{m}^3\text{/h}}{32\text{m/h}} = 0.5\text{m}^2 \tag{4.12}$$

The required column diameter (D_C) is given by equation 4.13.

$$D_{\text{C}} = \sqrt{\frac{4A}{\pi^2}} = \sqrt{\frac{4 \cdot 0.5\text{m}^2}{\pi^2}} = 0.8\text{m} \tag{4.13}$$

The column height is based on the number of theoretical trays, as described by the Kremser equation. A column efficiency of 20% and tray-spacing of 30 cm is assumed, which leads to a column height of 2.9 m. Table 4.17 shows the cost estimation of the extraction unit, based on the cost price of a reference unit (C_{ref}) [73]. The extraction unit is scaled using the diameter of the reference extraction unit (D_{ref}) and the diameter of the actual unit (D_{C}), powered by the scaling factor (n), as described by equation 4.14.

$$C_{\text{tpi}} = C_{\text{ref}} \cdot \left(\frac{D_{\text{C}}}{D_{\text{ref}}}\right)^n \tag{4.14}$$

Table 4.17: The total capital investment for the liquid-liquid extraction unit, estimations are based on the price of a reference unit. C_{tpi} is calculated using the values in this table with equation 4.14. $C_{tpi,Lang}$ is calculated from C_{tpi} via equation 4.15. $C_{tpi,€}$ is calculated from $C_{tpi,Lang}$ with the EU-dollar conversion rate.

C_{ref} (k$)	35 [73]
D_{ref} (m)	0.08 [73]
n	0.6 [74]
D_c	0.80
C_{tpi} (k$)	139
Lang factor	4.3 [75]
$C_{tpi,Lang}$ (k$)	594
$C_{tpi,€}$ (k€)	534

The Lang factor method is a rule of thumb to estimate the overall cost of a plant, based on the cost of the separate components. The total cost, including the Lang factor, is estimated by equation 4.15.

$$C_{tpi,Lang} = C_{tpi} * \text{Lang factor} \tag{4.15}$$

4.3.3. Crystallizer

The separation process consists of an extraction step followed by a crystallization step. First, both oxalic acid and TEACl are extracted with water from the propylene carbonate phase. After the extraction step, the oxalic acid and TEACl need to be separated from the water, to be recovered as solids. The separation of oxalic acid from water and TEACl is done by cooling crystallization between 60 °C and 20 °C. The solution is heated to 60 °C, and then low pressure is applied to evaporate the water and formic acid, until the solubility limit of oxalic acid in water at 60 °C (44 g/L) is reached. Then, the solution is slowly cooled down to 20 °C. In this step, the oxalic acid crystallizes. Then, the solution is heated again at reduced pressure to evaporate the remaining water, and TEACl is recovered. The assumption is made that 80% of the oxalic acid crystallizes. This assumption is based on the difference in solubility limit of oxalic acid at 60 °C (44 g/L) and the solubility limit of oxalic acid at 20 °C (9 g/L). The non-crystallized oxalic acid will be recovered together with TEACl and will be recycled into the system. In Figure 4.46 the process flow diagram of the assembly of crystallization units is given. In Table 4.18, the mass balance of the assembly of crystallization units is given.

The sizing of the heat exchanger units is based on an assumed specific heat flux of 20 kW/m^2. From the heating requirement of the unit, the area of the heat exchanger can be calculated. The cost estimation is done based on the method as described by Towler in Chemical Engineering Design [76], which is given in equation 4.16.

$$C_{unit} = a + bS^n \tag{4.16}$$

The total capital investment for the evaporation unit is based on the cost price of the evaporation unit, which is based on data of 2010. The Chemical Engineering Price Cost Index (CEPCI) of 2010 and 2019 is used to correct this price to the contemporary price level. To calculate the total capital investment, the cost price of the evaporation unit is multiplied by the Lang factor and by the price index, as described in equation 4.17.

Table 4.18: Mass balance of the assembly of crystallization units. The 80% of the oxalic acid crystallizes in the cooling crystallization unit, which is separated from the slurry by filtration.

	1	**2**	**3**	**4**	**5**	**6**	**7**	**8**	**9**
	ton/year	ton/ year	ton/ year	ton/year	ton/year	ton/year	ton/year	ton/year	ton/year
Water	52800	11986	40814	11986	11986			11986	52800
Oxalic acid	5000	5000		5000	1000	4000	1000		
TEACl	5133	5133		5133	5133		5133		
Formic acid	1022	232	790	232	232			232	1022

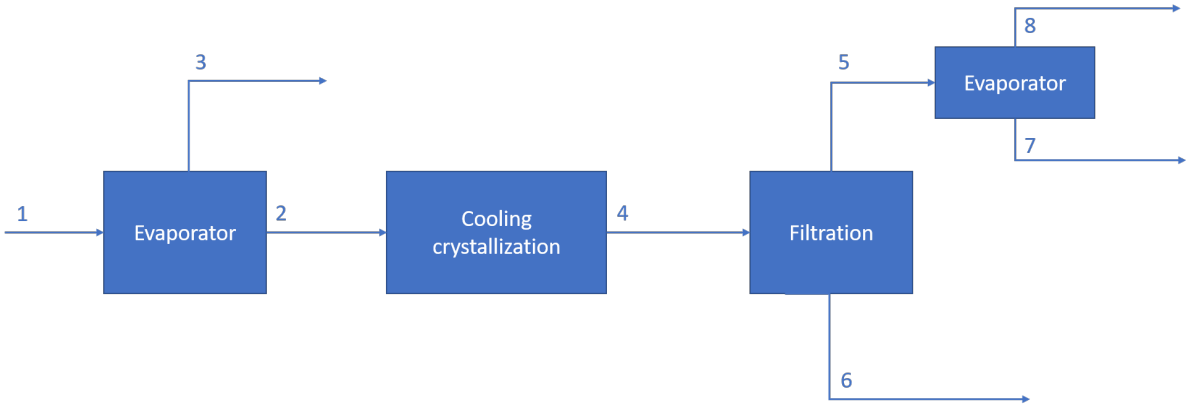

Figure 4.46: Process flow diagram for the assembly of crystallization units. The numbers correspond to stream numbers, of which the composition is described by the mass balance of the assembly of the crystallization units (table 4.18). The first evaporation unit is needed to create a concentrated oxalic acid stream, after which cooling crystallization occurs and 80% of oxalic acid crystallizes. This is separated from the rest of the stream by filtration. Solid TEACl with remaining oxalic acid is obtained by evaporation of remaining water and formic acid.

$$\mathrm{TCI_{unit}} = C_{\mathrm{unit}} \cdot \text{Lang factor} \cdot \frac{\mathrm{CEPCI_{2019}}}{\mathrm{CEPCI_{2010}}} \tag{4.17}$$

The cost price estimation for the first evaporation unit is given in table 4.19 and the estimation for the second unit is given in table 4.20.

The total capital investment of the crystallization unit is calculated based on the cost of a single batch vacuum crystallizer ($\mathrm{C_{cryst}}$) with the desired capacity, as described in equation 4.18. The cost price estimation of the

Table 4.19: The overall capital investment necessary for the first evaporator unit. The cost of the evaporation unit (C_{evap1}) is calculated with equation 4.16 with the following parameters a = 330, b= 36000, and n = 0.55 and S is the area of the evaporator unit which is calculated with the specific heat flux and the energy requirement of the evaporation unit. The total capital investment (TCI) is calculated from C_{evap1} by equation 4.17.

Specific heat flux (kW/(m^2)	20
$\mathrm{Q_{unit}}$ (kW)	3084
Area (m^2)	154
C_{evap1} (k€, 2010)	576
Lang factor	3.5
$\mathrm{CEPCI_{2010}}$	532.9
$\mathrm{CEPCI_{2019}}$	619.2
$\mathrm{TCI_{evap1,\ Lang}}$ (M$)	2.34
$\mathrm{TCI_{evap,\ €}}$ (M€)	2.11

Table 4.20: The overall capital investment necessary for the second evaporator unit. The cost of the evaporation unit (C_{evap2}) is calculated with equation 4.16 with the following parameters a = 330, b = 36000, and n = 0.55 and with the area which is calculated with the specific heat flux and the energy requirement of the evaporation unit. The total capital investment (TCI) is calculated from C_{evap2} by equation 4.17.

Specific heat flux (kW/m^2)	20
$\mathrm{Q_{unit}}$ (kW)	1170
Area (m^2)	58.5
C_{evap2} (k€, 2010)	3378
Lang factor	3.5
$\mathrm{CEPCI_{2010}}$	532.9
$\mathrm{CEPCI_{2019}}$	619.2
$\mathrm{TCI_{evap2,\ Lang}}$ (M$)	1.37
$\mathrm{TCI_{evap2,\ €}}$ (M€)	1.24

Table 4.21: The total capital investment for the crystallizer unit is based on the cost of a batch vacuum crystallizer as described by equation 4.18.

Capacity (m^3/h)	6.8
Residence time	1
Cost batch vacuum crystallizer (k€)	120 [77]
Lang factor	3.5
$CEPCI_{2014}$	576.1
$CEPCI_{2019}$	619.2
TCI_{Cryst} (k$)	452
TCI_{Cryst} (k$)	407

Table 4.22: The total capital investment for the belt filter unit, which is based on the the cost of 155 k€ for a belt filter of 5 m^2 in 2003 [3]. The total capital investment is calculated with equation 4.20.

Volume flowrate (m^3)	8.1
Volumetric flowrate per square meter (m^3/m^2)	0.9 [3]
Area (m^2)	9
C_{filter} (k€, 2003)	190
$CEPCI_{2003}$ (-)	402
$CEPCI_{2019}$ (-)	619.2
Lang factor (-)	2 [3]
TCI_{filter} (k€)	587

crystallizer unit is an estimation from Matche [77], and is given in Table 4.21.

$$\mathrm{TCI}_{\mathrm{cryst}} = C_{\mathrm{cryst}} \cdot \frac{\mathrm{CEPCI}_{2019}}{\mathrm{CEPCI}_{2014}} \cdot \text{Lang factor} \tag{4.18}$$

The sizing of the filtration unit is done based on a typical value for a volumetric flowrate per square meter, a reference price for a filtration unit and a sizing factor, all described by equation 4.19 [3]. The investment cost for the belt filter unit is given in Table 4.22.

$$C_{\mathrm{filter}} = \left(\frac{A_{\mathrm{unit}}}{A_{\mathrm{reference}}}\right)^n * C_{\mathrm{ref}} \tag{4.19}$$

From the investment cost for the belt filter, the total capital investment can be calculated by multiplication with the Lang factor and the chemical engineering price cost index, as described in equation 4.20.

$$\mathrm{TCI}_{\mathrm{filter}} = C_{\mathrm{filter}} \cdot \text{Lang factor} \cdot \frac{\mathrm{CEPCI}_{2019}}{\mathrm{CEPCI}_{2003}} \tag{4.20}$$

The operational cost for the assembly of crystallization units are based on the utilities needed for heating and cooling of the evaporation and condenser units. The total energy input for heating ($Q_{heating}$) is based on the total energy requirements of the separate units and is given by equation 4.21. The amount of steam (m_{steam}) needed per year is the energy requirement divided by the enthalpy of cooling and condensing of the steam (h_{steam}-h_{water}), as shown in equation 4.22.

$$Q_{\mathrm{heating}} = Q_{\mathrm{evap1}} + Q_{\mathrm{evap2}} \tag{4.21}$$

$$m_{\mathrm{steam}} = \frac{Q_{\mathrm{heating}}}{h_{\mathrm{water}} - h_{\mathrm{steam}}} \tag{4.22}$$

The total operational cost for heating is the amount of steam needed (m_steam) multiplied by the steam price ($€_{\mathrm{steam}}$), as shown in equation 4.23.

Table 4.23: The total operational cost for heating, based on the heating requirements for the crystallization process. The total steam cost (C_{steam}) is calculated from the values in this table, as described in equation 4.21, 4.22 and 4.23.

Q_{heating} (kJ/year)	$1.2^{*}\ 10^{11}$
h_{water} (kJ/kg)	417
h_{steam} (kJ/kg)	2674
m_{steam} (tonne/year)	54309
€$_{\text{steam}}$ (€/tonne)	25
C_{steam} (M€/year)	1.4

Table 4.24: The total operational cost for cooling, based on the cooling requirements for the crystallization process. The total steam cost (C_{cooling}) is calculated from the values in this table, as described in equation 4.24 and 4.25.

Q_{cooling} (kJ/year)	$1.0^{*}10^{11}$
$c_{p,\text{water}}$ (kJ/kg/K)	4.18
T_{out} (°C)	50
T_{in} (°C)	25
$m_{\text{coolingwater}}$ (m^3/year)	960000
€$_{cooling}$ (€/m^3)	0.00005
C_{cooling} (k€/year)	478

$$C_{\text{steam}} = €_{\text{steam}} \cdot m_{\text{steam}} \tag{4.23}$$

Table 4.23 shows the outcomes of the calculations as described in equation 4.21, 4.22 and 4.23. This all adds up to a cost for steam of 1.4M€ per year.

The amount of cooling water needed per year can be calculated with the total energy requirement for cooling of the crystallization unit (Q_{cooling}), the specific heat of water ($C_{p,\text{water}}$) and the temperature difference that needs to be obtained (ΔT) and is described by equation 4.24.

$$m_{\text{coolant}} = \frac{Q_{\text{cooling}}}{C_{p,\text{water}} \cdot \Delta T} \tag{4.24}$$

From the amount of cooling water (m_{coolant}) needed, the total cost of cooling can be calculated with the price of cooling water (€$_{\text{coolingwater}}$, as described by equation 4.25.

$$C_{\text{cooling}} = €_{\text{coolingwater}} \cdot m_{\text{coolant}} \tag{4.25}$$

Table 4.24 shows the outcomes of the calculations as described in equation 4.24 and 4.25. The total cost for cooling water per year is 478 k€.

4.3.4. Overall process

In Figure 4.47 the process flow diagram of the overall process is shown, combined of the flowsheets of the separate steps as discussed in previous sections. In Table 4.25, an overview is given of the CAPEX and OPEX of all the parts of the process. The CAPEX is the capital investment for the lifetime of the plant of 15 years. The OPEX is expressed as cost per year. To produce oxalic acid over the whole life time of the plant, the total operational cost are 15 times the OPEX given in Table 4.25. The production cost per kg of oxalic acid is calculated by dividing the total CAPEX and OPEX over the full life time of the plant by the amount of oxalic acid produced during the life time of the plant.

In Table 4.26 the total production cost for oxalic acid is given, based on the capital investment and operational cost over the full lifetime of the plant. With all the assumptions made, the production cost of oxalic acid was estimated to be €0.87/kg, which is lower than the current oxalic acid price of 1 €/kg. The cost of production is lower than the potential income, so the production of oxalic acid shows economic potential to replace the current production process of oxalic acid.

Table 4.25: Cost overview for the overall process, in terms of capital investment for the full lifetime of the plant (CAPEX) and operational costs per year (OPEX).

CAPEX	
Electrolyzer (M€)	7.2
Liquid-liquid extraction (M€)	0.54
Crystallization units (M€)	4.3
Total CAPEX (M€)	12.1
OPEX	
CO_2 cost (M€/year)	0.31
Electricity electrolyzer (M€/year)	0.96
Steam crystallizer (M€/year)	1.4
Cooling water crystallizer (M€/year)	0.05
Total OPEX (M€/year)	2.7

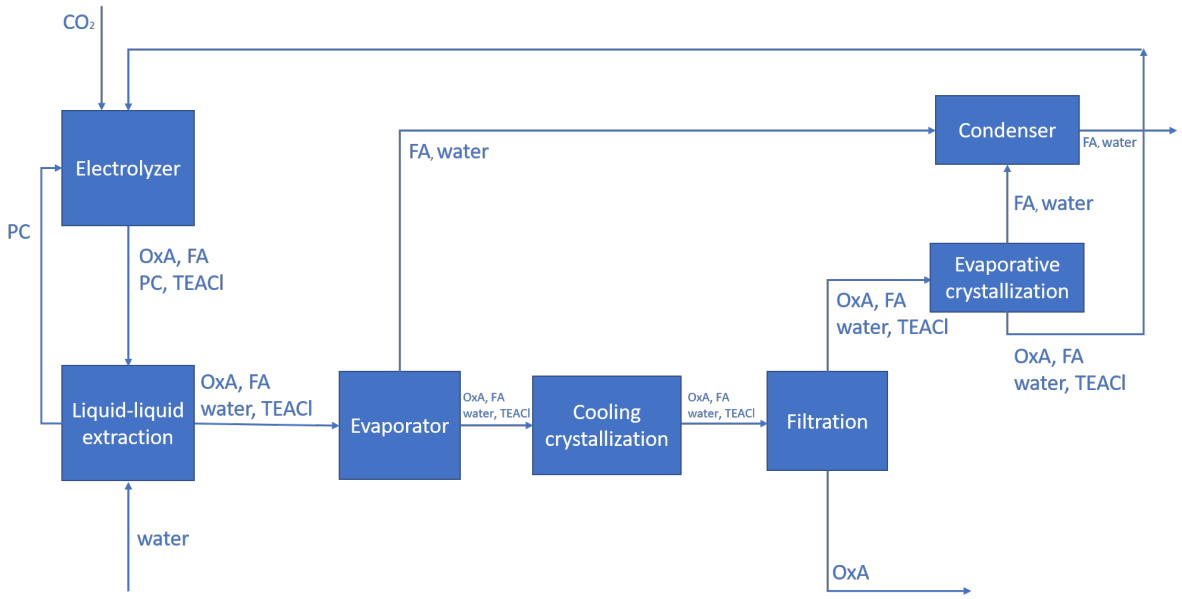

Figure 4.47: Process flow diagram for the full process, which is the combined flow diagrams of the electrolyzer unit (Figure 4.43), the liquid-liquid extraction (Figure 4.45 and the crystallization process (Figure 4.46). Abbreviations used are: PC = propylene carbonate, OxA = oxalic acid, FA = formic acid, TEACl = tetraethylammonium chloride.

Table 4.26: Estimated production cost of the oxalic acid production process for 4000 tonne/year oxalic acid production based on both the capital investment and operational cost over the full lifetime of the plant. The total production cost is 0.87€/kg, while the current oxalic acid price is 1 €/kg.

CAPEX (M€)	12.1
OPEX (M€/year)	2.7
lifetime plant	15
production (tonne/year)	4000
CAPEX (€/kg OxA)	0.20
OPEX (€/kg OxA)	0.67
CAPEX + OPEX (€/kg OxA)	0.87
Price OxA (€/kg OxA)	1

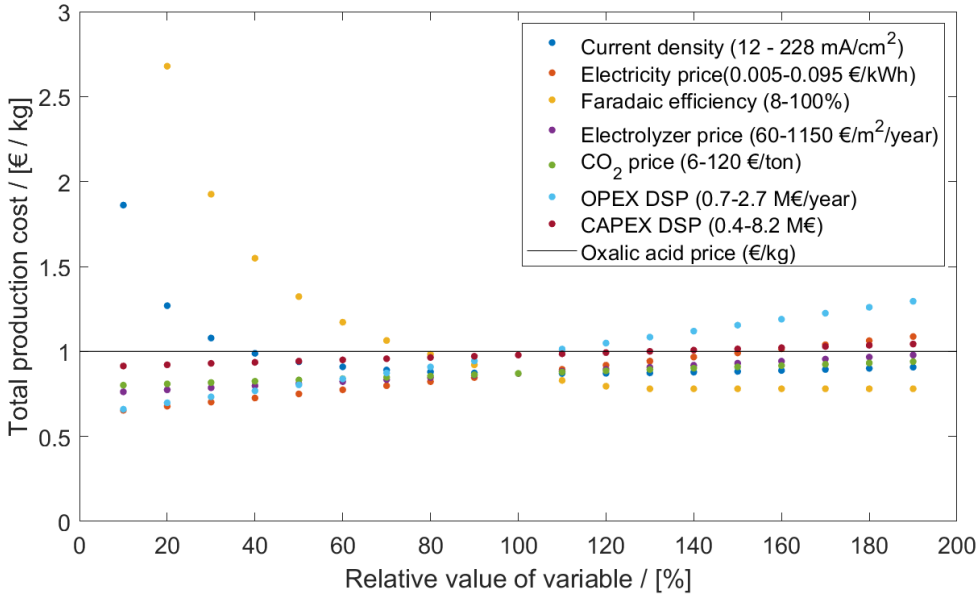

Figure 4.48: Sensitivity analysis for different process parameters on the total production cost of oxalic acid. The relative value of the variable at 100% represents the basecase. The total production cost of oxalic acid per kg is given as function of the relative value of several variables compared to the value of the variable in the base case. The parameters varied are the current density (blue), electricity price (red), faradaic efficiency (yellow), electrolyzer price (purple), CO_2 price (green), OPEX DSP (turquoise) and CAPEX DSP (bordeaux). The total oxalic acid production costs are compared with the current oxalic acid price (black line). As the basecase value of the faradaic efficiency is 80%, and it cannot exceed more than 100%, the faradaic efficiency is kept at 100% from 130-190 as relative value of the variable.

4.3.5. Sensitivity analysis

The techno-economic analysis uses a large amount of process parameters and it is useful to see the influence of the process parameter on the total production cost of oxalic acid (CAPEX + OPEX (€/kg)). In the sensitivity analysis, the influence of the curent density, electricity price, electrolyzer price, CO_2 price, faradaic efficiency and the total cost for both OPEX and CAPEX is analyzed. In Figure 4.48 is shown that the parameters influencing in the largest extent the total production costs of oxalic acid via electrolysis are the current density and the faradaic efficiency.

4.4. Summary and general remarks

A techno-economic analysis has been performed to get a sense of the economic potential of electrochemical oxalic acid production. The current oxalic acid price is approximately 1000 €/tonne and with this techno-economic analysis, the production cost for electrochemical production of oxalic acid has been estimated to be 870 €/tonne. Even though this is a rough estimate, based on many simplifications and assumptions, it is shown there is economic potential for the electrochemical production of oxalic acid. It should be noted that especially the low current density and the falling faradaic efficiency over time are the biggest technical issues, which could make oxalic acid production unviable. During the electrochemical conversion experiments maximum current densities obtained were 23 mA/cm^2. At the start of the experiment, faradaic efficiencies were obtained of over 80 %, but this decreased over the time period of the experiment. As is clearly seen from the sensitivity analysis, technical development should focus on stabilizing the obtained faradaic efficiency as well as increasing the current density. Another variable that clearly influences the price of the oxalic acid is the operational costs of the downstream process, which is mostly the steam needed to separate the water from both TEACl and oxalic acid. This cost is inherent to liquid-liquid extraction, which is the critical point for the economical potential of the downstream process.

5

Conclusions

In this thesis, the electrochemical reduction of CO_2 has been researched; both the electrochemical conversion and downstream processing were experimentally investigated. Based on the experimental results, a preliminary process design is proposed of which a techno-economic analysis is performed.

The influence of the cathode material, voltage, catholyte, anolyte, membrane, supporting electrolyte and temperature in a batch-scale reactor has been assessed. Lead (Pb) is found to be suitable as cathode for the electrochemical reduction of CO_2. The influence of the applied potential has been tested between -2.2V vs. Ag/AgCl and -2.7V vs. Ag/AgCl, a clear trade-off was observed. At -2.7V vs. Ag/AgCl, current density of maximum 17 mA/cm^2 and final oxalic acid concentration of 36 mM was obtained, while the cumulative faradaic efficiency towards oxalic acid at the end of the experiment was 45%. At -2.2V vs. Ag/AgCl, current density of -2 mA/cm^2 and final oxalic acid concentration of 6.4 mM was obtained, while the cumulative faradaic efficiency at the end of the experiment was 86%. The influence of the nature of the catholyte was studied by varying the catholyte from propylene carbonate to acetonitrile. Propylene carbonate showed 80% faradaic efficiency at the end of the experiment towards oxalic acid, acetonitrile showed only 7% faradaic efficiency to oxalic acid. The influence of the anolyte was studied by varying the anolyte from 0.1M TEACl in ACN to 0.5M H_2SO_4. With 0.1M TEACl in ACN the maximum current density obtained was -6 mA/cm^2, with 0.5M H_2SO_4 the maximum current density obtained was -9 mA/cm^2. Similar faradaic efficiencies were obtained with a cumulative faradaic efficiency of 80% at the end of the experiment. Therefore, the concentration of oxalic acid was higher at the end of the experiment. The influence of the ion selectivity of the membrane that separates the anodic of the cathodic compartment in the electrochemical reactor was tested. A cation exchange membrane (Nafion 117) an an anion exchange membrane (Fumasep) resulted in similar concentrations of the produced oxalic acid. However, the anion-exchange membrane degraded, which made the cation-exchange membrane the preferable choice. The influence of the salt used as supporting electrolyte in the catholyte was also examined. TEACl, TBAP and TEAAce were tested as supporting electrolyte. The conductivity of the catholyte varied with addition of different electrolyte, with a conductivity of 8.8 mS/cm for PC+TEACl, 4.3 mS/cm for PC+TBAP and 3.6 mS/cm for TEAAce. The lower conductivity resulted in lower current densities being reached of maximum -3 mA/cm^2 for TBAP and maximum -2 mA/cm^2 compared the maximum current density of -9 mA/cm^2 for PC+TEACl.

Another process parameter tested was the temperature of the catholyte, at which temperatures of 15, 55 and 75°C were compared. At 55 and 75°C, current densities of -10 mA/cm^2 were obtained compared to -3 mA/cm^2 at 15 °C. At the different temperatures, similar faradaic efficiency towards oxalic acid (63% after 5 hours) was found. It is believed that the higher current density obtained is induced by reduced mass transfer limitations, although increasing temperature may not be the most efficient method for reduction of mass transfer limitations.

All of these separate experiments conclude into the following optimal settings: Electrochemical reduction of CO_2 to oxalic acid with lead as cathode in a catholyte of PC+TEACl saturated with CO_2 and platinum as anode in an anolyte of 0.5M H_2SO_4, all of this separated by a cation-exchange membrane which lead, after applying a potential of -2.5V vs. Ag/AgCl for 5 hours with a 10 cm^2 cathode and a total catholyte volume of 160

mL, to an oxalic acid concentration of 27 mM. If maximum faradaic efficiency of 86% is desired, the optimal potential is -2.2V vs. Ag/AgCl. If high production of oxalic acid is desired, the optimal potential is -2.7V vs. Ag/AgCl, which leads to concentrations of 36 mM.

The first step to scaling-up this process was assessed by changing the batch reactor for a semi-continuous flow reactor where the CO_2 is pumped through the cell to have a continuous supply of reactant to reduce mass-transfer limitations. The electrochemical reduction of CO_2 has been performed in a flow-cell with the optimal settings obtained in the batch reactor. Several process parameters as applied potential and supporting electrolyte were also evaluated in the flow-cell. The main issue experienced with these experiments was the low reproducibility of the experiments, with different current densities and faradaic efficiencies observed in duplicated experiments. It has been shown that increasing water content leads to increasing current densities but decreasing faradaic efficiencies. In different duplicated experiments, large variations were found in the water content of the catholyte. This explains the large variations found in current density and faradaic efficiency for duplicated experiments. Compared to the H-cell experiments, the current densities obtained were higher, being the maximum current density obtained in the semi-continuous set-up with applied potential of -2.7 mA/cm^2 -23 mA/cm^2 while only -17 mA/cm^2 in the batch reactor. The faradaic efficiencies were significantly lower, being the faradaic efficiency obtained in the batch reactor 45% after 5 hours while only 25% in the semi-continuous set-up after 4.5 hours.

Several methods for the downstream processing of oxalic acid after the electrochemical conversion of CO_2 to oxalic acid were explored. The suitability of vacuum distillation, direct crystallization, liquid-liquid extraction followed by precipitation and crystallization, anti-solvent precipitation and direct further reaction have been discussed. Direct crystallization and direct methylation have been shown to be not suitable methods for downstream processing. On the other hand, the suitability of liquid-liquid extraction followed by both crystallization and precipitation, has been experimentally proved.

Based on the electrochemical conversion experiments and the proof-of-concepts performed for the downstream processing, a preliminary and simplified process design for the electrochemical formation of oxalic acid from CO_2 was proposed. For this process design, a techno-economic analysis has been performed. It is shown, that with this process design, the electrochemical production cost of oxalic acid (0.87€/kg) is lower than the current market price (1€/kg). It should be noted that the process design is based on a number of technical and economical assumptions, of which the obtained current density values and the assumed stability of the faradaic efficiency are the most influential. The state of the technology is not sufficiently mature to achieve the key performance indicators needed to achieve an economically viable process. The influence of several process parameters, such as current density, electricity price, faradaic efficiency, electrolyzer price, CO_2 price and both the operational cost and the capital investment for the downsteam process on the production cost of oxalic acid has been assessed. It is found that the stability of the faradaic efficiency over time, together with the increase of current densities to the desired value of 100-180 mA/cm^2 are the main technical challenges to focus on. From the techno-economic analysis it has been assessed that the liquid-liquid extraction step of the downstream processing is critical for the economical feasibility of the process. This is because the oxalic acid and supporting electrolyte need to be separated from the water and it is proposed to be done by evaporation - a very energy intensive process.

In conclusion, the electrochemical production of oxalic acid shows potential - both technically and economically - to become a commercialized industrial process if certain key performance indicators values can be experimentally achieved. For that, further optimization of the technical process needs to be addressed.

6

Recommendations

The opportunities for industrial-scale production of oxalic acid by electrochemical reduction of CO_2 have not been studied before. This research has shown both the technical state of the art and the economical potential of this production process. However, further optimization of the systems is required for the implementation of this technology in industry.

As briefly mentioned in the conclusions, the current densities obtained, as well as the stability of the faradaic efficiencies obtained over time are technical factors that largely influence the economic potential of the production process. A method to increase the obtained current density is by using Gas Diffusion Electrodes (GDEs), that eliminate mass transfer limitations by directly feeding gaseous reactants to the electrode. Electrochemical CO_2 reduction to ethylene, ethanol, carbon monoxide with and without using GDEs has been compared and shown tremendous increase in current density for all the products [78]. For the electrochemical CO_2 reduction to formic acid, current densities of up to 400 mA/cm^2 have been obtained using gas diffusion electrodes [79], while without the gas diffusion electrode maximum current densities of 55 mA/cm^2 are obtained [80]. Since current density values of 100-180 mA/cm^2 are required for the economical feasibility of the process and the highest current density observed using flat electrodes is 23 mA/cm^2, it is recommended to perform electrochemical reduction of CO_2 to oxalic acid with GDEs.
Another strategy to increase the current density and thereby the production of the desired product, is by performing the electrochemical reduction of CO_2 under higher pressure. The electrochemical reduction of CO_2 under high pressure (30 bar) has been performed in this thesis work in which increased current density values are measured compared to the flow-cell experiments, although lower flowrates were used. The faradaic efficiency to oxalic acid was low, but could be related to the high water content in the catholyte. At low pressure, the water content influenced the selectivity towards oxalic acid. With increasing water content, lower selectivity towards oxalic acid was observed. It is certainly recommended to further research the electrochemical reduction of CO_2 to oxalic acid under pressure and more specifically, to look for methods to reduce the amount of water in the set-up in order to obtain higher selectivities towards oxalic acid.

Another important parameter necessary for the implementation of this technology in industry, is the stability of the faradaic efficiency towards oxalic acid over time. The faradaic efficiency to oxalic acid decreases over time because the water content in the catholyte increases over time. The reason for the increasing water content in the catholyte is water cross-over through the membrane from anolyte (0.5M H_2SO_4) to catholyte (PC+0.7M TEACl). The membranes used are made for use in aqueous solutions, where some transport of water through the membrane is not a big concern. To guarantee the stability of the membrane, it is necessary to use an aqueous solution as anolyte. To reduce the water content in the catholyte, major improvements lie in the development or use of selective membranes that are stable in organic solvents. Tokuyama Soda has developed cation-exchange membranes made from vinyl monomers that have shown lower solvent and anion leakages in organic media compared to Nafion 117 [81]. Also, the application of Kevlar aramid nanofibers has lead to succesful fabrication of thin and robust organic solvent cation exchange membranes, although these are not commercially available yet [82]. To further clarify the role of the water content in the catholyte, a possible method to reduce the water content is the use of molecular sieves (3Å) which will aborb water that crosses from the anolyte to the catholyte compartment.

Up to now, only oxalic acid concentrations of up to 40 mM have been obtained. Subject of further research should focus on increasing the obtained concentrations to see the effect in the product distribution of the CO_2 reaction. Oxalic acid can be further reduced to glycolic acid and glyoxylic acid. With higher concentrations of oxalic acid, the reduction towards glycolic acid and glyoxalic acid may become more favorable.

As the reproducibility of the flow-cell experiments performed is low, an experimental method should be designed to achieve more consistent results. One of the reasons for the lack of reproducibility between experiments could be due to the differences in the surface of the electrode between experiments. In order to control the state of the surface of the electrode it can be characterized using different techniques, such as Scanning Electron Microscopy.

Chapter 2 discussed different electrocatalysts that have been used in small-scale and short-time experiments, that reduced the overpotential required for the electrochemical reduction of CO_2 to oxalic acid. As little is known about the stability of these electrocatalysts, it has not been part of this research. However, it is recommended to further study the options for using other electrocatalysts, as this could reduce the energy requirements of oxalic acid production.

Most of the recommendations focus on the improvement of the electrochemical process, as this part of the process strongly impacts OPEX and CAPEX. However, the separation process design also could use improvement, since it is also a large contribution to the overall production cost. Within the proposed process design, the oxalic acid and TEACl are extracted from propylene carbonate with water, which is a critical step. To recover the TEACl and to reach the solubility limit of TEACl in water, the water is evaporated which is very energy intensive. Furthermore, the assumption has been made that the oxalic acid has a concentration of 1M in propylene carbonate, which is a large concentration in which the further electrochemical reduction to glycolic and glyoxylic acid could become dominant. Therefore, other downstream processing methods should be experimentally explored, with non-artifical conditions obtained in the electrochemical system. This includes a wider product distribution and low oxalic acid concentrations. Future research should focus on finding an extractant that selectively extracts oxalic acid. This would eliminate the problem of the additional separation of oxalic acid and the supporting electrolyte (TEACl). Another potential downstream processing option could be the gas antisolvent process, as discussed in section 4.2, although still separation of oxalic acid and the supporting electrolyte is required. It is recommended to perform a proof-of-concept of this process.

Finally, the option to further electrochemically reduce oxalic acid to glycolic acid should be explored, since the glycolic acid market has a market size of 400 M$ by 2024 [83]. In addition, since the separation process of oxalic acid seems challenging, it would be interesting to research the feasibility of glycolic production and separation process.

Bibliography

[1] B. Eneau-Innocent, D. Pasquier, F. Ropital, J. M. Léger, and K. B. Kokoh. Electroreduction of carbon dioxide at a lead electrode in propylene carbonate: A spectroscopic study. *Applied Catalysis B: Environmental*, 2010. ISSN 09263373. doi: 10.1016/j.apcatb.2010.05.003.

[2] S. Ikeda, T. Takagi, and K. Ito. Selective formation of formic acid, oxalic acid, and carbon monoxide by electrochemical reduction of carbon dioxide. *Bulletin of the Chemical Society of Japan*, 60(7):2517–2522, 1987. doi: 10.1246/bcsj.60.2517. URL https://www.scopus.com/inward/record.uri?eid=2-s2.0-84975438667&doi=10.1246%2fbcsj.60.2517&partnerID=40&md5=287afff30c7767f64aea534c28329b37. cited By 213.

[3] R.J.C. Vaessen. *Development of scraped eutectic crystallizers*. PhD thesis, TU Delft, 06 2003.

[4] National Oceanic and Global Monitoring Division Atmospheric Administration, Earth System Research Laboratory. Recent daily average mauna loa co2. https://www.esrl.noaa.gov/gmd/ccgg/trends/monthly.html, 2020. accessed: 2020-02-20.

[5] IPCC. Climate change 2014 synthesis report summary chapter for policymakers. 2014.

[6] J M Lehn and R Ziessel. Photochemical generation of carbon monoxide and hydrogen by reduction of carbon dioxide and water under visible light irradiation. *Proceedings of the National Academy of Sciences of the United States of America*, 79(2):701–704, jan 1982. ISSN 0027-8424. doi: 10.1073/pnas.79.2.701. URL https://www.ncbi.nlm.nih.gov/pubmed/16593151https://www.ncbi.nlm.nih.gov/pmc/articles/PMC345815/.

[7] Ho Seok Whang, Jinkyu Lim, Min Suk Choi, Jonghyeok Lee, and Hyunjoo Lee. Heterogeneous catalysts for catalytic CO2 conversion into value-added chemicals. *BMC Chemical Engineering*, 1(1):9, 2019. ISSN 2524-4175. doi: 10.1186/s42480-019-0007-7. URL https://doi.org/10.1186/s42480-019-0007-7.

[8] Harri Nieminen, Arto Laari, and Tuomas Koiranen. CO_2 hydrogenation to methanol by a liquid-phase process with alcoholic solvents: A techno-economic analysis. *Processes*, 7(7):1–24, 2019. ISSN 22279717. doi: 10.3390/pr7070405.

[9] S.M. Javaid Zaidi. Overview of Conversion of Greenhouse Gas Carbon dioxide to Hydrocarbons. *Proceedings of the 2nd Annual Gas Processing Symposium*, pages 115–120, jan 2010. doi: 10.1016/S1876-0147(10)02013-6. URL https://www.sciencedirect.com/science/article/pii/S1876014710020136{#}bb0040.

[10] Eric E. Benson, Clifford P. Kubiak, Aaron J. Sathrum, and Jonathan M. Smieja. Electrocatalytic and homogeneous approaches to conversion of CO2to liquid fuels. *Chemical Society Reviews*, 38(1):89–99, 2009. ISSN 03060012. doi: 10.1039/b804323j.

[11] Oriol Gutiérrez Sánchez, Yuvraj Y. Birdja, Metin Bulut, Jan Vaes, Tom Breugelmans, and Deepak Pant. Recent advances in industrial CO 2 electroreduction. *Current Opinion in Green and Sustainable Chemistry*, 16:47–56, 2019. ISSN 24522236. doi: 10.1016/j.cogsc.2019.01.005. URL https://doi.org/10.1016/j.cogsc.2019.01.005.

[12] Andrew R. T. Morrison, Vincent van Beusekom, Mahinder Ramdin, Leo J. P. van den Broeke, Thijs J. H. Vlugt, and Wiebren de Jong. Modeling the Electrochemical Conversion of Carbon Dioxide to Formic Acid or Formate at Elevated Pressures. *Journal of The Electrochemical Society*, 166(4):E77–E86, 2019. ISSN 0013-4651. doi: 10.1149/2.0121904jes.

[13] Mahinder Ramdin, Andrew R.T. Morrison, Mariette De Groen, Rien Van Haperen, Robert De Kler, Leo J.P. Van Den Broeke, J. P. Martin Trusler, Wiebren De Jong, and Thijs J.H. Vlugt. High Pressure Electrochemical Reduction of CO 2 to Formic Acid/Formate: A Comparison between Bipolar Membranes and Cation

Exchange Membranes. *Industrial and Engineering Chemistry Research*, 58(5):1834–1847, 2019. ISSN 15205045. doi: 10.1021/acs.iecr.8b04944.

[14] Hirad S. Salehi, Mahinder Ramdin, Othonas A. Moultos, and Thijs J.H. Vlugt. Computing solubility parameters of deep eutectic solvents from Molecular Dynamics simulations. *Fluid Phase Equilibria*, 497: 10–18, 2019. ISSN 03783812. doi: 10.1016/j.fluid.2019.05.022. URL https://doi.org/10.1016/j.fluid.2019.05.022.

[15] Mar Pérez-Fortes, Jan C. Schöneberger, Aikaterini Boulamanti, Gillian Harrison, and Evangelos Tzimas. Formic acid synthesis using CO2 as raw material: Techno-economic and environmental evaluation and market potential. *International Journal of Hydrogen Energy*, 41(37):16444–16462, oct 2016. ISSN 0360-3199. doi: 10.1016/J.IJHYDENE.2016.05.199. URL https://www.sciencedirect.com/science/article/pii/S0360319915313835.

[16] Wenjun Zhang, Yi Hu, Lianbo Ma, Guoyin Zhu, Yanrong Wang, Xiaolan Xue, Renpeng Chen, Songyuan Yang, and Zhong Jin. Progress and Perspective of Electrocatalytic CO_2 Reduction for Renewable Carbonaceous Fuels and Chemicals. *Advanced Science*, 5(1), 2018. ISSN 21983844. doi: 10.1002/advs.201700275.

[17] K. Izutsu. John Wiley & Sons, 2009.

[18] Bor-Yih Yu and I-Lung Chien. Design and optimization of dimethyl oxalate (dmo) hydrogenation process to produce ethylene glycol (eg). *Chemical Engineering Research and Design*, 121:173 – 190, 2017. ISSN 0263-8762. doi: https://doi.org/10.1016/j.cherd.2017.03.012. URL http://www.sciencedirect.com/science/article/pii/S0263876217301454.

[19] E. Bowden. Org. synth. coll. vol. 2. 1943.

[20] Oxaquim. personal communication.

[21] Gen Consulting Co. Oxalic acid market size, share, trends & forecasts (2019-2025). https://www.researchcosmos.com/reports/oxalic-acid-market-research-report-global-industry-analysis-and-f 1727181519, 2019. accessed: 2020-02-20.

[22] T. Suzuki A. Sanada E. Yonemitsu, T. Isshika. Process for producing oxalic acid, 1969.

[23] S. Fujitus K. Masunaga H. Yanagisawa H. Miyazaki, Y. Shiomi. Process for the preparation of oxalic acid diesters, 1982.

[24] Plastics Insight. Mono-ethylene glycol (meg): Production, market, price and its properties. https://www.plasticsinsight.com/resin-intelligence/resin-prices/mono-ethylene-glycol-meg/, 2019. accessed: 2020-02-20.

[25] Maria A. Murcia Valderrama, Robert-Jan van Putten, and Gert-Jan M. Gruter. The potential of oxalic – and glycolic acid based polyesters (review). towards CO_2 as a feedstock (carbon capture and utilization – ccu). *European Polymer Journal*, 119:445 – 468, 2019. ISSN 0014-3057. doi: https://doi.org/10.1016/j.eurpolymj.2019.07.036. URL http://www.sciencedirect.com/science/article/pii/S0014305719309164.

[26] National Academies of Sciences and Engineering. *Gaseous Carbon Waste Streams Utilization: Status and Research Needs*. National Academies Press, 2020.

[27] Hideshi Ooka, Marta C. Figueiredo, and Marc T.M. Koper. Competition between Hydrogen Evolution and Carbon Dioxide Reduction on Copper Electrodes in Mildly Acidic Media. *Langmuir*, 33(37):9307–9313, 2017. ISSN 15205827. doi: 10.1021/acs.langmuir.7b00696.

[28] DEAN JA. *Lange's Handbook of Chemistry, 15th edition*. McGraw-Hill, 1999.

[29] Donald G Kaufman. *Biosphere 2000 : protecting our global environment*. Kendall/Hunt Pub. Co., 1996.

[30] Armando Gennaro, Abdirisak A. Isse, Maria Gabriella Severin, Elio Vianello, Iqbal Bhugun, and Jean Michel Savéant. Mechanism of the electrochemical reduction of carbon dioxide at inert electrodes in media of low proton availability. *Journal of the Chemical Society - Faraday Transactions*, 92(20):3963–3968, 1996. ISSN 09565000. doi: 10.1039/FT9969203963.

[31] Yuyu Liu, Zhibao Huo, Dongmei Sun, Rongzhi Chen, Yu Chen, Suddhasatwa Basu, Feng Hong, Fangming Jin, Xiaomin Wang, Jinli Qiao, and Jiujun Zhang. *Electrochemical Reduction of Carbon Dioxide: Fundamentals and Technologies*. 06 2016. ISBN 9781482258240.

[32] Ennis C. McConnell R. Spence M. Eggins, B.R. Improved yields of oxalate, glyoxylate and glycolate from the electrochemical reduction of carbon dioxide in methanol. *Journal of Applied Electrochemistry*, 1997.

[33] Brian R. Eggins, Eleanor M. Brown, E. Anne McNeill, and James Grimshaw. Carbon dioxide fixation by electrochemical reduction in water to oxalate and glyoxylate. *Tetrahedron Letters*, 29(8):945–948, 1988. ISSN 00404039. doi: 10.1016/S0040-4039(00)82489-2.

[34] Johann Desilvestro and Stanley Pons. The cathodic reduction of carbon dioxide in acetonitrile: An electrochemical and infrared spectroelectrochemical study. *Journal of Electroanalytical Chemistry and Interfacial Electrochemistry*, 267(1-2):207–220, aug 1989. ISSN 0022-0728. doi: 10.1016/0022-0728(89)80249-9. URL https://www.sciencedirect.com/science/article/pii/0022072889802499.

[35] J. Fischer, Th Lehmann, and E. Heitz. The production of oxalic acid from CO_2 and H_2O, volume = 11, year = 1981. *Journal of Applied Electrochemistry*, (6):743–750. ISSN 0021891X. doi: 10.1007/BF00615179.

[36] Wei Xin Lv, Rui Zhang, Peng Ran Gao, Chun Xia Gong, and Li Xu Lei. Electrochemical reduction of carbon dioxide on stainless steel electrode in acetonitrile. *Advanced Materials Research*, 807-809:1322–1325, 2013. ISSN 10226680. doi: 10.4028/www.scientific.net/AMR.807-809.1322.

[37] E. Lamy, L. Nadjo, and J.M. Saveant. Standard potential and kinetic parameters of the electrochemical reduction of carbon dioxide in dimethylformamide. *Journal of Electroanalytical Chemistry and Interfacial Electrochemistry*, 78(2):403–407, may 1977. ISSN 0022-0728. doi: 10.1016/S0022-0728(77)80143-5. URL https://www.sciencedirect.com/science/article/pii/S0022072877801435?via{%}3Dihub.

[38] Yoshinori Kushi, Hirotaka Nagao, Takanori Nishioka, Kiyoshi Isobe, and Koji Tanaka. Oxalate Formation in Electrochemical CO_2 Reduction Catalyzed by Rhodium-Sulfur Cluster , 1994. ISSN 0366-7022.

[39] M. Rudolph, S. Dautz, and E. G. Jager. Macrocyclic [N4/2-] coordinated nickel complexes as catalysts for the formation of oxalate by electrochemical reduction of carbon dioxide. *Journal of the American Chemical Society*, 122(44):10821–10830, 2000. ISSN 00027863. doi: 10.1021/ja001254n.

[40] Raja Angamuthu, Philip Byers, Martin Lutz, Anthony L. Spek, and Elisabeth Bouwman. Electrocatalytic CO_2 conversion to oxalate by a copper complex. *Science*, 327(5963):313–315, 2010. ISSN 00368075. doi: 10.1126/science.1177981.

[41] James Y. Becker, Baruch Vainas, Rivka Eger, and Leah Kaufman. Electrocatalytic reduction of CO_2 to oxalate by Ag" and Pd" porphyrins. *Journal of the Chemical Society - Series Chemical Communications*, (21):1471–1472, 1985. ISSN 00224936. doi: 10.1039/C39850001471.

[42] P .A. Christensen and S . J. Higgins. The electrochemical reduction of to oxalate at a Pt electrode immersed in acetonitrile and coated with polyvinylalcohol/[Ni(dppm)$_2$C1$_2$]. *Journal of electroanalytical chemistry*, 8(387):127–132, 1995. ISSN 00220728.

[43] Aubrey R. Paris and Andrew B. Bocarsly. High-Efficiency Conversion of CO_2 to Oxalate in Water Is Possible Using a Cr-Ga Oxide Electrocatalyst. *ACS Catalysis*, 9(3):2324–2333, 2019. ISSN 21555435. doi: 10.1021/acscatal.8b04327.

[44] David M. Weekes, Danielle A. Salvatore, Angelica Reyes, Aoxue Huang, and Curtis P. Berlinguette. Electrolytic CO_2 Reduction in a Flow Cell. *Accounts of Chemical Research*, 51(4):910–918, 2018. ISSN 15204898. doi: 10.1021/acs.accounts.8b00010.

[45] Zum Mechanismus der elektrochemischen Dimerisierung von CO_2 zu Oxalsäure. *Berichte der Bunsengesellschaft für physikalische Chemie*, 77(10-11):818–823, oct 1973. ISSN 0005-9021. doi: 10.1002/bbpc.19730771018. URL https://doi.org/10.1002/bbpc.19730771018.

[46] Electrochemistry in nonaqueous solutions, sep 2009. URL https://doi.org/10.1002/9783527629152.ch1.

[47] Armando Gennaro, Abdirisak Ahmed Isse, and Elio Vianello. Solubility and electrochemical determination of CO_2 in some dipolar aprotic solvents. *Journal of Electroanalytical Chemistry and Interfacial Electrochemistry*, 289(1):203 – 215, 1990. ISSN 0022-0728. doi: https://doi.org/10.1016/0022-0728(90)87217-8. URL http://www.sciencedirect.com/science/article/pii/0022072890872178.

[48] Volodymyr Koverga, Yevheniia Smortsova, François-Alexandre Miannay, Oleg Kalugin, Toshiyuki Takamuku, Pál Jedlovszky, Bogdan Marekha, and Abdenacer Idrissi. Distance angle descriptors of the interionic and ion-solvent interactions in imidazolium-based ionic liquid mixtures with aprotic solvents: A molecular dynamics simulation study. *The journal of physical chemistry. B*, 123, 06 2019. doi: 10.1021/acs.jpcb.9b03838.

[49] Timothy C. Berto, Linghong Zhang, Robert J. Hamers, and John F. Berry. Electrolyte dependence of CO_2 electroreduction: Tetraalkylammonium ions are not electrocatalysts. *ACS Catalysis*, 5(2):703–707, 2015. ISSN 21555435. doi: 10.1021/cs501641z.

[50] Yeonji Oh and Xile Hu. Organic molecules as mediators and catalysts for photocatalytic and electrocatalytic CO_2 reduction. *Chem. Soc. Rev.*, 42:2253–2261, 2013. doi: 10.1039/C2CS35276A. URL http://dx.doi.org/10.1039/C2CS35276A.

[51] Rune Halseid, Tomáš Bystroň, and Reidar Tunold. Oxygen reduction on platinum in aqueous sulphuric acid in the presence of ammonium. *Electrochimica Acta*, 51:2737–2742, 03 2006. doi: 10.1016/j.electacta.2005.08.011.

[52] Steven T. Ahn, Ismael Abu-Baker, and G.Tayhas R. Palmore. Electroreduction of CO_2 on polycrystalline copper: Effect of temperature on product selectivity. *Catalysis Today*, 288:24 – 29, 2017. ISSN 0920-5861. doi: https://doi.org/10.1016/j.cattod.2016.09.028. URL http://www.sciencedirect.com/science/article/pii/S092058611630582X. Electrochemical Reduction of Carbon Dioxide by heterogenous and homogeneous catalysts: Experiment and Theory.

[53] Bonis M.R. Crolet, J.L. ph measurements in aqueous CO_2 solutions under high pressure and temperature. *CORROSION*, 39:39–46, 1983.

[54] Angelica Reyes Aoxue Huang David M. Weekes, Danielle A. Salvatore and Curtis P. Berlinguette. Electrolytic CO_2 reduction in a flow cell. *Accounts of Chemical Research*, 51:910–918, 2018. doi: 10.1021/acs.accounts.8b00010.

[55] H. Yu H.B. Yu Q.N. Wang, H. Dong. Enhanced performance of gas diffusion electrode for electrochemical reduction of carbon dioxide to formate by adding polytetrafluoroethylene into catalyst layer. *J. Power Sources*, 279:1–5, 2015.

[56] M Kubota. Decomposition of oxalic acid with nitric acid. *Journal of Radioanalytical Chemistry*, 75(1):39–49, 1982. ISSN 1588-2780. doi: 10.1007/BF02519972. URL https://doi.org/10.1007/BF02519972.

[57] ECHA. Oxalic acid - registration dossier. https://echa.europa.eu/registration-dossier/-/registered-dossier/14786/4/3/?documentUUID=c4515a70-69c9-4cd2-9d40-91d13194f2e2, 2000. accessed: 2020-02-10.

[58] Inchem. Icsc 0529 - oxalic acid. http://www.inchem.org/documents/icsc/icsc/eics0529.htm, 2009. accessed: 2020-02-10.

[59] N. Rodriguez-Hornedo and J. T. Carstensen. Crystallization kinetics of oxalic acid dihydrate: Nonisothermal desupersaturation of solutions. *Journal of Pharmaceutical Sciences*, 75(6):552–558, 1986. doi: 10.1002/jps.2600750606. URL https://onlinelibrary.wiley.com/doi/abs/10.1002/jps.2600750606.

[60] Issei Nakamori Haruo Hayashida, Kiichi Teruya. Liquid-liquid equilibria of the system, propylene carbonate-water-acid. *Chemical Engineering*, 36:221–223, 1972. doi: https://doi.org/10.1252/kakoronbunshu1953.36.221.

[61] C Srinivasakannan, R Vasanthakumar, K Iyappan, and P G Rao. A Study on Crystallization of Oxalic Acid in Batch Cooling Crystallizer. 16(3):125–129, 2002.

[62] Gerhard Muhrer, Cheng Lin, and Marco Mazzotti. Modeling the Gas Antisolvent Recrystallization Process. *Industrial & Engineering Chemistry Research*, 41(15):3566–3579, jul 2002. ISSN 0888-5885. doi: 10.1021/ie020070+. URL https://doi.org/10.1021/ie020070+.

[63] Matthew Jouny, Wesley Luc, and Feng Jiao. General Techno-Economic Analysis of CO_2 Electrolysis Systems. 2018. doi: 10.1021/acs.iecr.7b03514.

[64] Exchange rates UK. Live euro to dollar exchange rate (eur/usd) today. https://www.exchangerates.org.uk/Euros-to-Dollars-currency-conversion-page.html, 2020. accessed: 2020-01-31.

[65] Mahinder Ramdin, Andrew R T Morrison, Mariette De Groen, Rien Van Haperen, Robert De Kler, Erdem Irtem, Antero T Laitinen, Leo J P Van Den Broeke, Tom Breugelmans, J P Martin Trusler, Wiebren De Jong, and Thijs J H Vlugt. High-Pressure Electrochemical Reduction of CO_2 to Formic Acid/Formate: Effect of pH on the Downstream Separation Process and Economics. *Industrial & Engineering Chemistry Research*, 58:22718–22740, 2019. ISSN 0888-5885. doi: 10.1021/acs.iecr.9b03970.

[66] Alibaba Xian Kig technology Co. Lead alloy anode plate. https://www.alibaba.com/product-detail/Lead-Alloy-Anode-Plate-for-Electrowinning_60727843447.html?spm=a2700.galleryofferlist.0.0.1ca47975vAOZbA, 2017. accessed: 2020-02-19.

[67] Alibaba Xian Kig technology Co. Alkaline water electrolysis cell 4 plates. https://www.alibaba.com/product-detail/alkaline-water-electrolysis-cell-4-plates_62438618937.html?spm=a2700.galleryofferlist.0.0.57907421frG9kl, 2017. accessed: 2020-02-19.

[68] Fuel Cell Earth. Nafion membrane ne 1035. https://www.fuelcellearth.com/fuel-cell-products/ne1035-membrane/, 2016. accessed: 2020-02-19.

[69] Nancy L. Garland. Doe's fuel cell catalyst r&d activities. https://www.energy.gov/sites/prod/files/2014/03/f9/2_cwg_may2012_garland.pdfs, 2012. accessed: 2020-02-19.

[70] Jennie M Moton Genevieve Saur Colella, Whitney G. and Todd Ramsden. Techno-economic analysis of pem electrolysis for hydrogen production. https://www.energy.gov/sites/prod/files/2014/08/f18/fcto_2014_electrolytic_h2_wkshp_colella1.pdf, 2014. accessed: 2020-02-19.

[71] J. D. Seader, Ernest J. Henley, and D. Keith Roper. *Separation process principles, 3rd edition.* John Wiley Incorporated, 2011.

[72] Lyle Frederick Albright. *Albright's Chemical Engineering Handbook.* CRC Press, 2009.

[73] Alibaba. Extraction column. https://www.alibaba.com/product-detail/YYCQ-Extraction-column_62276340236.html?spm=a2700.galleryofferlist.0.0.2d8e7260SvTnvS, 2019. accessed: 2020-02-18.

[74] Roger Williams. Six-tenths factor aids in approximating costs. 1947.

[75] Max Peters, Klaus Timmerhaus, and Ronald West. *Plant Design and Economics for Chemical Engineers.* McGrawHill, 2003.

[76] Ray Sinnot Gavin Towler. *Chemical Engineering Design, 2nd Edition.* Butterworth-Heinemann, 2012.

[77] Matches. Crystallizer cost estimate. http://matche.com/equipcost/Crystallizer.html, 2014. accessed: 2020-02-19.

[78] Drew Higgins, Christopher Hahn, Chengxiang Xiang, Thomas F Jaramillo, and Adam Z Weber. Gas-Diffusion Electrodes for Carbon Dioxide Reduction: A New Paradigm. *ACS Energy Letters*, 4(1):317–324, jan 2019. doi: 10.1021/acsenergylett.8b02035. URL https://doi.org/10.1021/acsenergylett.8b02035.

[79] Xu Lu, Dennis Y. C. Leung, Huizhi Wang, and Jin Xuan. A high performance dual electrolyte microfluidic reactor for the utilization of CO_2. *Applied Energy*, 194:549–559, 5 2017. ISSN 0306-2619. doi: 10.1016/j.apenergy.2016.05.091.

[80] Xueli Zheng, Phil De Luna, F. Pelayo García de Arquer, Bo Zhang, Nigel Becknell, Michael B. Ross, Yifan Li, Mohammad Norouzi Banis, Yuzhang Li, Min Liu, Oleksandr Voznyy, Cao Thang Dinh, Taotao Zhuang, Philipp Stadler, Yi Cui, Xiwen Du, Peidong Yang, and Edward H. Sargent. Sulfur-modulated tin sites enable highly selective electrochemical reduction of CO_2 to formate. *Joule*, 1(4):794 – 805, 2017. ISSN 2542-4351. doi: https://doi.org/10.1016/j.joule.2017.09.014. URL http://www.sciencedirect.com/science/article/pii/S2542435117300880.

[81] Feina Xu, Christophe Innocent, and Gérald Pourcelly. Electrodialysis with ion exchange membranes in organic media. *Separation and Purification Technology*, 43(1):17 – 24, 2005. ISSN 1383-5866. doi: https://doi.org/10.1016/j.seppur.2004.09.009. URL http://www.sciencedirect.com/science/article/pii/S1383586604002667.

[82] Yan Zhao, Yi Li, Jiajie Zhu, Amaia Lejarazu-Larrañaga, Shushan Yuan, Emily Ortega, Jiangnan Shen, Congjie Gao, and Bart Van der Bruggen. Thin and robust organic solvent cation exchange membranes for ion separation. *J. Mater. Chem. A*, 7:13903–13909, 2019. doi: 10.1039/C9TA03550H. URL http://dx.doi.org/10.1039/C9TA03550H.

[83] Markets and Markets. Glycolic acid market by grade (cosmetic, technical), application (personal care & dermatology, industrial, household) and region (apac, north america, europe, south america, middle east & africa) - global forecast to 2024. https://www.marketsandmarkets.com/Market-Reports/glycolic-polyglycolic-acid-market-1090.html, 2019. accessed: 2020-03-26.